Spring 6-9-2016

Three Novel Seminaphthorhodamines: Synthesis, Structure, and Spectral Properties

Chris Schweizer
Portland State University

Three Novel Seminaphthorhodamines: Synthesis, Structure, and Spectral Properties

By

Christopher Schweizer

An undergraduate honors thesis submitted in partial fulfillment of the requirements for the degree of

Bachelor of Science

in

University Honors

And

Chemistry

Thesis Advisor

Robert M. Strongin

Portland State University

2016

Acknowledgements

I would like to thank Dr. Strongin for teaching me organic chemistry in my sophomore year and giving me a place to develop my skills as a chemist. I'd like to thank Lei Wang for all his guidance and patience in the lab and his help with data processing; without him this thesis would not exist, Dr. Sibrian-Vasquez for the foundational synthetic work she did that made this thesis possible, and finally, Dr. Mark Lowry for his help with understanding fluorophore chemistry and his helpful suggestions.

Abstract

A series of three new seminaphthorhodamine analogs were synthesized via the condensation of 7-amino-2-naphthol and amino substituted hydroxy-benzophenones. Absorption, excitation, and emission spectra were taken in a variety of solvents and pH values. At biological pH, the molecules showed increasing Stokes shifts (from 40 to 95 nm) and longer wavelength emission in phosphate buffer with increased alkylation of the rhodamine nitrogen moiety. The fluorescent properties of the compounds were pH insensitive and variable in organic solvents. Two of the compounds exhibited significant emission at long wavelengths on the edge of the near infrared region of the electromagnetic spectrum.

Contents

Introduction

Fluorescent compounds (heretofore referred to as fluorophores) are a diverse class of molecules that absorb and emit light at different frequencies. This change in wavelength (the Stokes shift) is due to excited state relaxation processes such as vibratory energy loss to solvent molecules. Fluorophores have found countless applications in the fields of medicine and industry and are a primary topic of research for organic chemists. Special attention has recently been paid to fluorophores that emit in the near infrared (NIR) region of the electromagnetic spectrum. NIR radiation is better able to penetrate live tissue and experiences decreased interference from fluorescing proteins.[1] They are therefore better suited to certain biological imaging applications than fluorophores that emit in the visible region. Although considerable work has been done in developing such NIR dyes, the library of available fluorophores that show NIR emission is small compared to those that fluoresce at shorter wavelengths.[1]

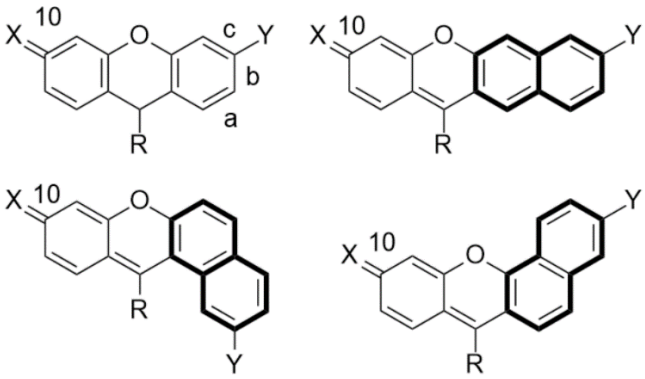

Figure 1: The benzoxanthene framework. Clockwork from top left: the xanthene skeleton, a benzo[c]xanthene, benzo[b]xanthene, and benzo[a]xanthene.

Benzoxanthenes are one class of fluorophores which consist of a substituted xanthene skeleton with a linear (b) or branched (a, c) benzannulation (Figure 1).[2] They are desirable synthetic targets due to their low cost, sensitivity, and ease of functionalization.[3]

Benzoxanthene design strategy makes use of not only the pattern of benzannulation, but also of the regiochemistry of functional groups (usually hydroxyl or

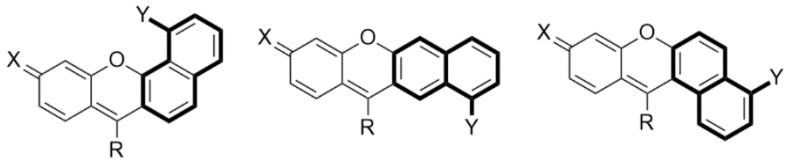

Figure 2: Alternate benzoxanthene substitution patterns than those shown in Figure 1.

amino) to tune the desired spectroscopic properties.[4] Figure 2 shows some alternate substitution patterns for benzoxanthene dyes that have been explored in recent work.[3] The benzoxanthenes have found varied applications in live cell imaging, light emitting diodes (LEDs), and as ratiometric pH probes.[2,5,6] Although most benzoxanthene dyes emit in the visible region, recently developed seminaphtharhodofluorones (SNAFR, which are substituted with oxygen at position 10) and seminaphtharhodofluors (SNARF, which are nitrogen substituted at the 10 position) have been shown to exhibit large Stokes shifts (~200 nm) and NIR emissions.[7,3]

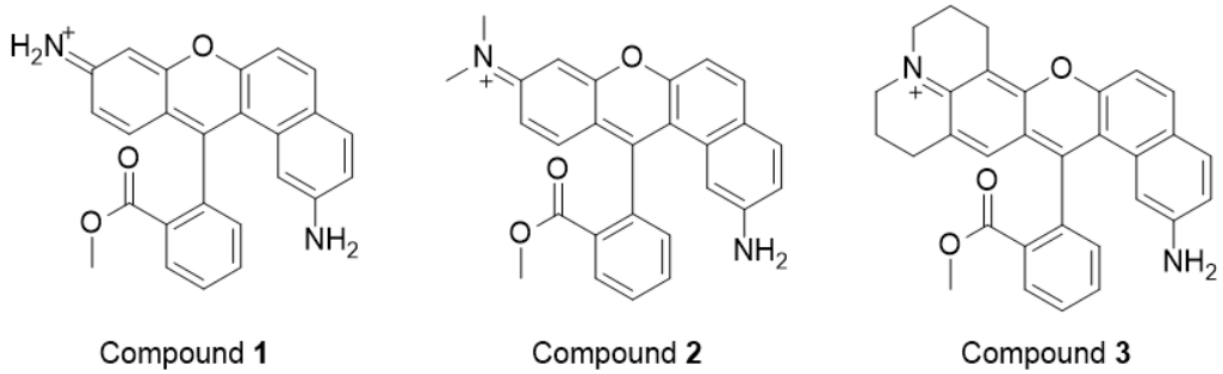

Compound **1** Compound **2** Compound **3**

*Figure 3: Three new SNARF compounds based on a benzo[a]xanthene skeleton. They vary at the 10 position, with compound **1** (left) containing a free amine, compound **2** (center) containing two methyl groups, and compound **3** (right) based on julolidine.*

With the goal of expanding the library of available fluorophores, herein is presented the synthesis of three new type a benzoxanthene dyes of the seminaphthorhodamine class, as seen in Figure 3. The free amine (**1**), dimethyl (**2**), and

julolidine (**3**) moieties at the 10 position have all been investigated and shown promising chemical properties.[1, 6] The general synthetic strategy was the condensation of an appropriately substituted benzophenone with a disubstituted naphthol under acidic conditions, with subsequent ring opening and esterification, as previously reported.[6] Based on the characterization of recently synthesized benzannulated xanthene dyes, it was hypothesized that the target compounds would display long wavelength fluorescence and possibly find use in biological applications.[3,7] To test the hypothesis, the ultraviolet-visible (UV-vis) absorption, excitation, and emission (EEM) spectra of the target compounds were measured in a range of organic and aqueous media.

Results and Discussion

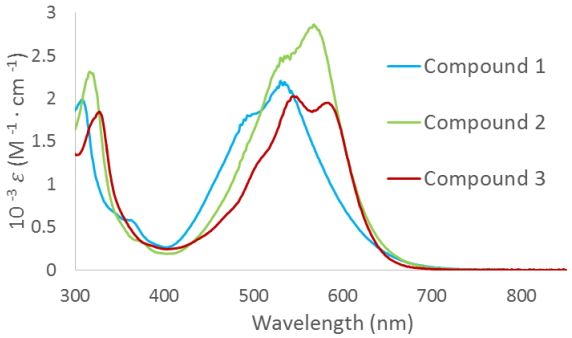

*Figure 4: Overlaid UV-vis absorption spectra for compounds **1**, **2**, and **3** in pH 7.4 phosphate buffer (10% DMSO).*

The spectral properties of the compounds were found to be pH insensitive. Overlaid absorption spectra in pH 7.4 phosphate buffer can be seen in Figure 4. Organic solvents tended to shift the absorbance maxima to longer wavelengths with increasing polarity (Table 1). The emission maxima were also greater or equal in organic solvents than those in phosphate buffer. All three compounds showed two local absorption maxima in certain solvents and one predominant one in others. With increased alkylation of the nitrogen at position 10, the appearance of the two maxima is apparent in phosphate buffer. The converse is true in organic solvents,

with DMSO and MeOH showing two absorption maxima with the free amine, and only one pronounced peak with the julolidine type.

*Table 1: Absorbance maxima and emission maxima, extinction coefficients, and Stokes shifts for compounds **1-3** in pH 7.4 phosphate buffer (10% DMSO), MeOH (10% DMSO), and DMSO. All measurements were taken at 15 μM concentration.*

	Absorbance λ_{max} (nm)	Extinction coefficient (M^{-1} cm^{-1})	Emission λ_{max} (nm)	Stokes Shift (nm)
Compound **1** pH 7.4	530	2.21×10^4	570	40
Compound **1** DMSO	582	2.05×10^4	620	38
Compound **1** MeOH	567	1.80×10^4	610	43
Compound **2** pH 7.4	568	2.86×10^4	640	72
Compound **2** DMSO	606	2.67×10^4	650	54
Compound **2** MeOH	584	2.61×10^4	640	56
Compound **3** pH 7.4	545	2.03×10^4	650	95
Compound **3** DMSO	606	2.02×10^4	660	54
Compound **3** MeOH	592	2.17×10^4	670	78

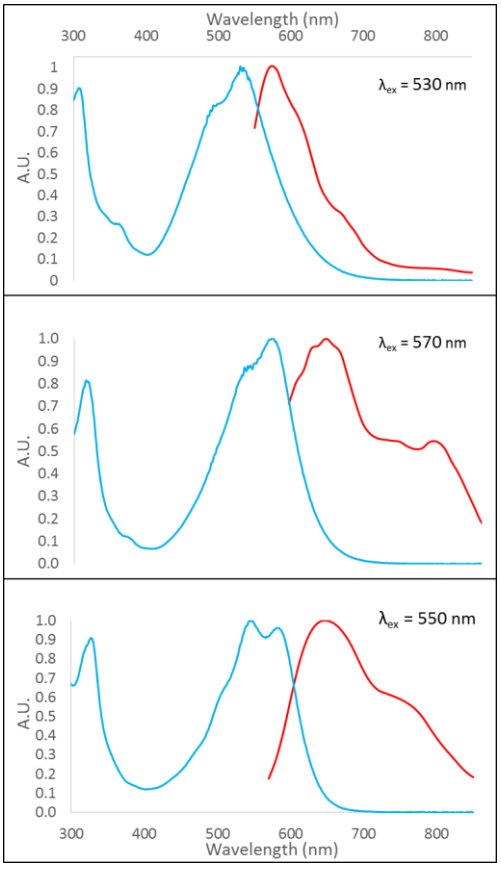

*Figure 5: Stokes shift of compounds **1** (top), **2** (center), and **3** (bottom) in pH 7.4 phosphate buffer (10% DMSO).*

The Stokes shift of each compound in phosphate buffer with 10% DMSO can be seen in Figure 5. In aqueous solution, the Stokes shift is more pronounced with increased alkylation of the nitrogen at position 10, likely due to the electron donating abilities of the N-alkyl groups.[8] The extinction coefficients, absorption maxima, and Stokes shift of each compound can be seen in Table 1 in the various solvents probed. Stokes shifts grew larger with increasing alkylation of the position 10 nitrogen in aqueous solvents. Stokes shifts were lower in organic solvents than in buffered solutions for all the

compounds studied. Extinction coefficients were largest with compound **2** and similar in compounds **1** and **3.**

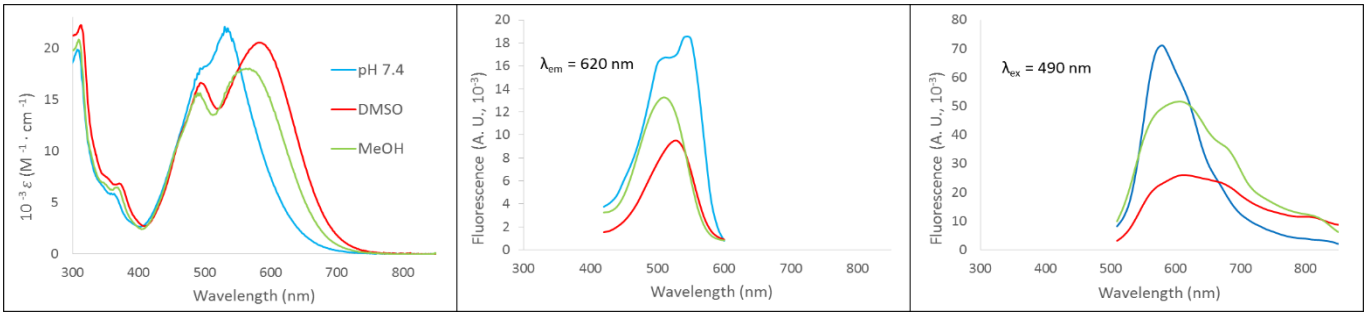

*Figure 6: UV-vis absorption (left), excitation (center), and emission (right) spectra for compound **1** (15 μM) in pH 7.4 phosphate buffer (10% DMSO), MeOH (10% DMSO) and DMSO. The legend is seen at top left. The fluorescence axis in the emission spectrum at right has been normalized to the absorbance at the excitation wavelength so that the intensity is proportional to the brightness of emission.*

The UV-vis absorption, emission, and excitation spectra with EEM wavelengths chosen near commonly available laser lines for compound **1** in phosphate buffer, DMSO, and MeOH are shown in Figure 6. Emission intensity was greatest in phosphate buffer at all excitation wavelengths. This compound emits most strongly in the yellow to red region of the spectrum. The emission intensity at top right in Figures 6-8 have been divided by the absorbance at the excitation wavelength so that the intensity is proportional to the brightness of the compound's fluorescent emission. Compound **1** had the brightest emission in aqueous solvent, then **3** (60% of **1**), then **2** (30% of **1**).

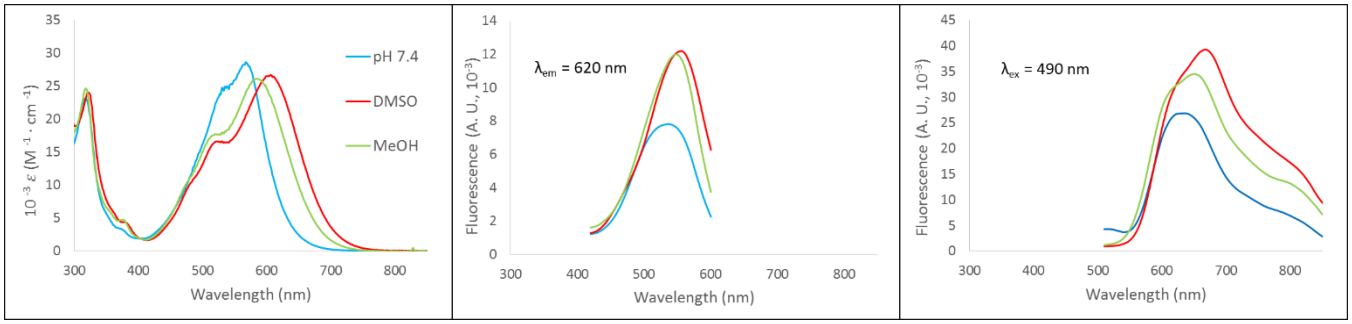

*Figure 7: UV-vis absorption (left), excitation (center), and emission (right) spectra for compound **2** (15 μM) in pH 7.4 phosphate buffer (10% DMSO), MeOH (10% DMSO) and DMSO. The legend is seen at left. The fluorescence axis in the emission spectrum at right has been normalized to the absorbance at the excitation wavelength so that the intensity is proportional to the brightness of emission.*

The UV-vis and EEM spectra for compound **2** are seen in Figure 7 above. This compound showed less spectral sensitivity to solvent conditions than compounds **2** and **3**, with solvation in DMSO and MeOH yielding stronger emission than the aqueous phase fluorophore. Emission was weaker than that of compound **1** but roughly equal to compound **2**. Emission was primarily in the red and the start of the NIR region.

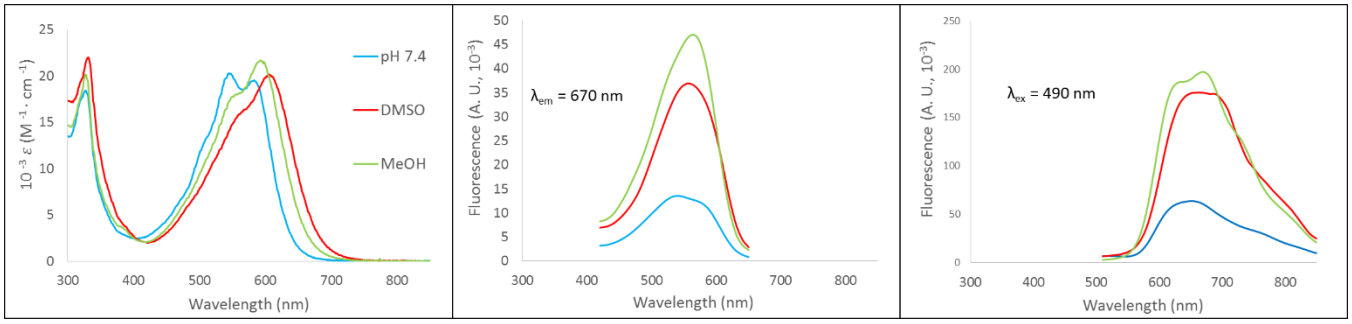

*Figure 8: UV-vis absorption (left), excitation (center), and emission (right) spectra for compound **3** (15 μM) in pH 7.4 phosphate buffer (10% DMSO), MeOH (10% DMSO) and DMSO. The legend is seen at top left. The fluorescence axis in the emission spectrum at right has been normalized to the absorbance at the excitation wavelength so that the intensity is proportional to the brightness of emission.*

Compound **3**'s UV-vis and EEM spectra appear in Figure 8. Emission intensity was roughly four times stronger in organic solvents than in phosphate buffer. In aqueous solution, emission intensity was about double that of compound **2** and two-thirds that of compound **1**. Like compound **2**, compound **3** showed two local absorption maxima in all the solvent systems probed (most pronounced in phosphate buffer), and exhibited emissions into the red region of the spectrum and into the beginning of the NIR region.

The same trend of increased alkylation of the position 10 nitrogen leading to higher Stokes shifts in aqueous solution can be seen affecting the emission wavelengths of the target compounds, with the dimethyl and julolidine substituted compounds seeing increased emission in the red and NIR regions. This is most likely

due to the electron donating effects of the alkyl groups to the conjugated π-system, which are strengthened in the excited state.[8] The decreased rotational freedom and rigidity of the julolidine rings also extend the orbital overlap with the π system.[8]

Overall, the three compounds show promising spectral properties, but more work needs to be done to truly characterize their potential applications. Time dependent density functional theory calculations could better predict the excited state electronic structures of the target compounds and help explain their behavior in various media.[9]

Experimental

Instrumentation

Unless otherwise indicated, all commercially available starting materials were used directly without further purification. Silica gel Sorbent Technologies 32-63 μm was used for flash column chromatography. ^{1}H-NMR was obtained on an ARX-400 Advance Bruker spectrometer. Chemical shifts (δ) are given in ppm relative to d_6-DMSO (2.50 ppm, ^{1}H, 39.52 ^{13}C). MS (HRMS, ESI) spectra were obtained at the PSU Bioanalytical Mass Spectrometry Facility on a ThermoElectron LTQ-Orbitrap high resolution mass spectrometer with a dedicated Accela HPLC system.

Absorbance spectra were collected on a Cary 50 UV−vis spectrophotometer. Fluorescent excitation and emission spectra were collected on a Cary Eclipse fluorescence spectrophotometer (Agilent Technologies). Absorbance spectra were baseline corrected. Fluorescence spectra were corrected for the

wavelength dependent response of the R928 photomultiplier tube using a manufacturer generated correction file.

SNARF Synthesis

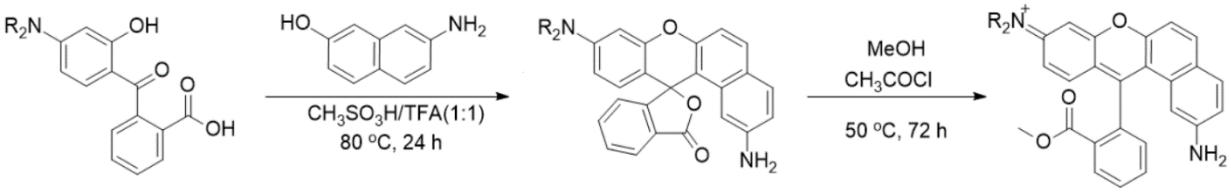

*Figure 9: General synthetic scheme for compounds **1**-**3**. The appropriately substituted benzophenone is condensed with 7-amino-2-naphthol in acidic conditions. The resulting spiro compound is then opened and esterified with acetyl chloride and MeOH.*

The three SNARF-4 compounds that form the basis of this paper were synthesized in two steps. The appropriately substituted hydroxybenzophenone was condensed with 7-amino-2-naphthol in a mixture of CH_3SO_3H:TFA 1:1 at 80 °C for 16-24 h to produce the corresponding spiro lactone (labelled spiro **1**-**3** in the supporting information section to correspond to compounds **1**-**3**). Subsequent ring opening and Fisher esterification is carried out in MeOH with catalytic acetyl chloride to produce the methyl ester. The required starting materials; 2-(2,4-dihydroxybenzoyl)benzoic acid, 2-(4-amino-2-hydroxybenzoyl)benzoic acid, 2-(8-hydroxy-1,2,3,5,6,7-hexahydropyrido[3,2,1-ij]quinoline-9-carbonyl)benzoic acid and 7-amino-2-naphthol are synthesized according to described or modified literature protocols. In general, overall good yields are obtained for the fluorophores included in this series. All compounds were isolated by flash column chromatography, if necessary, and characterized by NMR and HR ESI MS. The reaction scheme for the synthesis of compounds

1-**3** can be seen in Scheme 1. Unlike compounds **2** and **3**, compound **1**'s precursor benzophenone was prepared from hydrolysis of rhodamine-110 due to unsuccessful attempts to synthesize it from condensation of phthalic anhydride and *m*-aminophenol. This condensation was successful in the case of the dimethyl and julolidine compounds (**2** and **3**, respectively). The expanded synthetic procedures can be seen in the supporting information section.

Conclusion

Presented herein are the synthesis, spectral properties, and structural characterization of three new benzo[a]xanthene seminaphthorhodamine compounds. The compounds showed fluorescent properties, with increased alkylation of the position 10 nitrogen producing longer wavelength emission and bigger Stokes shifts in aqueous media. This was most likely due to increased rigidity, coplanarity, orbital overlap with the π system, as well as increased electron donation from the N-alkyl groups. Further research is needed to fully probe the potential applications of these new fluorophores.

References

1) Yuan, L., Lin, W., Yang, Y., & Chen, H. (2012). A unique class of near-infrared functional fluorescent dyes with carboxylic-acid-modulated fluorescence ON/OFF switching: rational design, synthesis, optical properties, theoretical calculations, and applications for fluorescence imaging in living animals. *Journal of the American Chemical Society*, *134*(2), 1200-1211.

2) Whitaker, J. E., Haugland, R. P., & Prendergast, F. G. (1991). Spectral and photophysical studies of benzo [c] xanthene dyes: dual emission pH sensors. *Analytical biochemistry*, *194*(2), 330-344.

3) Yang, Y., Lowry, M., Schowalter, C. M., Fakayode, S. O., Escobedo, J O., Xu, X., ... & Strongin, R. M. (2006). An organic white light-emitting fluorophore. *Journal of the American Chemical Society*, *128*(43), 14081-14092.

4) Brémond, É., Alberto, M. E., Russo, N., Ricci, G., Ciofini, I., & Adamo, C. (2013). Photophysical properties of NIR-emitting fluorescence probes: insights from TD-DFT. *Physical Chemistry Chemical Physics, 15*(25), 10019-10027.

5) Arppe, R., Näreoja, T., Nylund, S., Mattsson, L., Koho, S., Rosenholm, J. M., ... & Schäferling, M. (2014). Photon upconversion sensitized nanoprobes for sensing and imaging of pH. *Nanoscale*, *6*(12), 6837-6843.

6) Han, J., & Burgess, K. (2009). Fluorescent indicators for intracellular pH. *Chemical reviews*, *110*(5), 2709-2728.

7) Yang, Y., Lowry, M., Xu, X., Escobedo, J. O., Sibrian-Vazquez, M., Wong, L., ... & Strongin, R. M. (2008). Seminaphthofluorones are a family of water-soluble, low molecular weight, NIR-emitting fluorophores. *Proceedings of the National Academy of Sciences*, *105*(26), 8829-8834.

8) Albota, M., Beljonne, D., Brédas, J. L., Ehrlich, J. E., Fu, J. Y., Heikal, A. A., ... & McCord-Maughon, D. (1998). Design of organic molecules with large two-photon absorption cross sections. *Science, 281*(5383), 1653-1656.

9) Improta, R., Scalmani, G., Frisch, M. J., & Barone, V. (2007). Toward effective and reliable fluorescence energies in solution by a new state specific polarizable continuum model time dependent density functional theory approach. *The Journal of chemical physics*, *127*(7), 074504.

Supporting Information

Synthesis

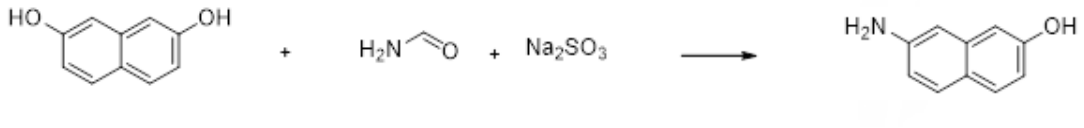

Synthesis of 7-amino-2-naphthol. 2,7-dihydroxy naphthalene, formamide and sodium sulfite were suspended in 50 mL of DI water. The mixture was refluxed 12 h. The solid formed was collected by filtration and washed with water (100 mL). The solid was dissolved in 100 mL of diethyl ether, then transferred to a 500 mL separatory funnel. The organic phase was washed with 100 mL of 6 N HCl. The aqueous layer was basified to pH 13 with 50% NaOH. The aqueous layer was washed with 100 mL of diethyl ether. The aqueous layer was neutralized to pH 7 with HCl. The aqueous layer was extracted with ethyl acetate (3 x 100 mL). The organic extracts were combined, dried over Na_2SO_4 and the solvent evaporated under vacuum. Yield 76%.[1] 1H NMR (400 MHz, DMSO-d_6) δ 9.30 (s, 1H), 7.44 (d, J = 8.8 Hz, 1H), 7.41 (d, J = 8.8 Hz, 1H), 6.72 (d, J = 2.4 Hz, 1H), 6.67 (dd, J = 8.9, 2.1 Hz 1H), 6.65 (dd, J = 8.9, 2.4 H, 1H), 6.59 (d, J = 2.1 Hz, 1H), 5.20 (s, 2H). ^{13}C NMR (101 MHz, DMSO) δ 155.35, 146.75, 136.51, 128.89, 128.27, 121.17, 115.16, 113.34, 106.30, 104.53.

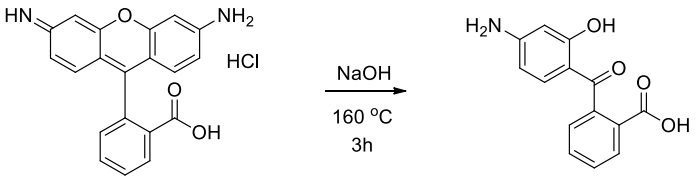

Synthesis of 2-(4-amino-2-hydroxybenzoyl)benzoic acid. Rhodamine 110 hydrochloride (0.2 g, 0.545 µmol) was mixed with NaOH (0.375g, 9.27 mmol) and 200 µL of water. The mixture was stirred and heated at 160 °C for two hours, 0.5 mL of 50% NaOH were added in one portion and the mixture heated and stirred at 160 °C for an additional one hour. The mixture was allowed to cool down to room temperature and diluted with 10 mL of water. The mixture was acidified to pH 1 with concentrated HCl. The resulting mixture was extracted with ethyl ether (2 × 50 mL), the organic extracts combined, dried over Na_2SO_4, filtered and the solvent evaporated under vacuum to leave a pale yellow solid. Yield: 130 mg, 93%. ^{1}H NMR (400 MHz, DMSO-d_6) δ 13.01

(s, 1H), 12.60 (s, 1H), 7.95 (dd, J = 7.2, 1.2 Hz, 1H), 7.67 (td, J = 7.5, 1.4 Hz, 1H), 7.60 (td, J = 7.5, 1.4 Hz, 1H), 7.37 (dd, J = 7.6, 1.2 Hz, 1H), 6.71 (d, J = 8.5 Hz, 1H), 6.44 (s, 2H), 6.02 (dd, J = 8.3, 2.1 Hz 1H), 6.00 (d, J = 2.2, 1H). ^{13}C NMR (101 MHz, DMSO) δ 198.29, 166.89, 164.95, 156.79, 140.04, 134.45, 131.92, 129.81, 129.67, 129.28, 127.65, 109.76, 106.45, 106.15, 98.13, 48.56.

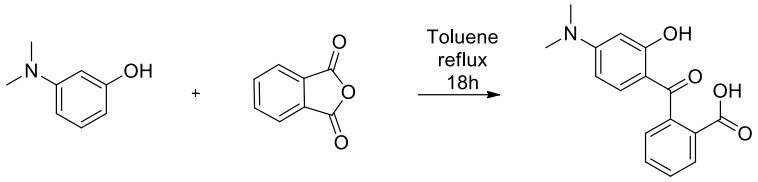

Synthesis of compound 2-(4-(dimethylamino)-2-hydroxybenzoyl)benzoic acid: 3-dimethyl amino phenol (5 g, 36.44 mmol) and phthalic anhydride (5.39 g, 36.44 mmol) were dissolved in 30 mL of toluene and refluxed 18 h. The solvent was evaporated under vacuum to leave a purple residue. The residue was dissolved in ethyl acetate and the mixture passed through a plug of silica gel using EtOAc:Hexanes 1:1, EtOAc:Hexanes 3:1, and EtOAc for elution. Yield 4.32 g, 42%. ^{1}H NMR (400 MHz, DMSO-d_6) δ 13.07 (s, 1H), 12.54 (s, 1H), 7.97 (dd, *J* = 7.8, 1.0 Hz, 1H), 7.69 (td, *J* = 7.5, 1.4 Hz, 1H), 7.61 (td, *J* = 7.6, 1.4 Hz, 1H), 7.38 (dd, *J* = 7.7, 1.2 Hz, 1H), 6.81 (d, *J* = 9.1 Hz, 1H), 6.21 (dd, *J* = 9.2, 2.5 Hz, 1H), 6.10 (d, *J* = 2.5 Hz, 1H), 3.00 (s, 6H). ^{13}C NMR (101 MHz, DMSO) δ 198.74, 166.88, 164.29, 155.71, 140.03, 133.88, 132.05, 129.87, 129.70, 129.45, 127.64, 109.67, 104.33, 97.03, 40.15

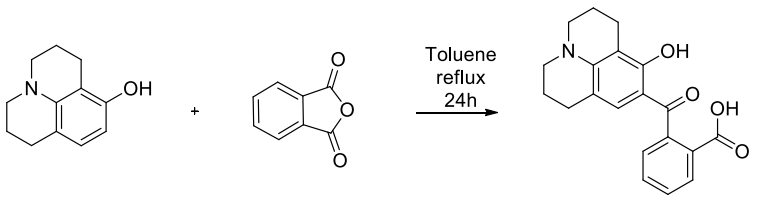

Synthesis of compound 2-(8-hydroxy-1,2,3,5,6,7-hexahydropyrido[3,2,1-ij]quinoline-9-carbonyl)benzoic acid: Phthalic anhydride (0.392 g 2.64 mmol) and 8-

hydroxyjulolidine (0.5 g, 2.64 mmol) were dissolved in 12 mL of toluene. The mixture was refluxed 24 h, then the solvent evaporated under vacuum to leave a deep red residue. The target compound was isolated as a pale yellow solid by flash column chromatography on silica gel using CH_2Cl_2:MeOH 95:5 for elution. Yield: 622 mg, 70%. ^{1}H NMR (400 MHz, DMSO-d_6) δ 12.94 (s, 2H), 7.94 (dd, *J* = 7.8, 1.3 Hz, 1H), 7.66 (td, *J* = 7.5, 1.4 Hz, 1H), 7.58 (td, *J* = 7.6, 1.4 Hz, 1H), 7.33 (dd, *J* = 7.5, 1.3 Hz, 1H), 6.39 (s, 1H), 3.24 (td, *J* = 7.2, 5.2 Hz, 4H), 2.59 (t, *J* = 6.4 Hz, 2H), 2.40 (t, *J* = 6.2 Hz, 2H), 1.90 – 1.80 (m, 2H), 1.80 – 1.70 (m, 2H). ^{13}C NMR (101 MHz, DMSO) δ 197.93, 167.03, 159.73, 148.75, 140.12, 131.72, 129.94, 129.82, 129.63, 129.15, 127.66, 112.39, 108.34, 104.58, 49.36, 48.91, 48.56, 39.15, 26.63, 21.06, 20.07, 19.54.

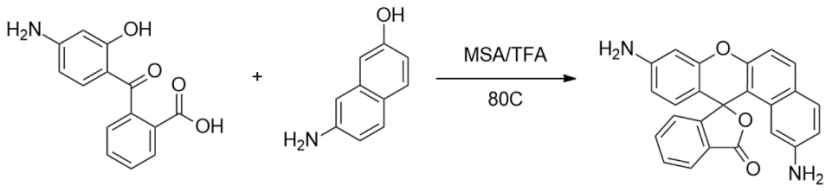

Synthesis of spiro 1: 2-(4-amino-2-hydroxybenzoyl)benzoic acid (0.389 mmol) and 7-amino-2-naphthol (0.389 mmol) were dissolved in 750 µL of methanesulfonic acid (MSA), then 1.5 µL of trifluoroacetic acid (TFA) was added. The mixture was heated and stirred at 80 ^{o}C for 16-24 h. The reaction mixture was allowed to warm to room temperature, then poured into 50 mL of DI water. The mixture was neutralized to pH 6-7 by portion wise addition of solid $NaHCO_3$. The resulting precipitate was filtered, washed with DI water and air dried. The target compound isolated by flash column chromatography on silica gel. Yield: 60 mg, 42%. ^{1}H NMR (400 MHz, DMSO-d_6) δ 8.06 (ddd, *J* = 8.7, 2.87, 0.6 Hz, 1H), 7.78 (d, *J* = 8.7 Hz, 1H), 7.70 – 7.63 (m, 2H), 7.56 (d, *J* = 8.6 Hz, 1H), 7.13 – 7.08 (m, 1H), 7.06 (d, *J* = 8.8 Hz, 1H), 6.71 (dd, *J* = 8.6, 2.0 Hz, 1H), 6.39 (d, *J* = 2.2 Hz, 1H), 6.32 (dd, *J* = 8.7, 2.2 Hz, 1H), 6.23 (d, *J* = 8.7 Hz, 1H), 5.84 (d, *J* = 2.0 Hz, 1H), 5.58 (s, 2H), 5.20 (s, 2H). ^{13}C NMR (101 MHz, DMSO) δ 169.37, 154.69, 150.87, 150.56, 149.85, 147.67, 135.42, 133.09, 132.34, 130.28, 129.42, 127.62, 126.50, 125.26, 123.36, 123.01, 115.67, 112.33, 111.45, 106.67, 105.37, 103.20, 98.38, 84.06.

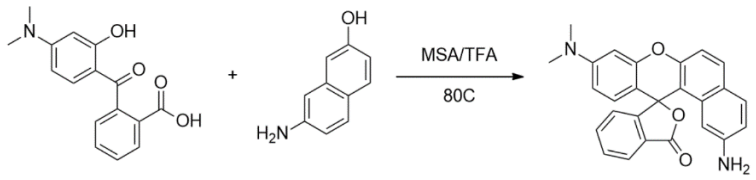

Synthesis of spiro 2: 2-(4-(dimethylamino)-2-hydroxybenzoyl)benzoic acid (0.351 mmol) and 7-amino-2-naphthol (0.351 mmol) were dissolved in 750 µL of methanesulfonic acid (MSA), then 750 µL of trifluoroacetic acid (TFA) was added. The mixture was heated and stirred at 80 ^{o}C for 16-24 h. The reaction mixture was allowed to warm to room temperature, then poured into 50 mL of DI water. The mixture was neutralized to pH 6-7 by portion wise addition of solid $NaHCO_3$. The resulting precipitate was filtered, washed with DI water and air dried. The target compound isolated by flash column chromatography on silica gel. Yield: 70 mg, 49%. ^{1}H NMR (400 MHz, DMSO-d_6) δ 8.16 – 8.08 (m, 1H), 7.95 (d, J = 8.9 Hz, 1H), 7.75 – 7.65 (m, 3H), 7.24 (d, J = 8.9 Hz, 1H), 7.19 – 7.12 (m, 1H), 6.88 (dd, J = 8.6, 2.0 Hz, 1H), 6.62 (d, J = 9.0 Hz, 1H), 6.59 (s, 1H), 6.46 (s, 1H), 6.11 (d, J = 1.9 Hz, 1H), 2.98 (s, 6H). ^{13}C NMR (101 MHz, DMSO) δ 168.90, 158.33, 157.98, 135.37, 132.60, 130.81, 129.70, 127.80, 124.68, 123.66, 117.19, 116.73, 114.28, 97.13, 39.14.

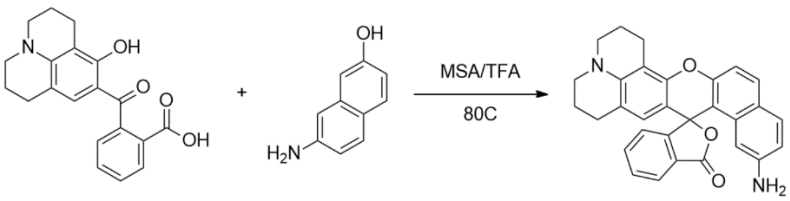

Synthesis of spiro 3: 2-(8-hydroxy-1,2,3,5,6,7-hexahydropyrido[3,2,1-ij]quinoline-9-carbonyl)benzoic acid (0.351 mmol) and 7-amino-2-naphthol (0.351 mmol) were dissolved in 750 µL of methanesulfonic acid (MSA), then 750 µL of trifluoroacetic acid (TFA) was added. The mixture was heated and stirred at 80 ^{o}C for 16-24 h. The reaction mixture was allowed to warm to room temperature, then poured into 50 mL of DI water. The mixture was neutralized to pH 6-7 by portion wise addition of solid

$NaHCO_3$. The resulting precipitate was filtered, washed with DI water and air dried. The target compound isolated by flash column chromatography on silica gel. Yield: 30 mg, 18%. ^{1}H NMR (400 MHz, DMSO-d_6) δ 8.08 – 8.02 (m, 1H), 7.79 – 7.73 (m, 1H), 7.70 – 7.61 (m, 2H), 7.55 (d, *J* = 8.7 Hz, 1H), 7.13 – 7.05 (m, 2H), 6.70 (dd, *J* = 8.6, 2.1 Hz, 1H), 5.89 (s, 1H), 5.82 (d, *J* = 2.0 Hz, 1H), 5.18 (s, 2H), 3.15 (t, *J* = 5.6 Hz, 2H), 3.10 (ddd, *J* = 7.1, 4.7, 2.9 Hz, 2H), 2.87 (t, *J* = 6.5 Hz, 2H), 2.49 – 2.33 (m, 2H), 1.99 – 1.88 (m, 2H), 1.77 (d, *J* = 6.5 Hz, 2H). ^{13}C NMR (101 MHz, DMSO) δ 169.40, 154.62, 150.82, 147.63, 145.15, 143.55, 135.39, 133.03, 132.20, 130.26, 129.41, 126.50, 125.24, 123.31, 123.28, 123.05, 117.64, 115.57, 112.47, 106.02, 105.75, 105.18, 103.22, 84.46, 48.98, 48.54, 26.90, 21.23, 20.58, 20.47.

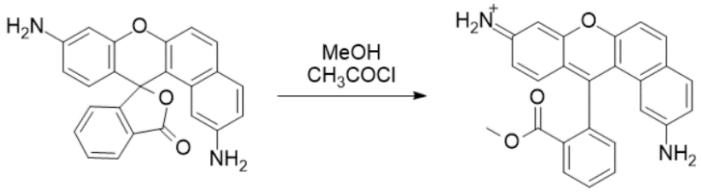

Synthesis of compound 1: Spiro precursor 1 (140 µmol) was dissolved in 20 mL of MeOH and chilled in an ice bath. Acetyl chloride (750 µL) was added dropwise. The mixture was stirred and kept at 50 ^{o}C for 48h. Additional acetyl chloride (300 µL) was added dropwise and the mixture kept at 50 ^{o}C for an additional 24h to complete conversion. The mixture was allowed to cool down to room temperature and the solvent evaporated under vacuum. Yield: 29 mg, 54%. ^{1}H NMR (400 MHz, DMSO-d_6) δ 9.00 (s, 1H), 8.81 (s, 1H), 8.38 – 8.34 (m, 1H), 8.34 – 8.29 (m, 1H), 7.91 (pd, *J* = 7.5, 1.6 Hz, 2H), 7.81 (d, *J* = 8.7 Hz, 1H), 7.54 (d, *J* = 8.7 Hz, 1H), 7.43 – 7.37 (m, 1H), 7.08 (dd, *J* = 9.4, 2.0 Hz, 1H), 7.03 (d, *J* = 2.0 Hz, 1H), 6.97 (d, *J* = 9.4 Hz, 1H), 6.94 (dd, *J* = 8.7, 2.1 Hz, 1H), 5.96 (d, *J* = 2.0 Hz, 1H), 5.84 (s, 2H), 3.57 (s, 3H). ^{13}C NMR (101 MHz, DMSO) δ 165.20, 160.89, 160.82, 157.26, 157.18, 150.76, 141.40, 137.13, 134.42, 132.44, 132.33, 131.56, 131.32, 130.66, 128.51, 128.33, 123.17, 120.22, 116.85, 116.83, 114.27, 110.60, 106.80, 95.87, 52.41.

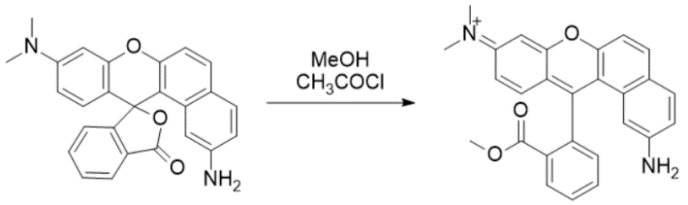

Synthesis of compound 2: Spiro precursor 2 (160 µmol) was dissolved in 20 mL of MeOH and chilled in an ice bath. Acetyl chloride (750 µL) was added dropwise. The mixture was stirred and kept at 50 ^{o}C for 48h. Additional acetyl chloride (300 µL) was added dropwise and the mixture kept at 50 ^{o}C for an additional 24h to complete conversion. The mixture was allowed to cool down to room temperature and the solvent evaporated under vacuum. Yield: 47mg, 70%. ^{1}H NMR (400 MHz, DMSO-d_6) δ 8.42 – 8.36 (m, 1H), 8.35 (d, *J* = 6.4 Hz, 1H), 7.99 – 7.87 (m, 2H), 7.83 (d, *J* = 8.7 Hz, 1H), 7.52 (d, *J* = 8.8 Hz, 1H), 7.46 – 7.39 (m, 1H), 7.32 (dd, *J* = 9.7, 2.5 Hz, 1H), 7.20 (d, *J* = 2.5 Hz, 1H), 6.99 – 6.92 (m, 2H), 6.02 (d, *J* = 2.0 Hz, 1H), 5.89 (s, 2H), 3.58 (s, 3H), 3.35 (s, 6H). ^{13}C NMR (101 MHz, DMSO) δ 165.21, 160.91, 157.62, 157.47, 156.55, 150.95, 141.76, 137.12, 134.48, 132.50, 132.46, 131.58, 130.73, 130.12, 128.46, 128.35, 123.15, 117.82, 116.88, 116.55, 114.62, 110.43, 106.92, 95.40, 52.45, 48.55, 40.86, 40.03, 39.40, 39.17.

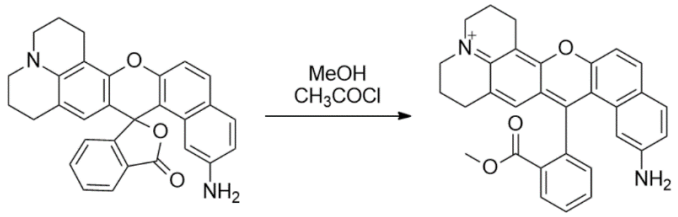

Synthesis of compound 3: Spiro precursor 3 (160 µmol) was dissolved in 20 mL of MeOH and chilled in an ice bath. Acetyl chloride (750 µL) was added dropwise. The mixture was stirred and kept at 50 ^{o}C for 48h. Additional acetyl chloride (300 µL) was added dropwise and the mixture kept at 50 ^{o}C for an additional 24h to complete conversion. The mixture was allowed to cool down to room temperature and the solvent

evaporated under vacuum. Yield: 28 mg, 37%. ^{1}H NMR (400 MHz, DMSO-d_6) δ 8.34 (dd, *J* = 7.4, 1.5 Hz, 1H), 8.29 (d, *J* = 8.7 Hz, 1H), 7.97 – 7.86 (m, 2H), 7.83 (d, *J* = 8.6 Hz, 1H), 7.61 (d, *J* = 8.6 Hz, 1H), 7.43 – 7.33 (m, 1H), 6.99 (dd, *J* = 8.6, 1.9 Hz, 1H), 6.58 (s, 1H), 5.98 (s, 1H), 3.65 (d, *J* = 5.8 Hz, 2H), 3.59 (d, *J* = 5.8 Hz, 2H), 3.05 (d, *J* = 7.7 Hz, 2H), 2.68 (s, 2H), 2.04 (d, *J* = 8.3 Hz, 2H), 1.87 (s, 2H). ^{13}C NMR (101 MHz, DMSO) δ 165.15, 157.43, 156.16, 152.70, 151.29, 139.74, 137.24, 134.36, 132.01, 131.93, 131.59, 130.61, 128.94, 128.40, 127.92, 125.12, 117.28, 117.04, 114.04, 103.98, 52.36, 50.93, 50.51, 27.01, 19.74, 18.92, 18.72.

NMR

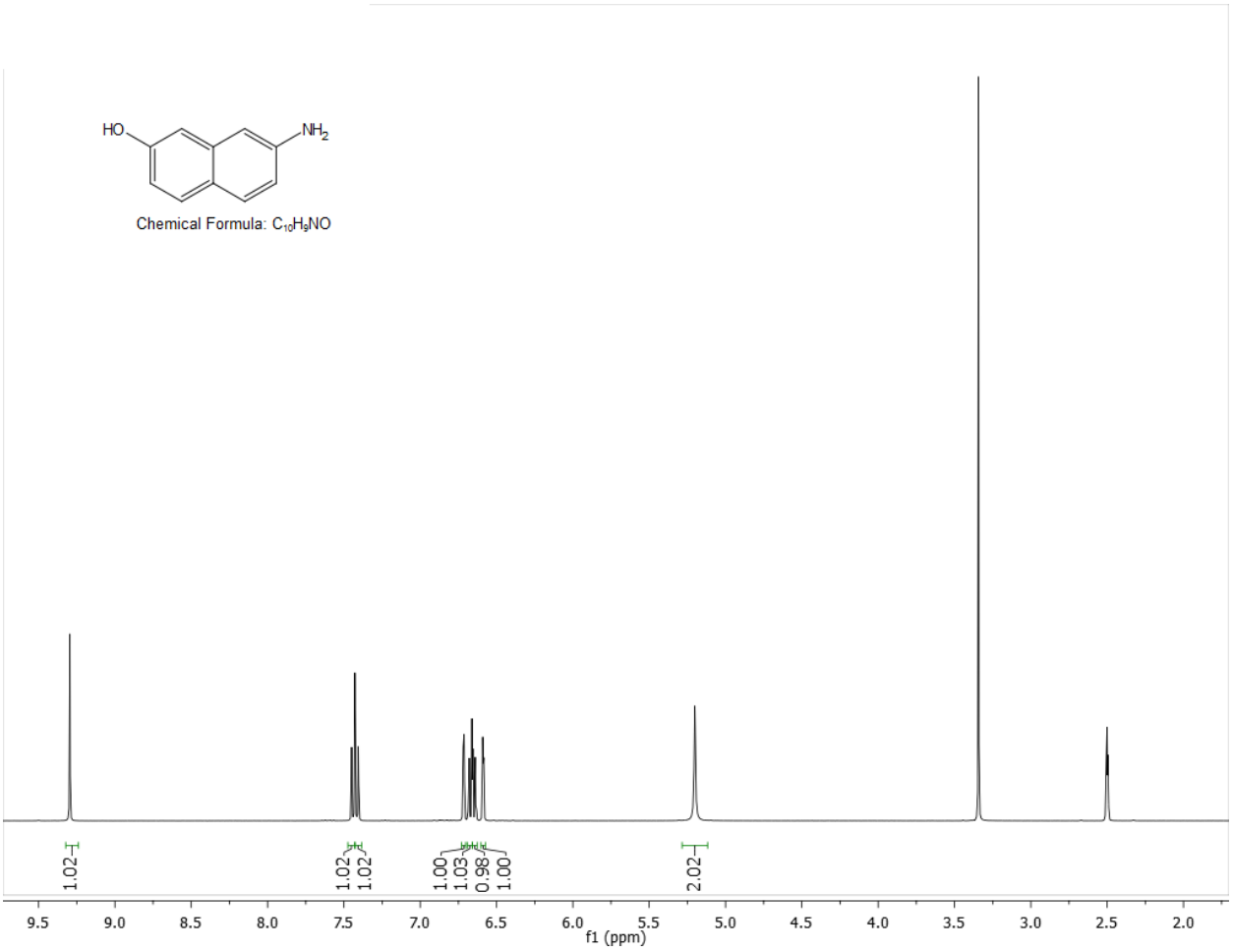

Figure S1: ^{1}H NMR spectrum for 7-amino-2-naphthol.

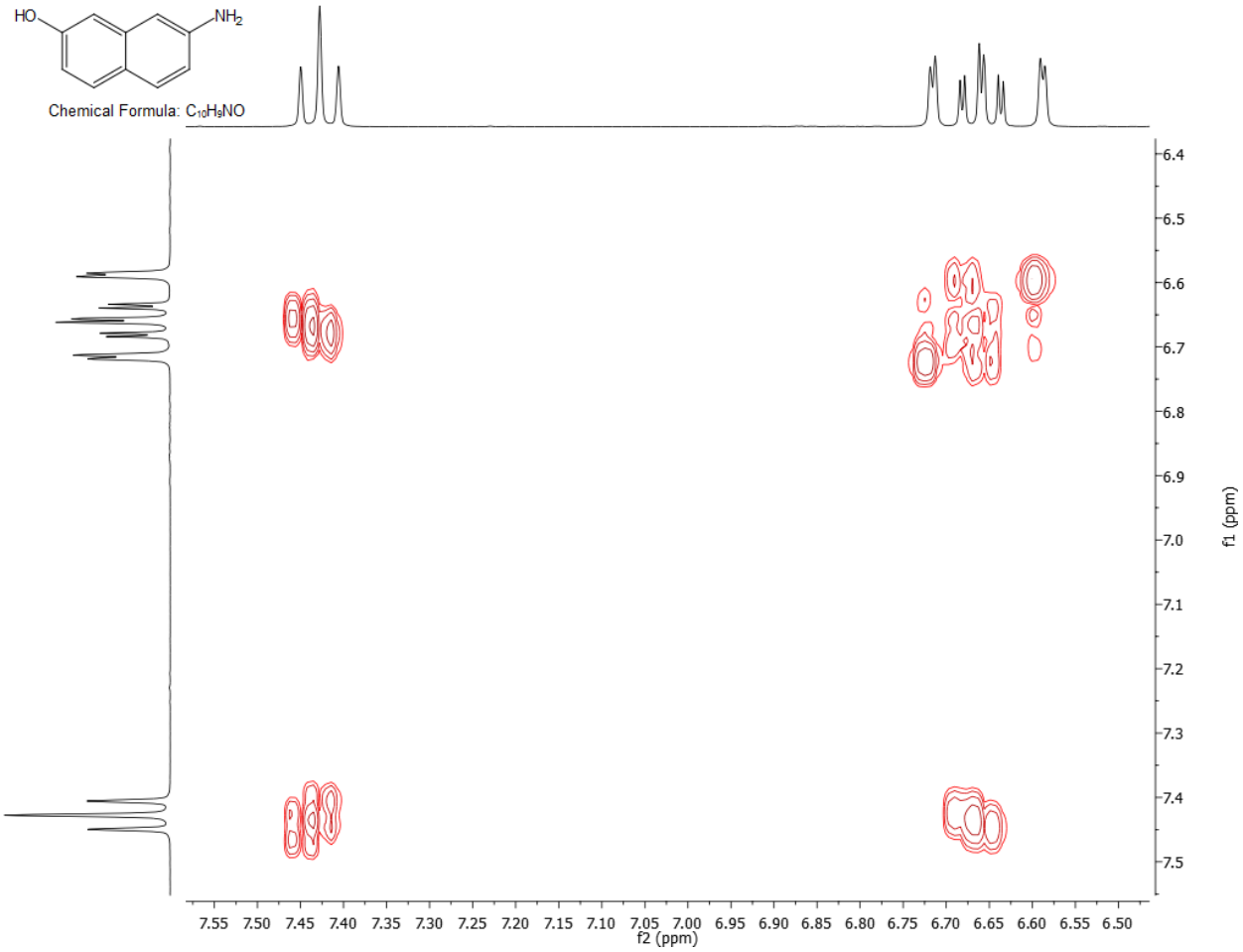

Figure S2: ^{1}H 2D correlation (COSY) NMR spectra for 7-amino-2-naphthol.

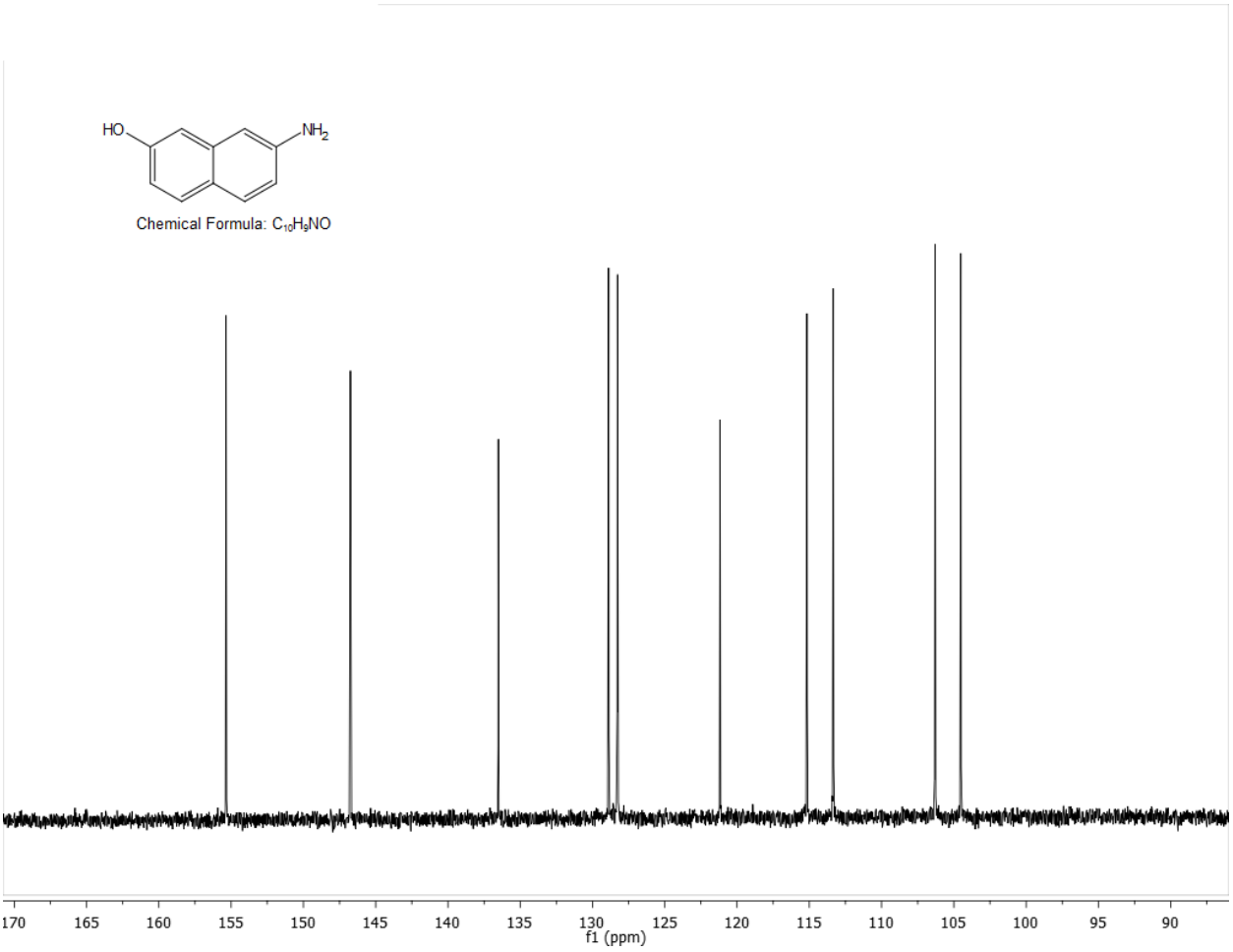

Figure S3: ^{13}C NMR spectrum for 7-amino-2-naphthol.

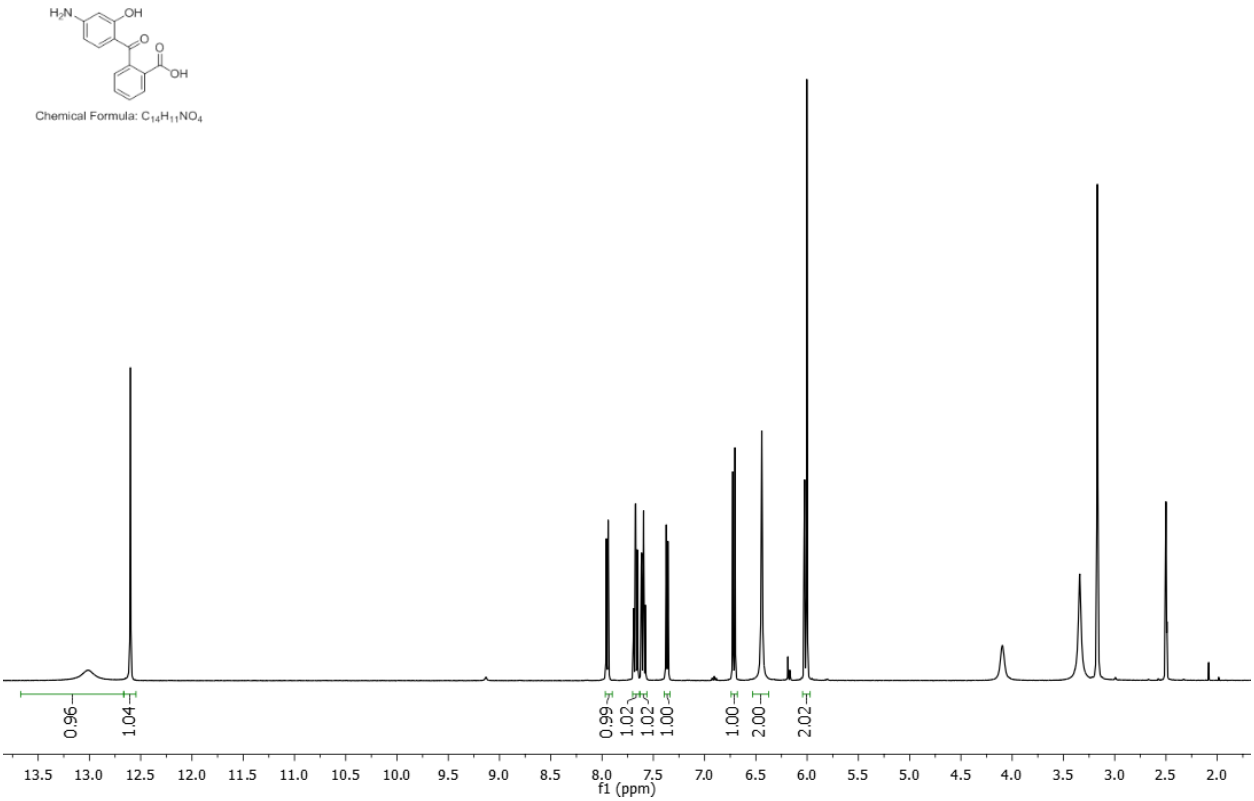

Figure S4: ^{1}H NMR spectrum for 2-(4-amino-2-hydroxybenzoyl)benzoic acid.

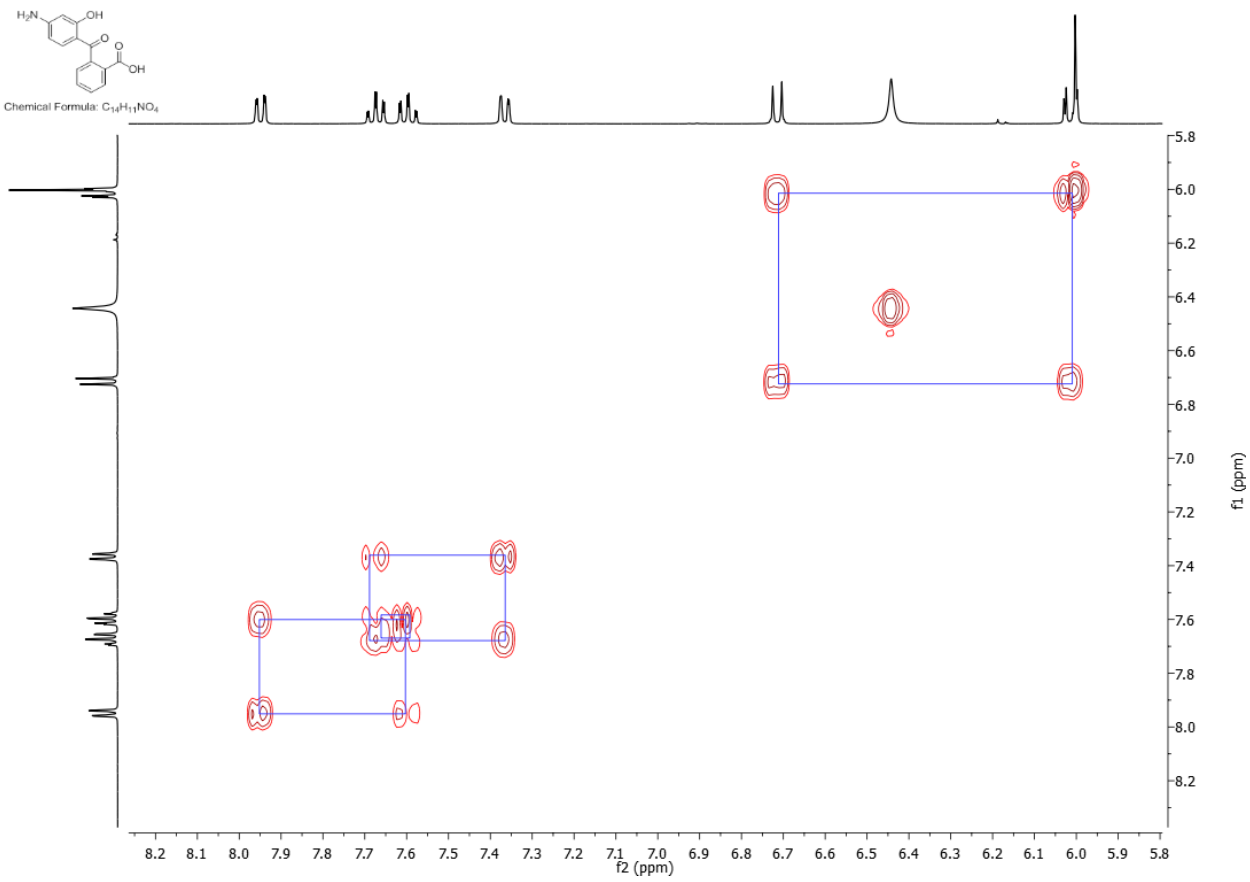

Figure S5: ^{1}H 2D correlation (COSY) NMR spectra for 2-(4-amino-2-hydroxybenzoyl)benzoic acid.

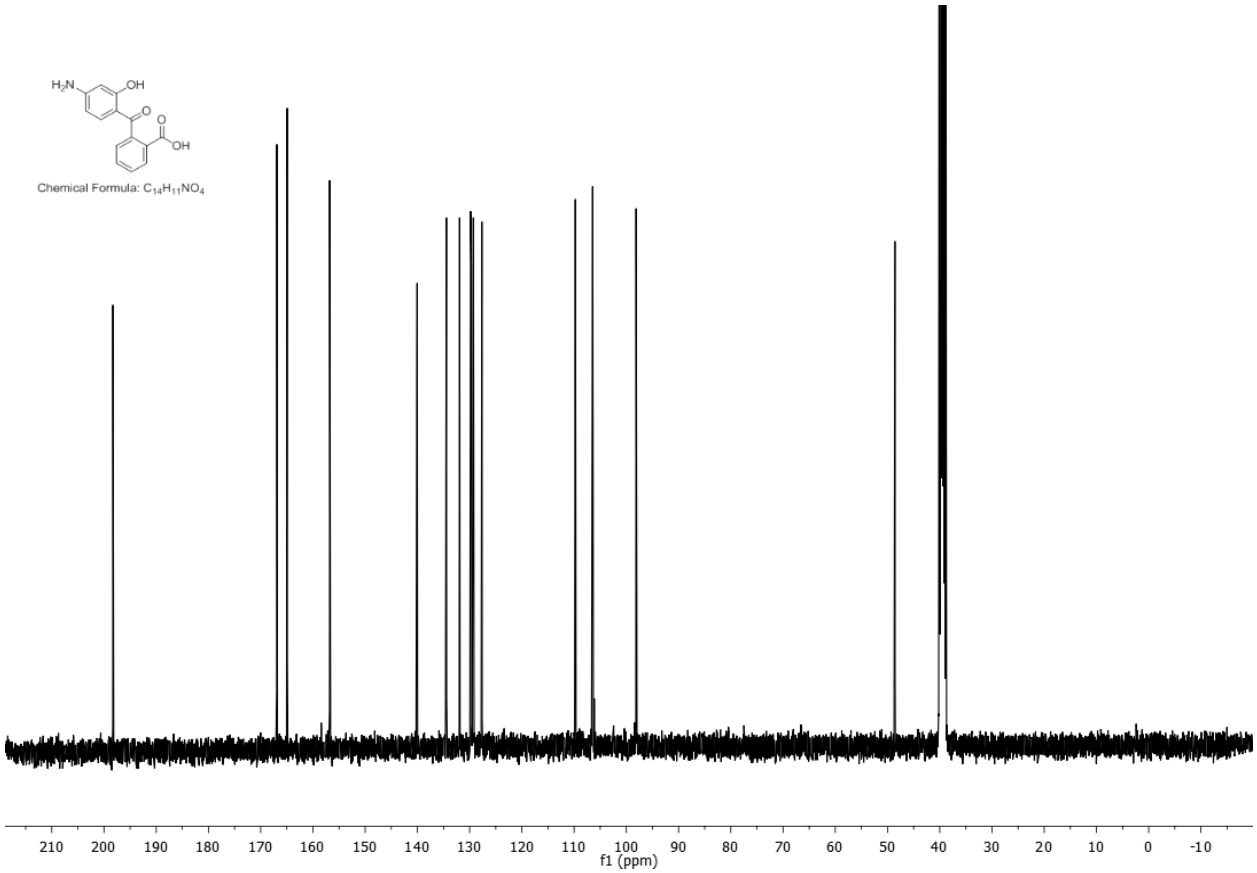

Figure S6: ^{13}C NMR spectrum for 2-(4-amino-2-hydroxybenzoyl)benzoic acid.

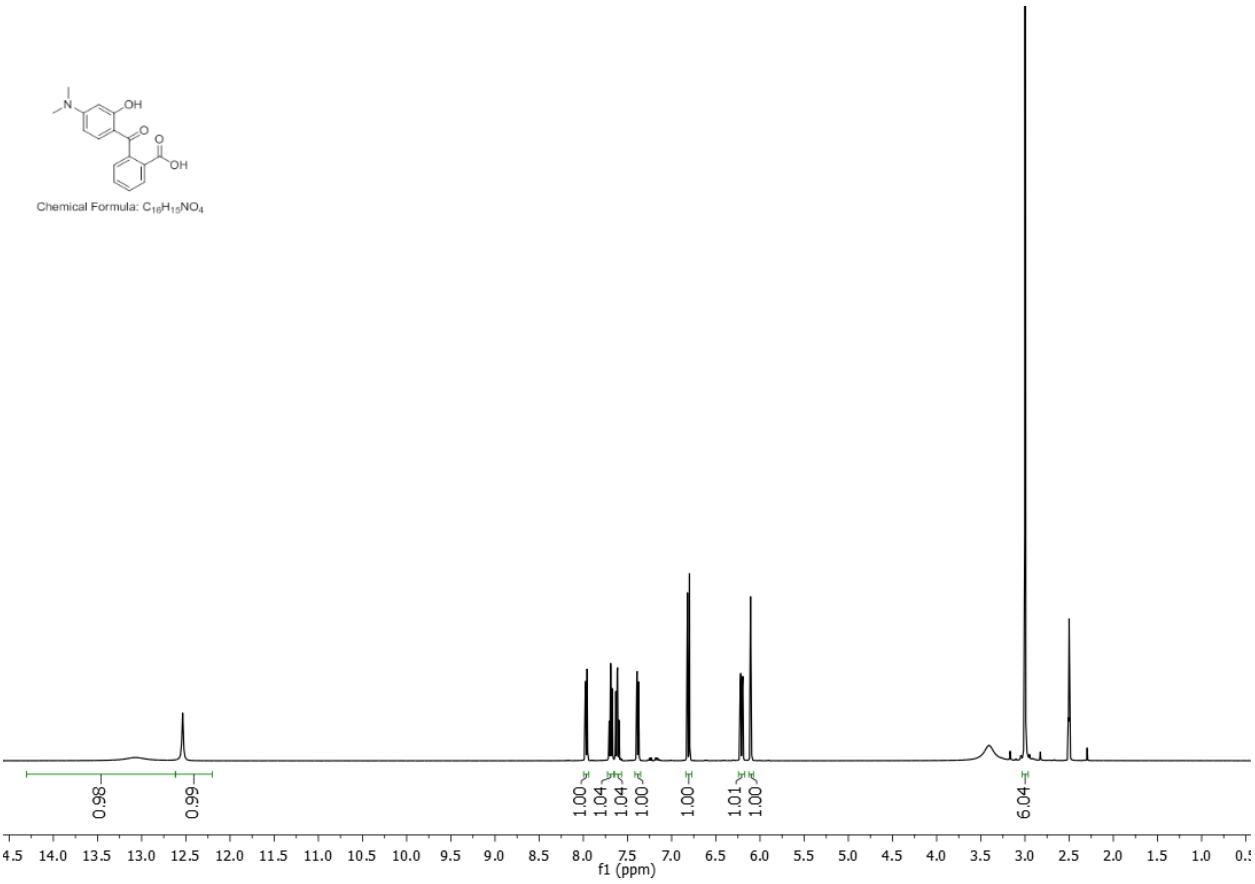

Figure S7: ^{1}H NMR spectrum for 2-(4-(dimethylamino)-2-hydroxybenzoyl)benzoic acid.

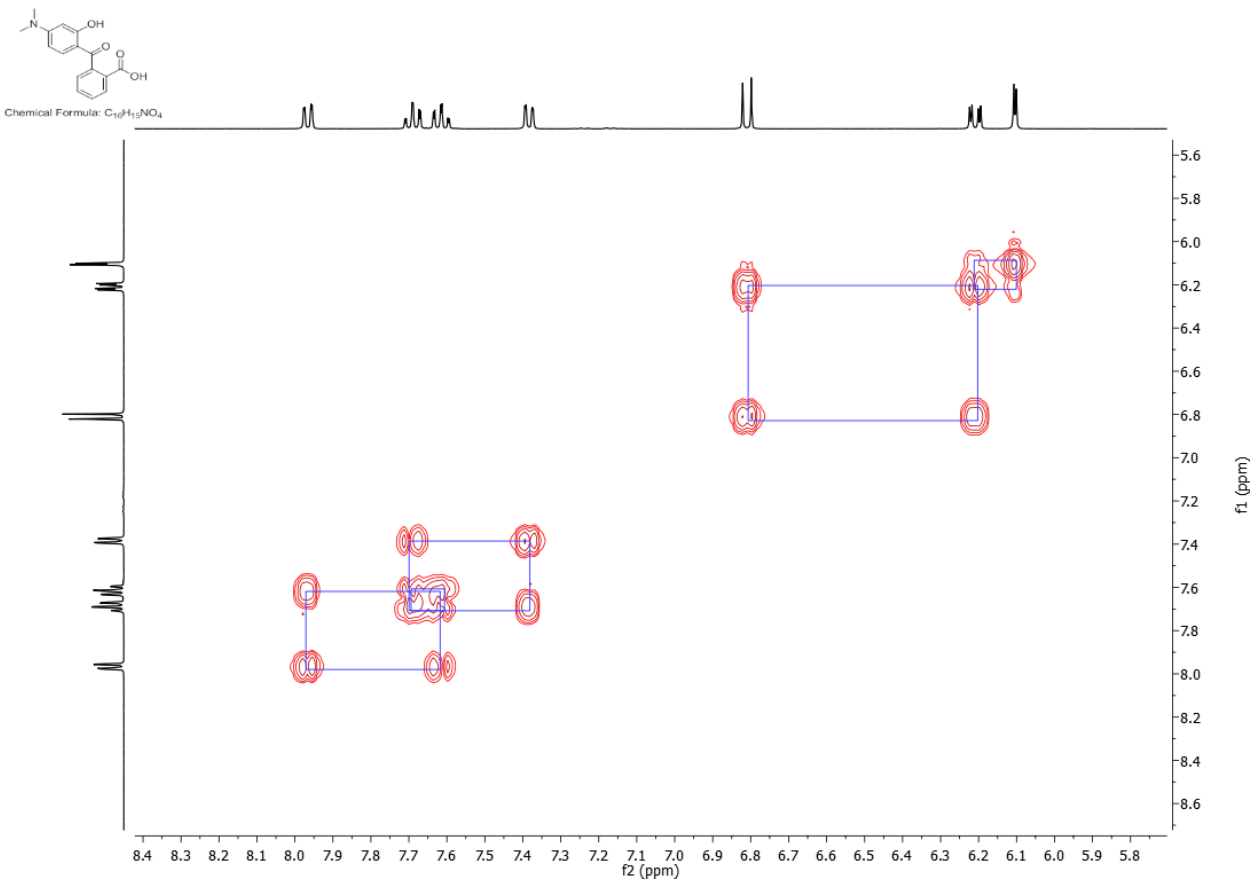

Figure S8: ^{1}H 2D correlation (COSY) NMR spectra for 2-(4-(dimethylamino)-2-hydroxybenzoyl)benzoic acid.

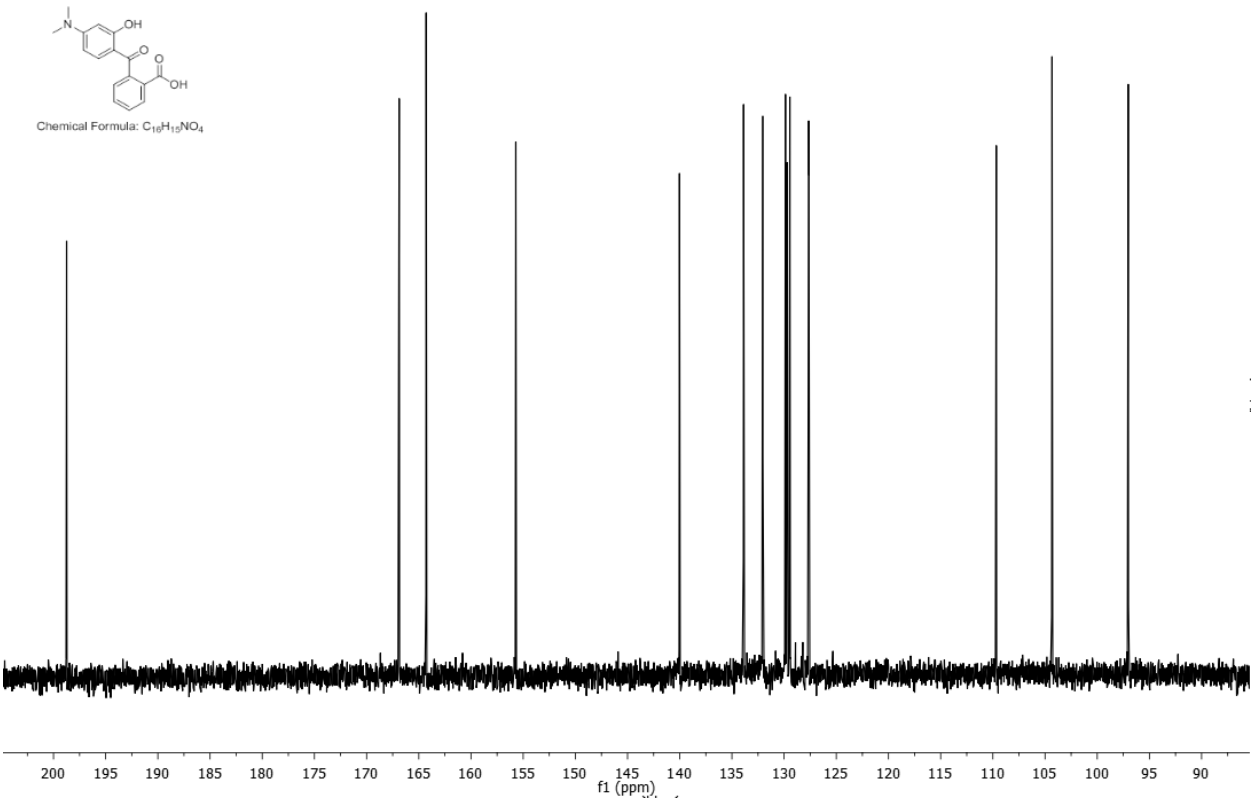

Figure S9: ^{13}C NMR spectrum for 2-(4-(dimethylamino)-2-hydroxybenzoyl)benzoic acid.

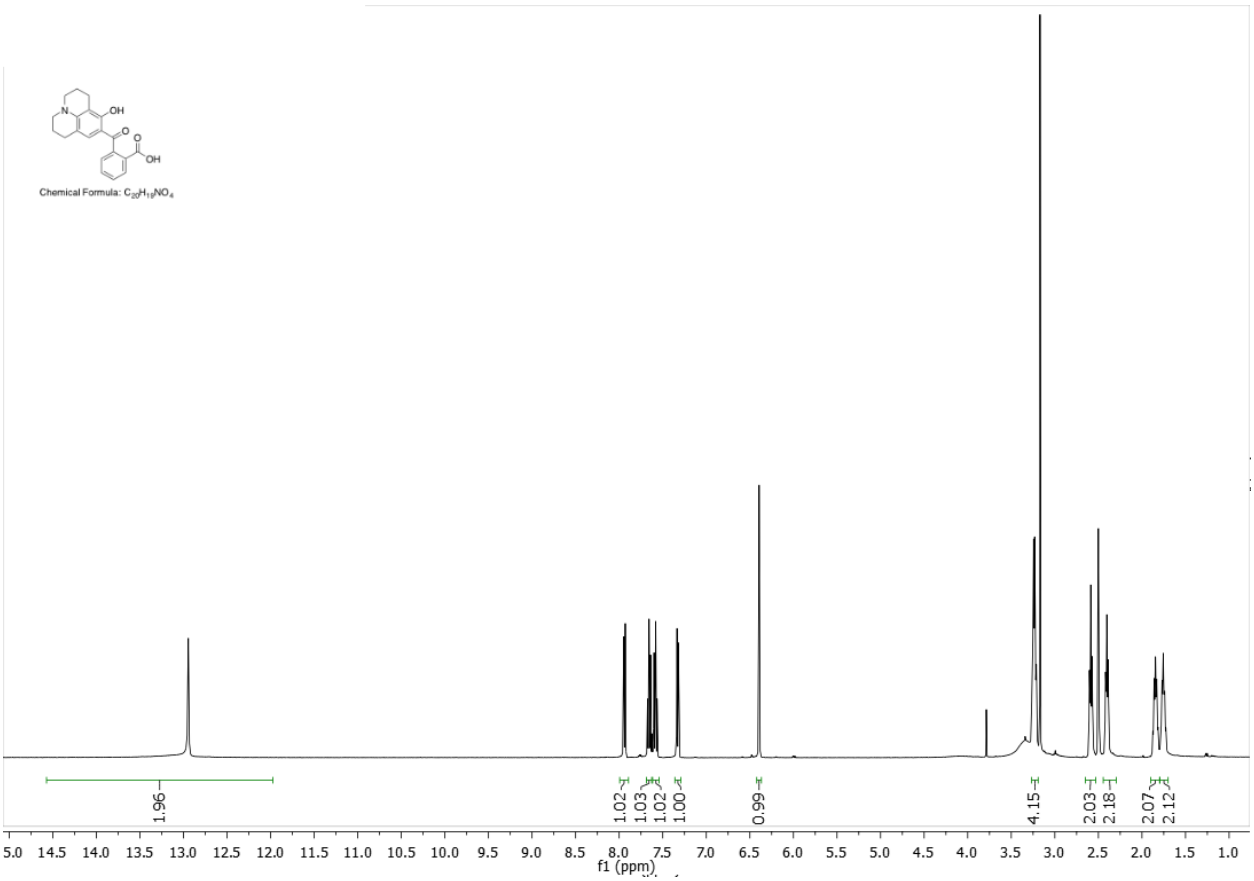

Figure S10: [1]H NMR spectrum for 2-(8-hydroxy-1,2,3,5,6,7-hexahydropyrido[3,2,1-ij]quinoline-9-carbonyl)benzoic acid.

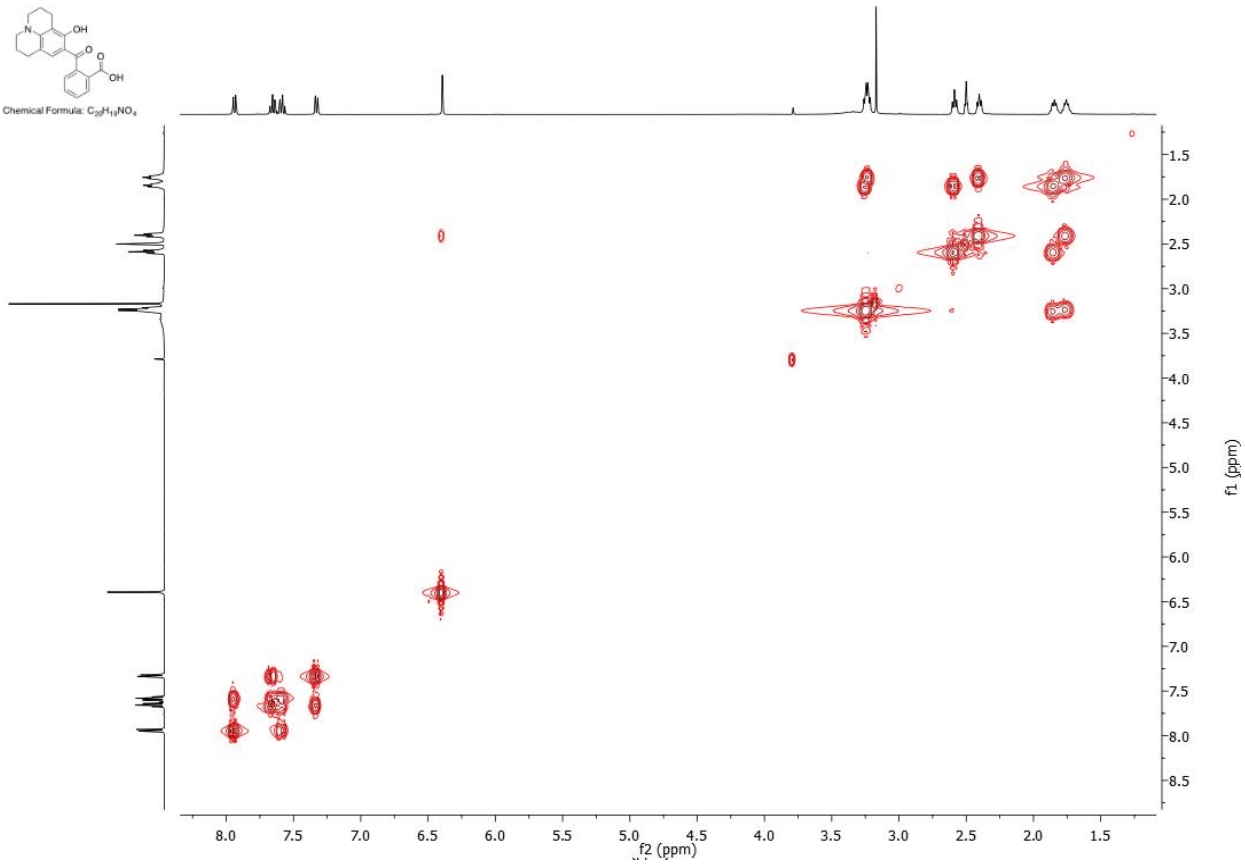

Figure S11: [1]H 2D correlation (COSY) NMR spectra for 2-(8-hydroxy-1,2,3,5,6,7-hexahydropyrido[3,2,1-ij]quinoline-9-carbonyl)benzoic acid.

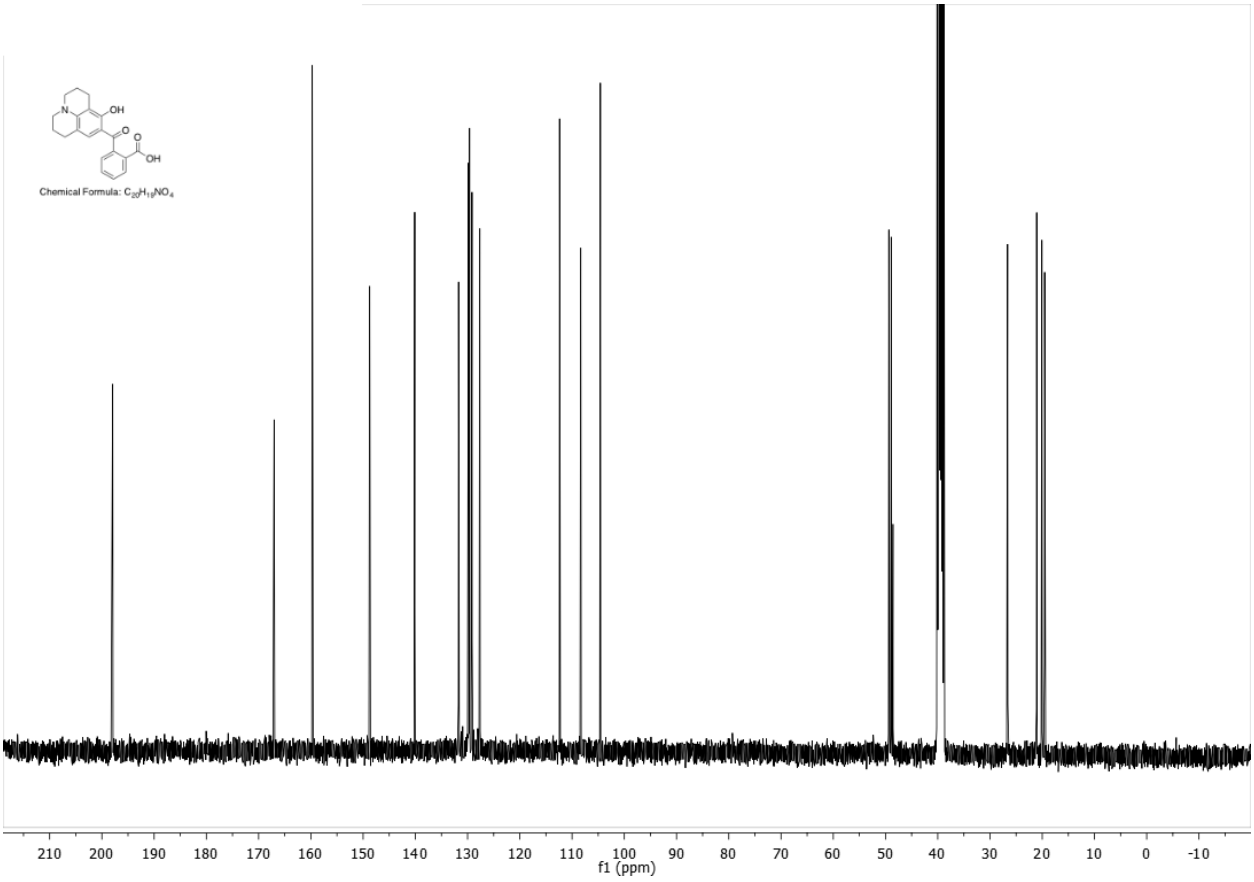

Figure S12: ^{13}C NMR spectrum for 2-(8-hydroxy-1,2,3,5,6,7-hexahydropyrido[3,2,1-ij]quinoline-9-carbonyl)benzoic acid.

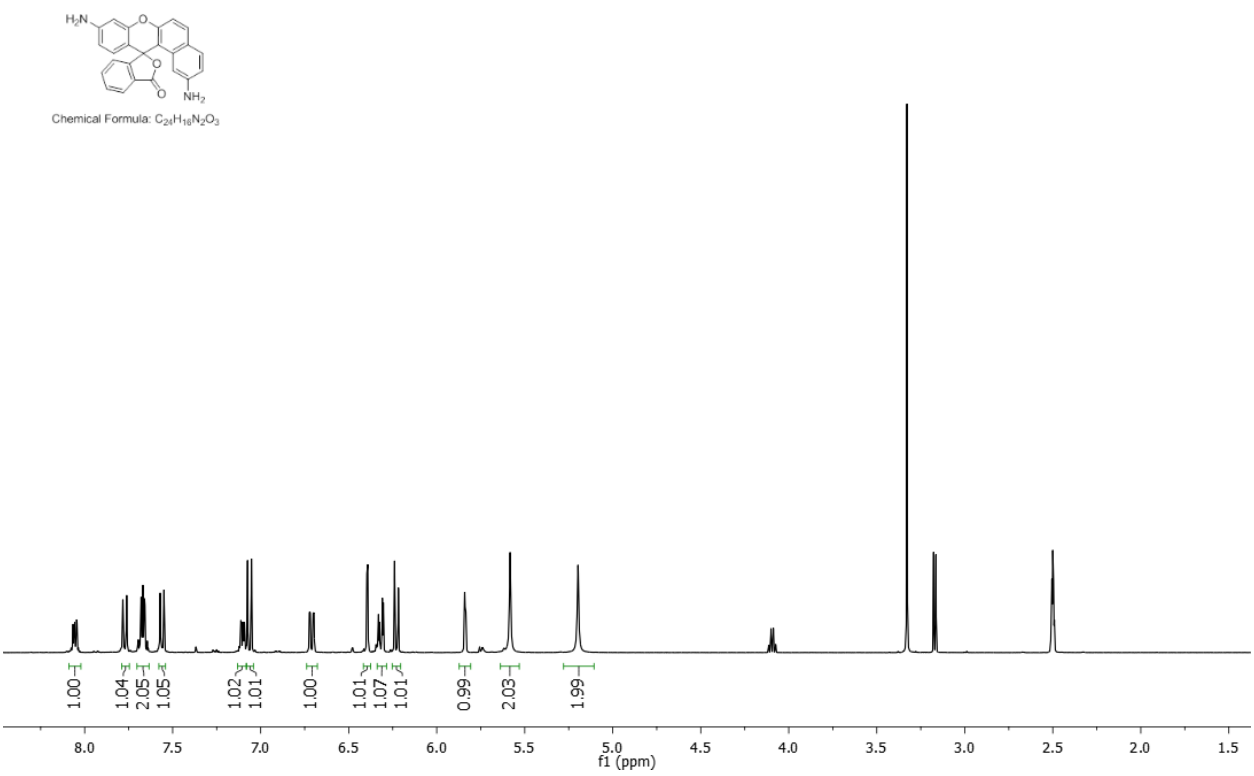

*Figure S13: ^{1}H NMR spectrum for spiro **1**.*

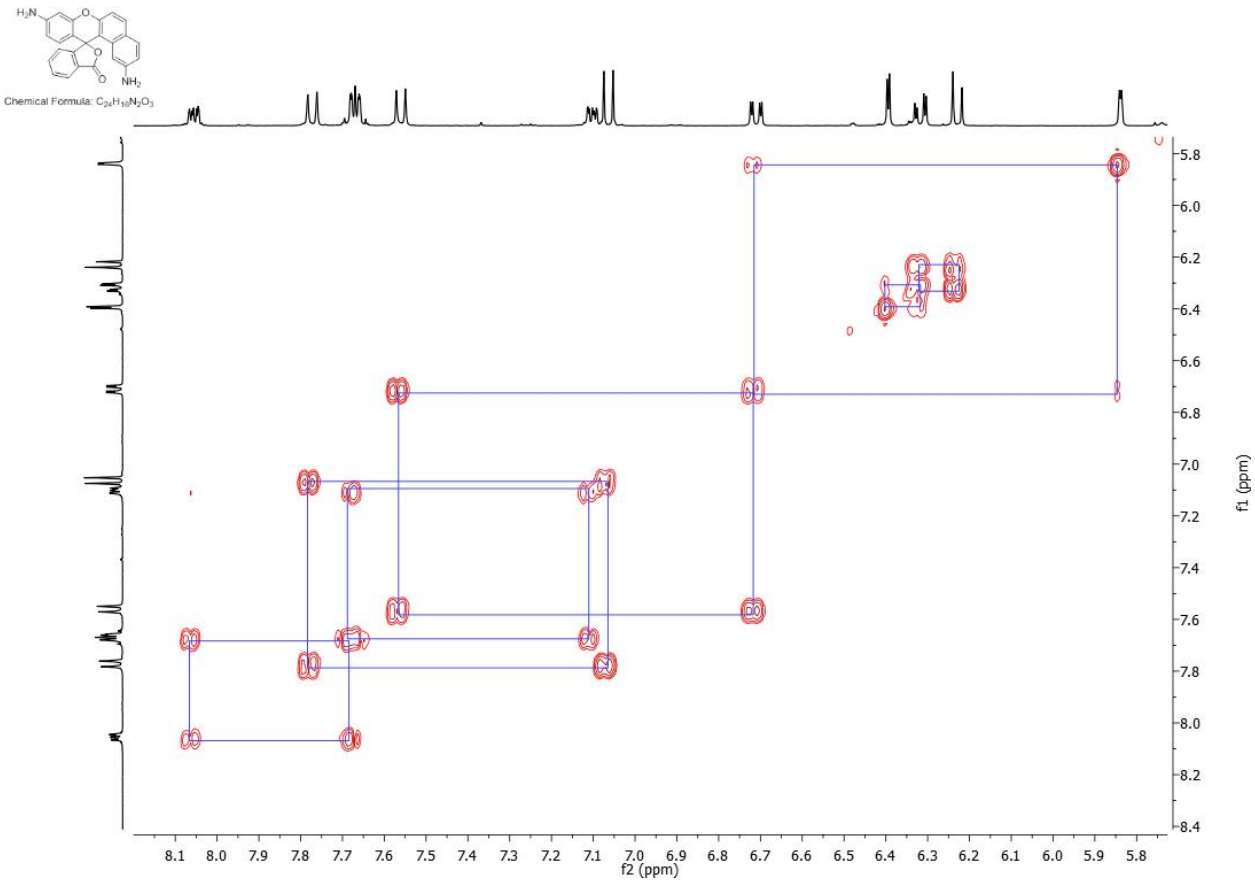

*Figure S14: ^{1}H 2D correlation (COSY) NMR spectra for spiro **1**.*

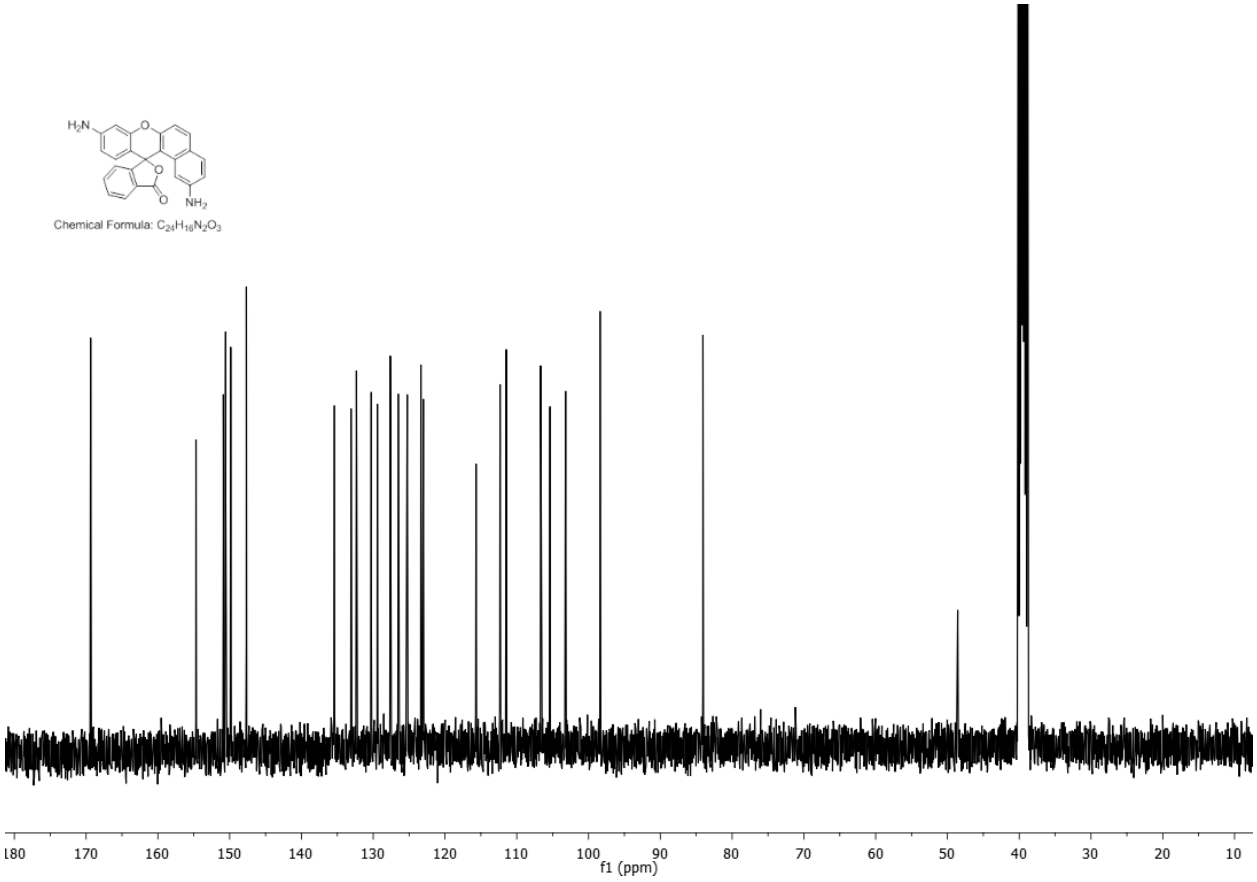

*Figure S15: ^{13}C NMR spectrum for spiro **1**.*

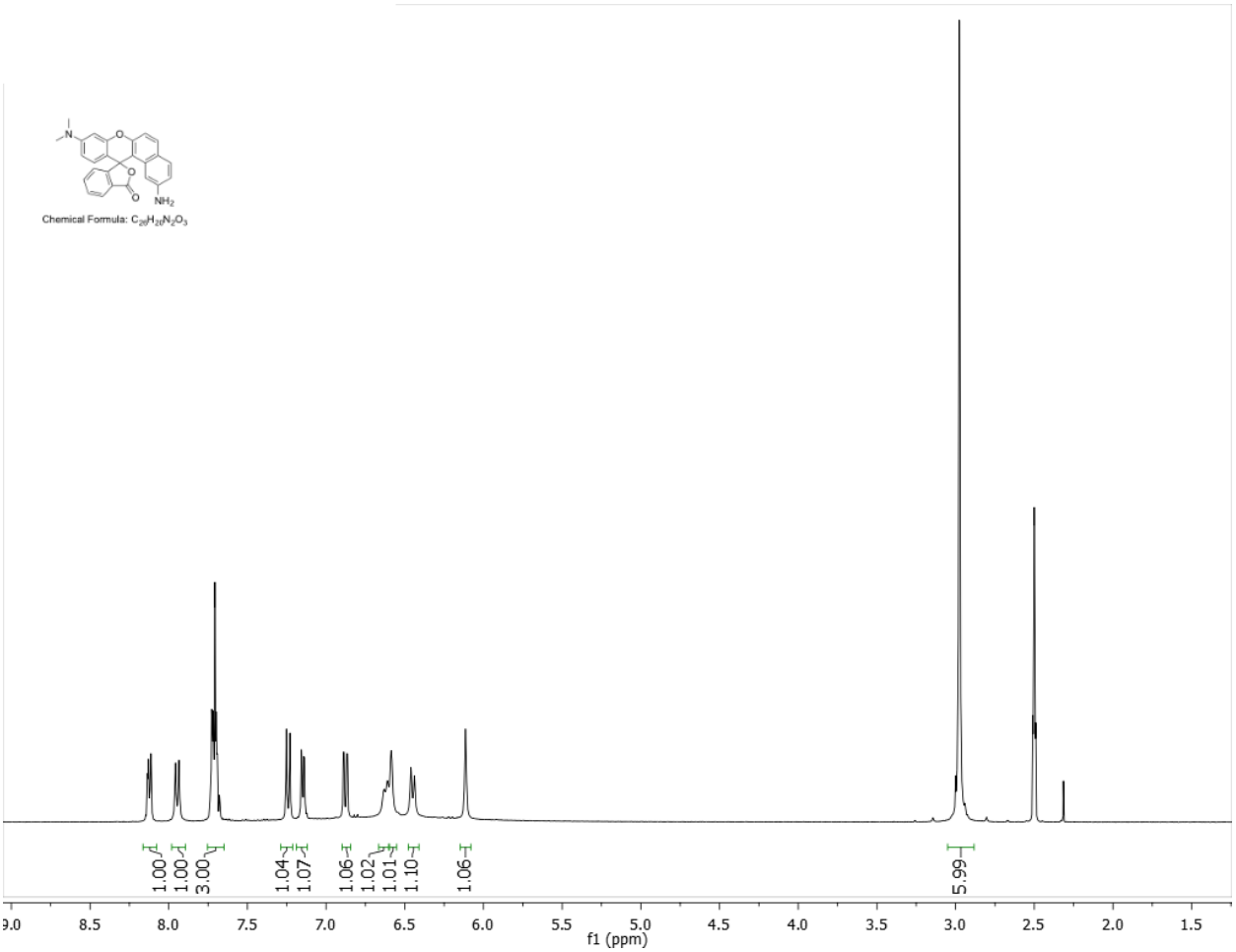

*Figure S16: ^{1}H NMR spectrum for spiro **2**.*

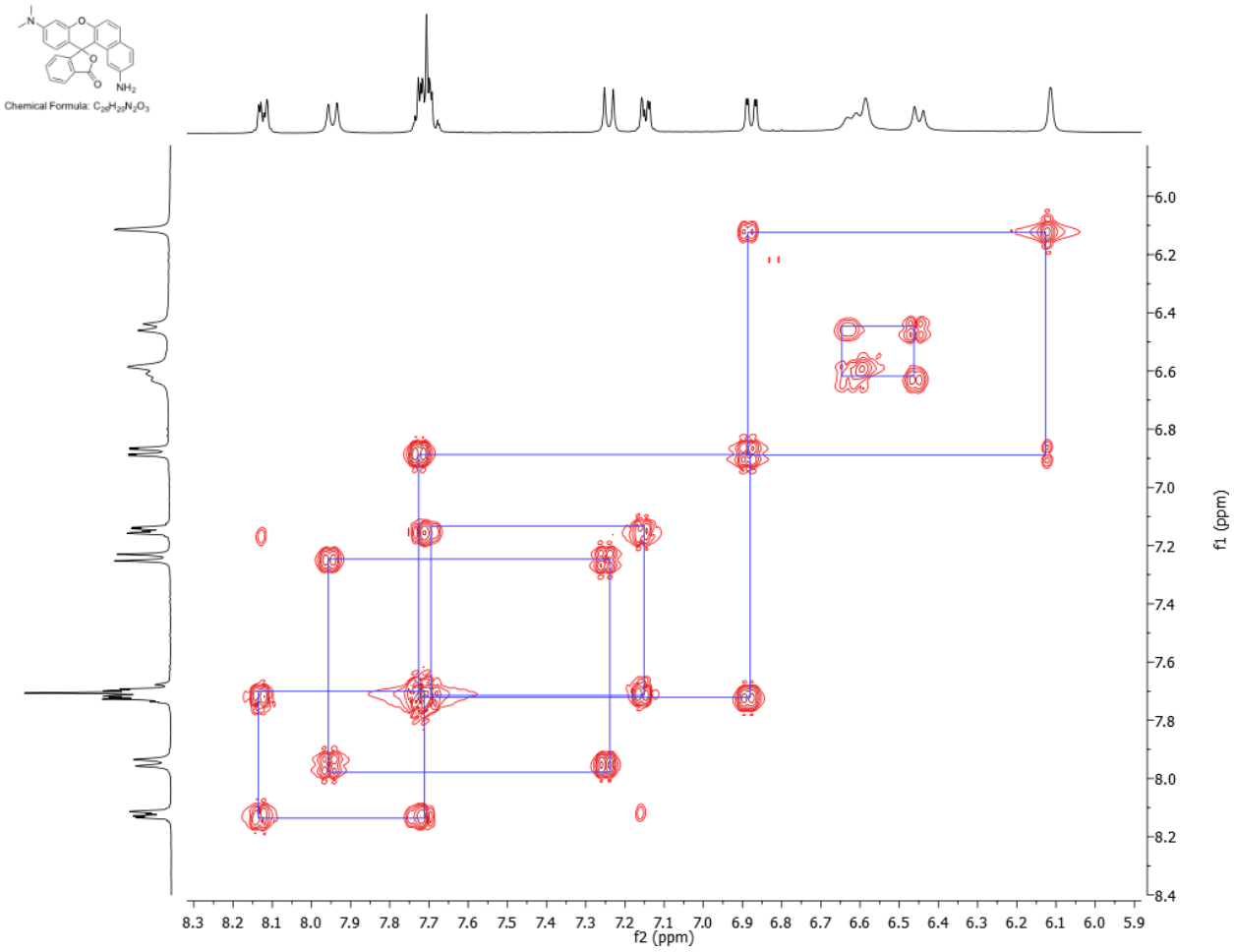

*Figure S17: ^{1}H 2D correlation (COSY) NMR spectra for spiro **2**.*

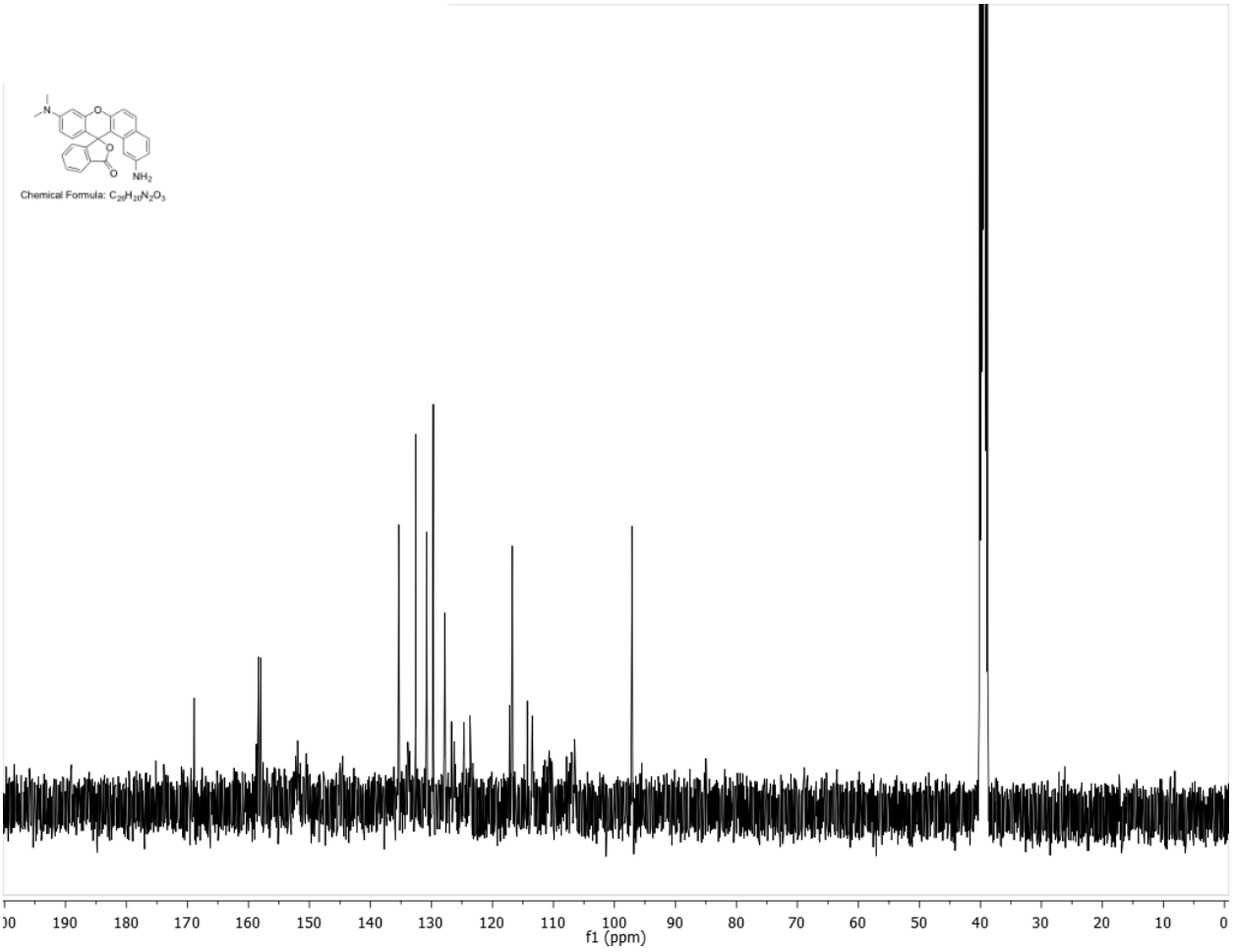

*Figure S18: ^{13}C NMR spectrum for spiro **2**.*

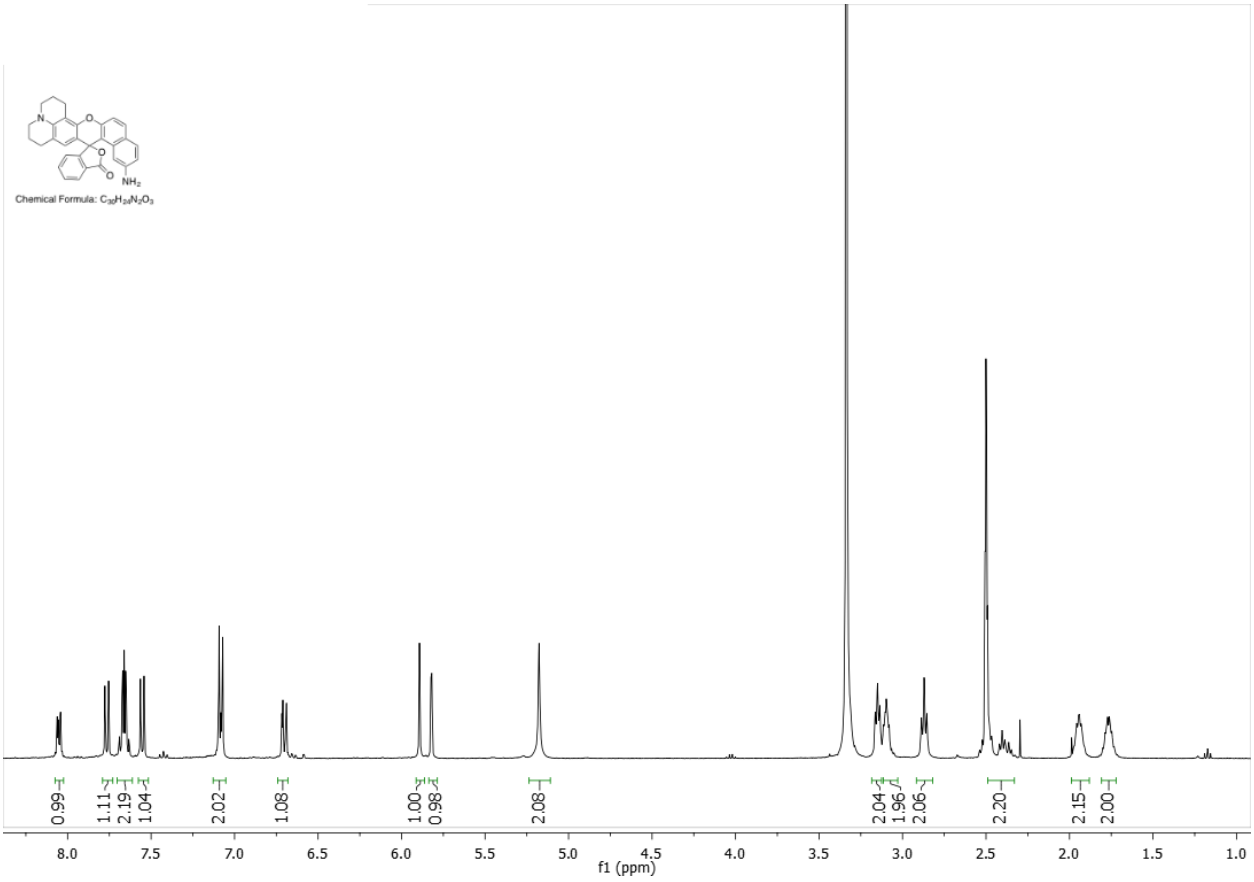

*Figure S19: ^{1}H NMR spectrum for spiro **3**.*

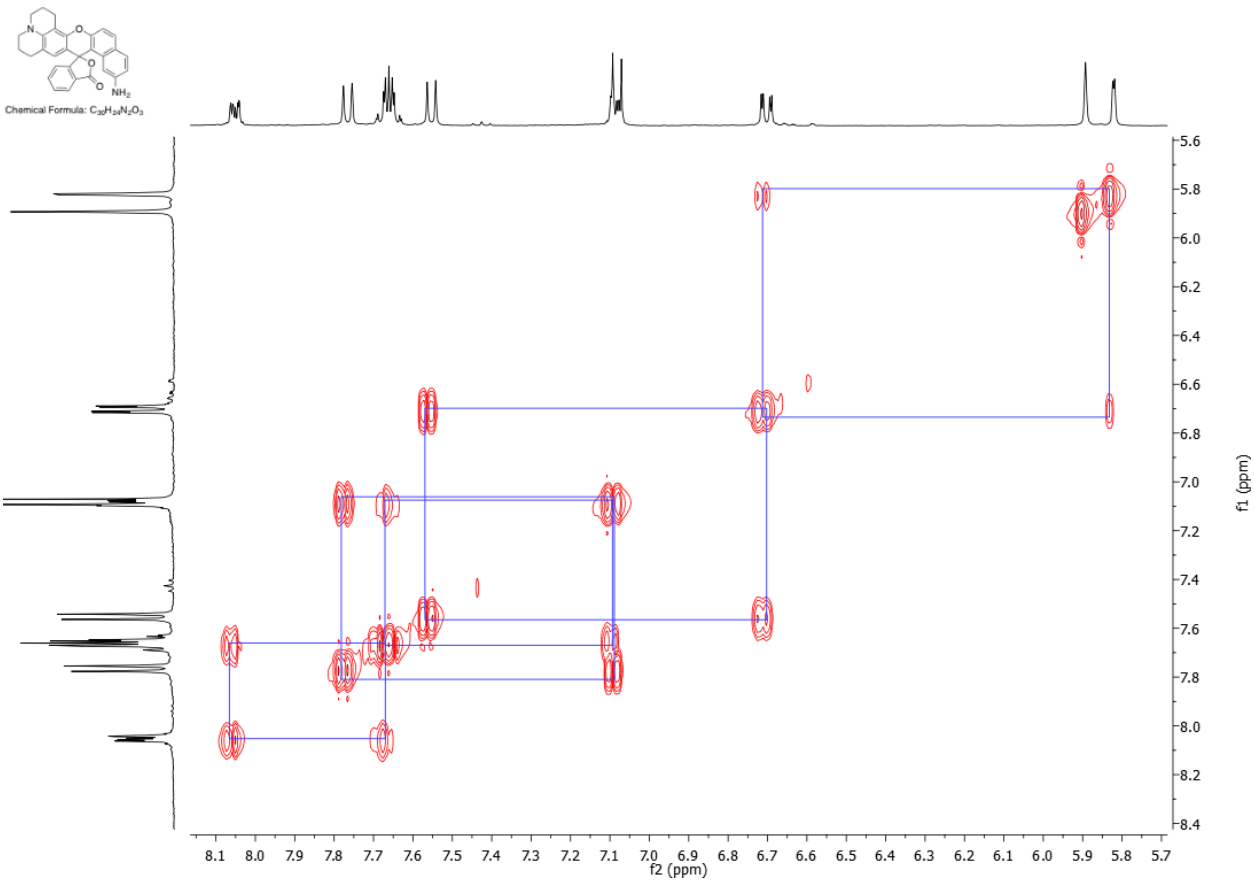

*Figure S20: ^{1}H 2D correlation (COSY) NMR spectra for spiro **3**.*

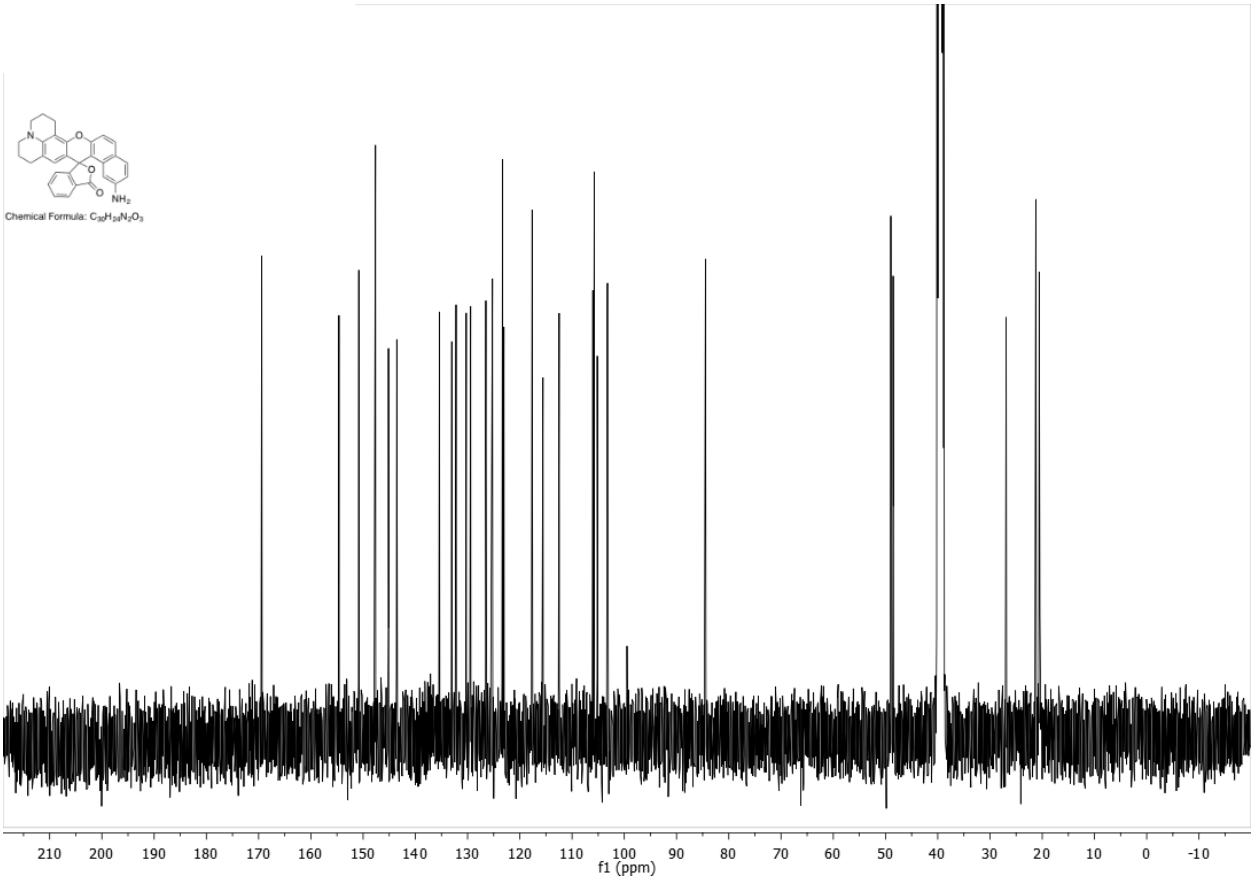

*Figure S21: ^{13}C NMR spectrum for spiro **3**.*

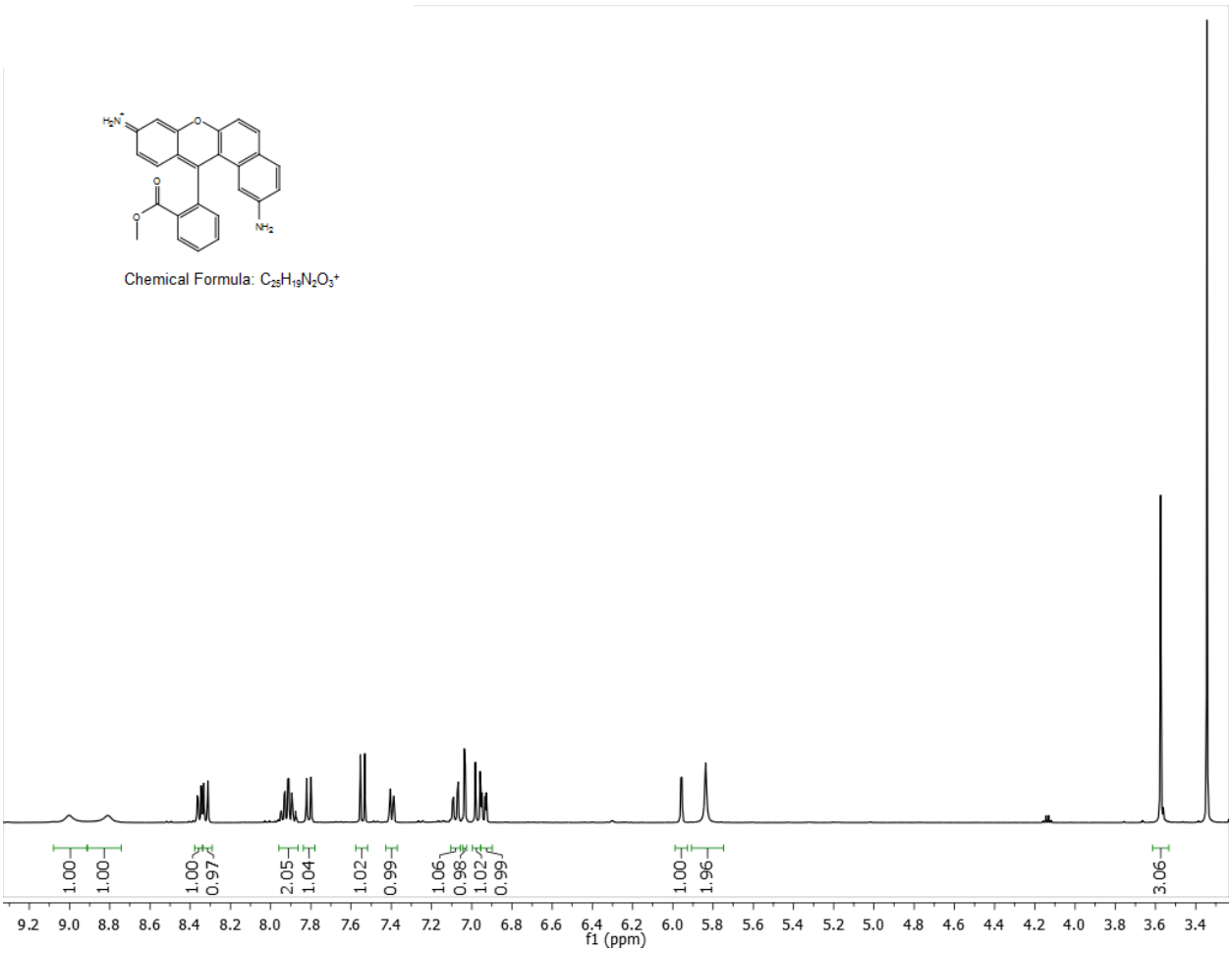

*Figure S22: ^{1}H NMR spectrum for Compound **1**.*

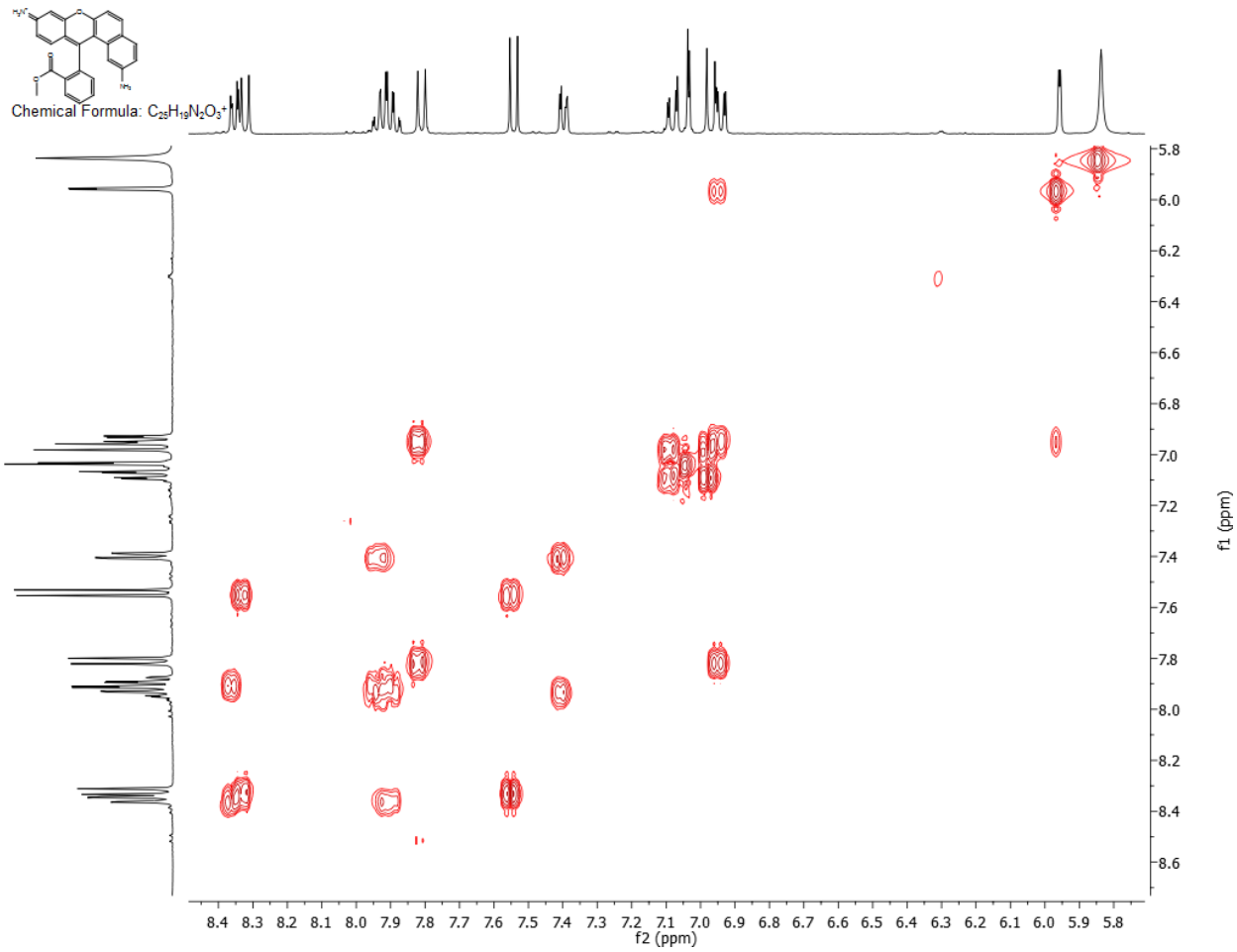

*Figure S23: ^{1}H 2D correlation (COSY) NMR spectra for Compound **1**.*

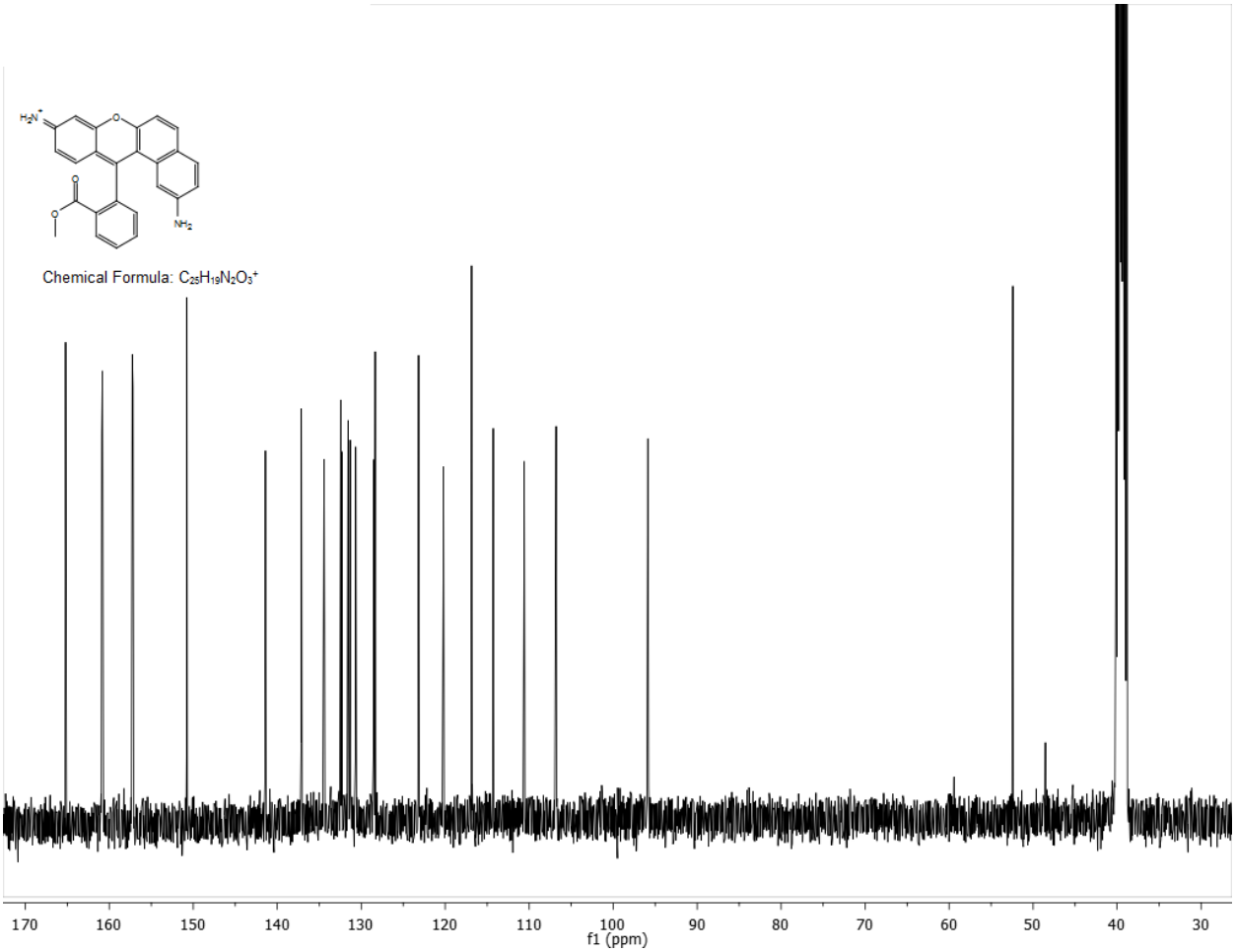

*Figure S24: ^{13}C NMR spectrum for Compound **1**.*

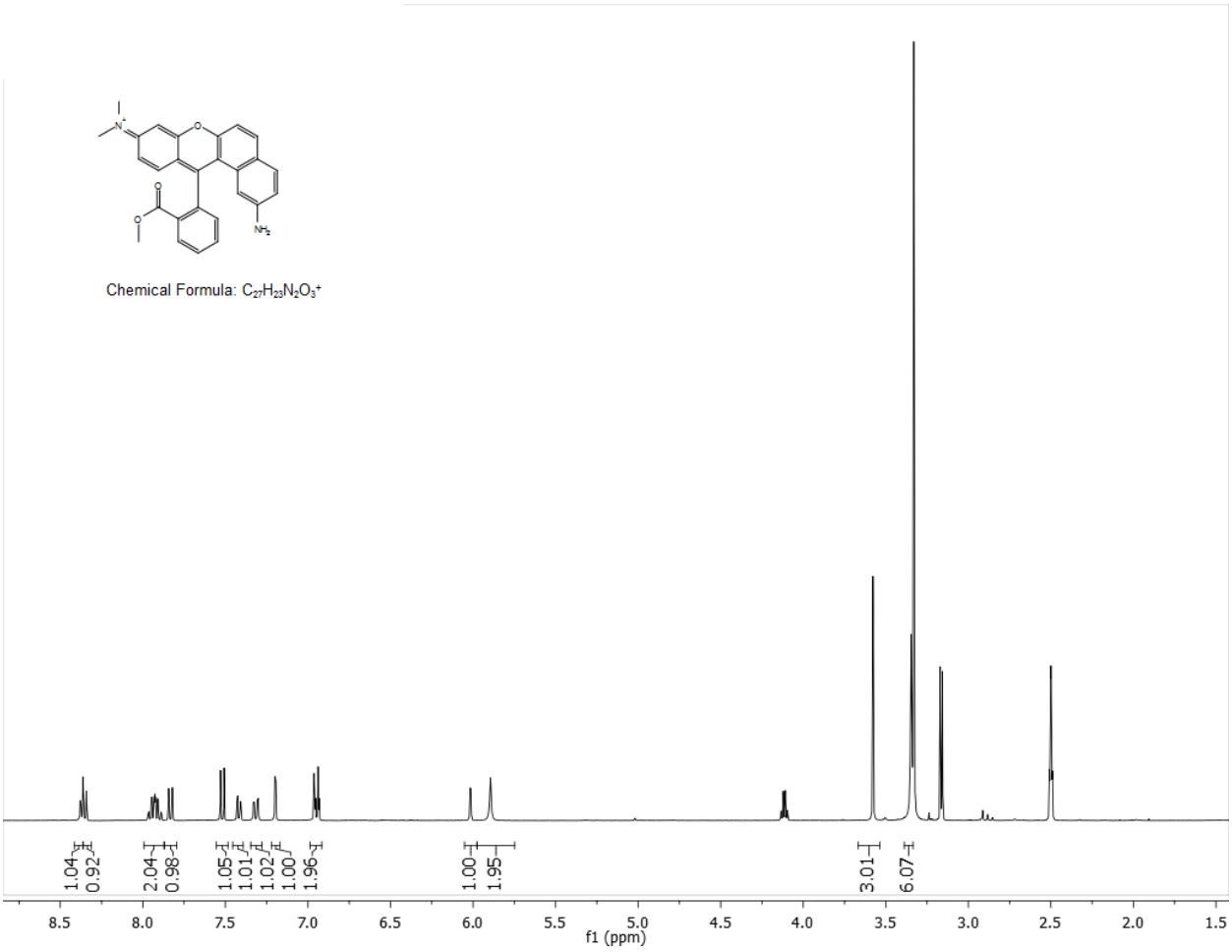

*Figure S25: ^{1}H NMR spectrum for Compound **2**.*

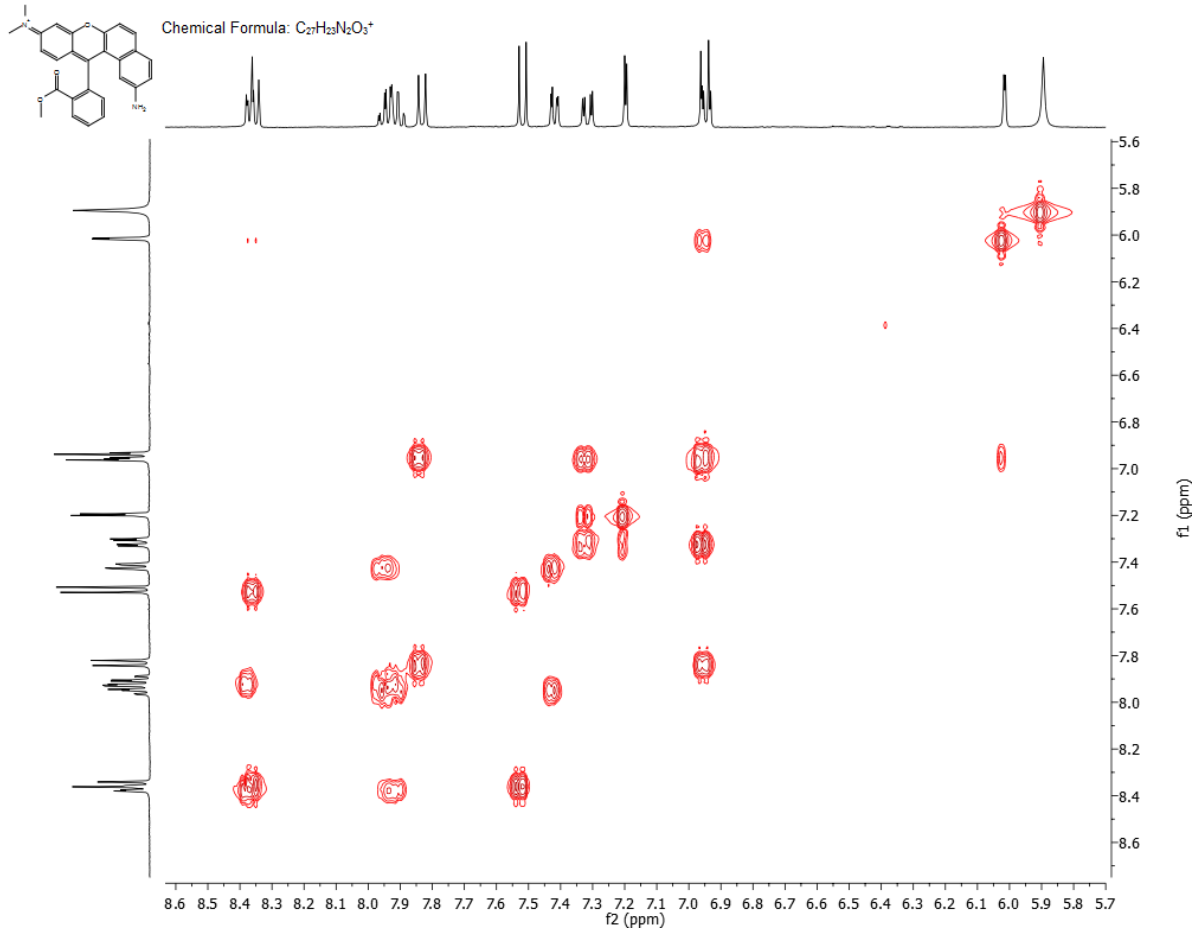

*Figure S26: ^{1}H 2D correlation (COSY) NMR spectra for Compound **2**.*

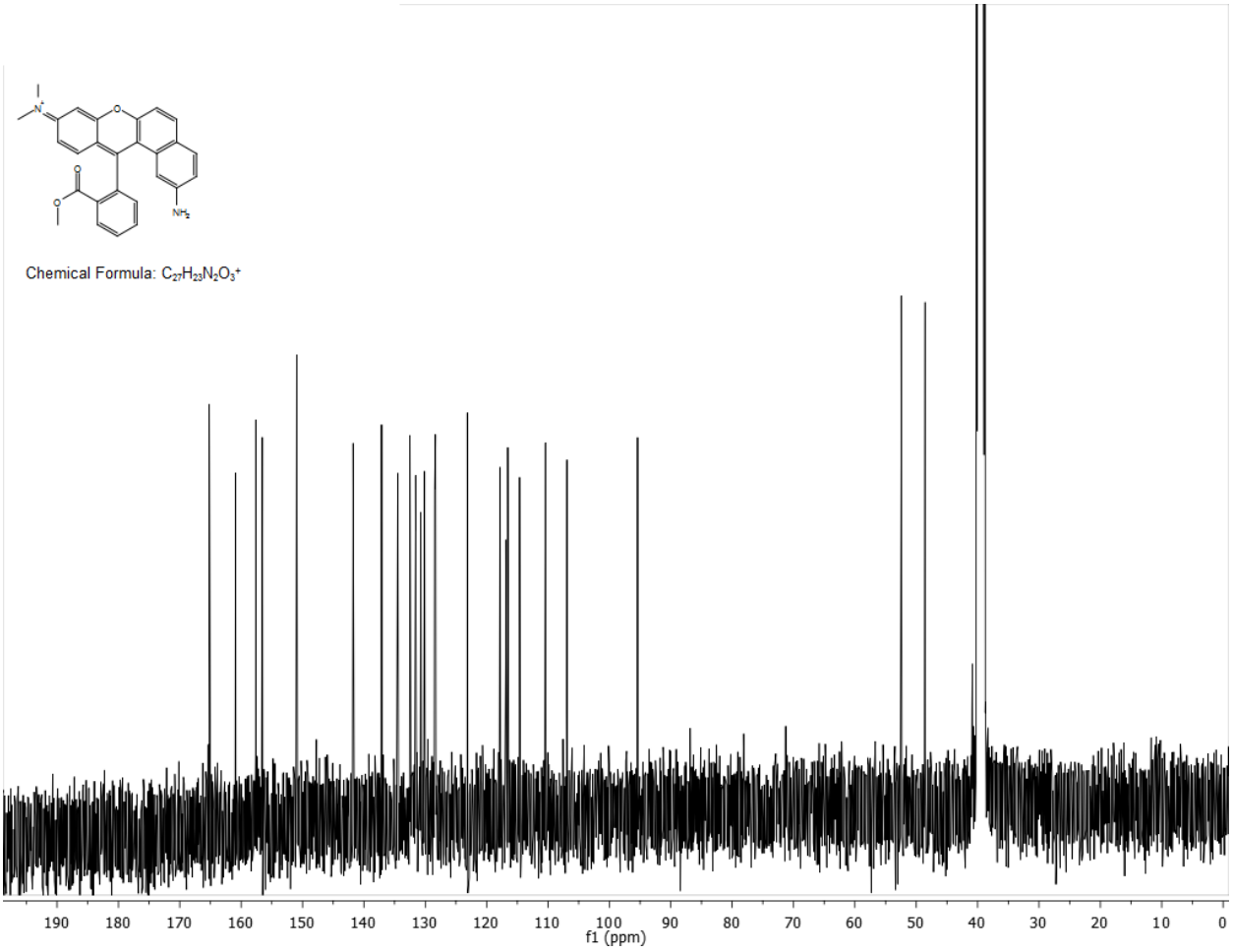

*Figure S27: ^{13}C NMR spectrum for Compound **2**.*

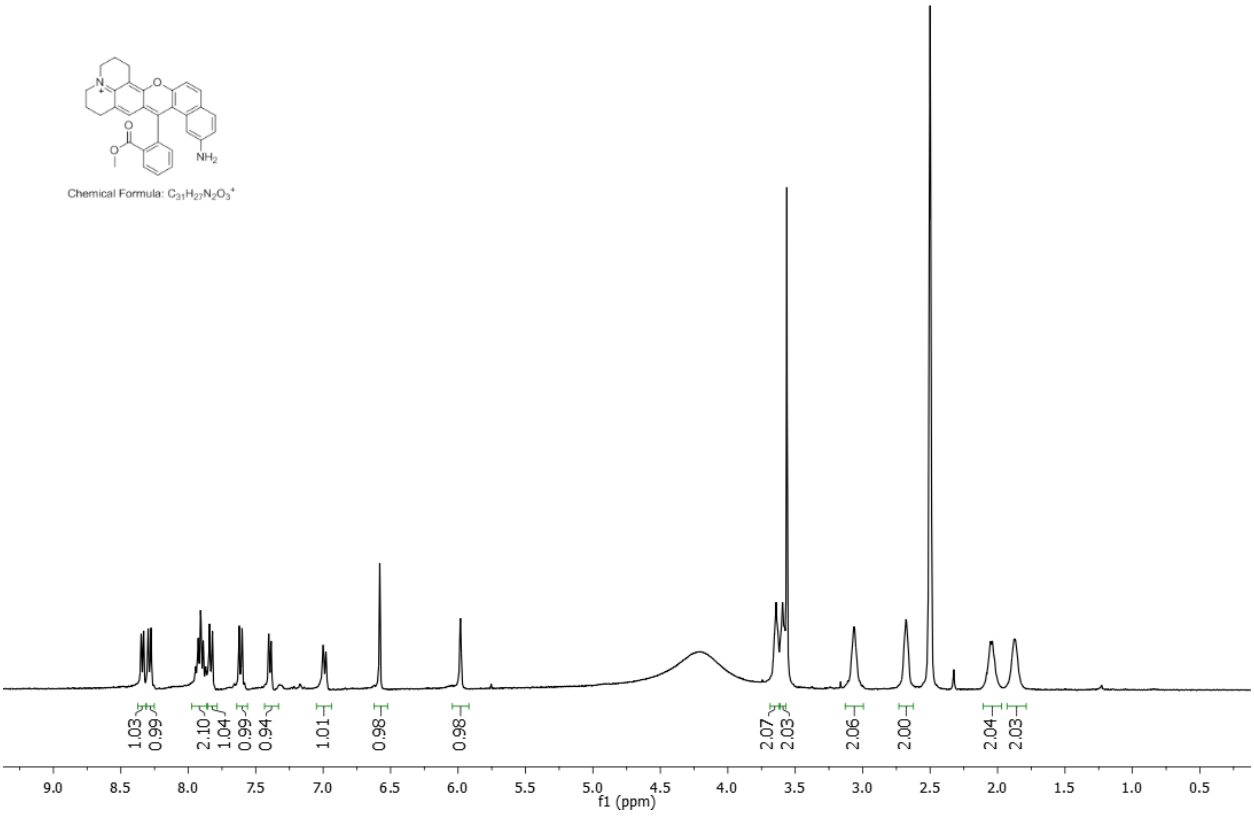

*Figure S28: ^{1}H NMR spectrum for Compound **3**.*

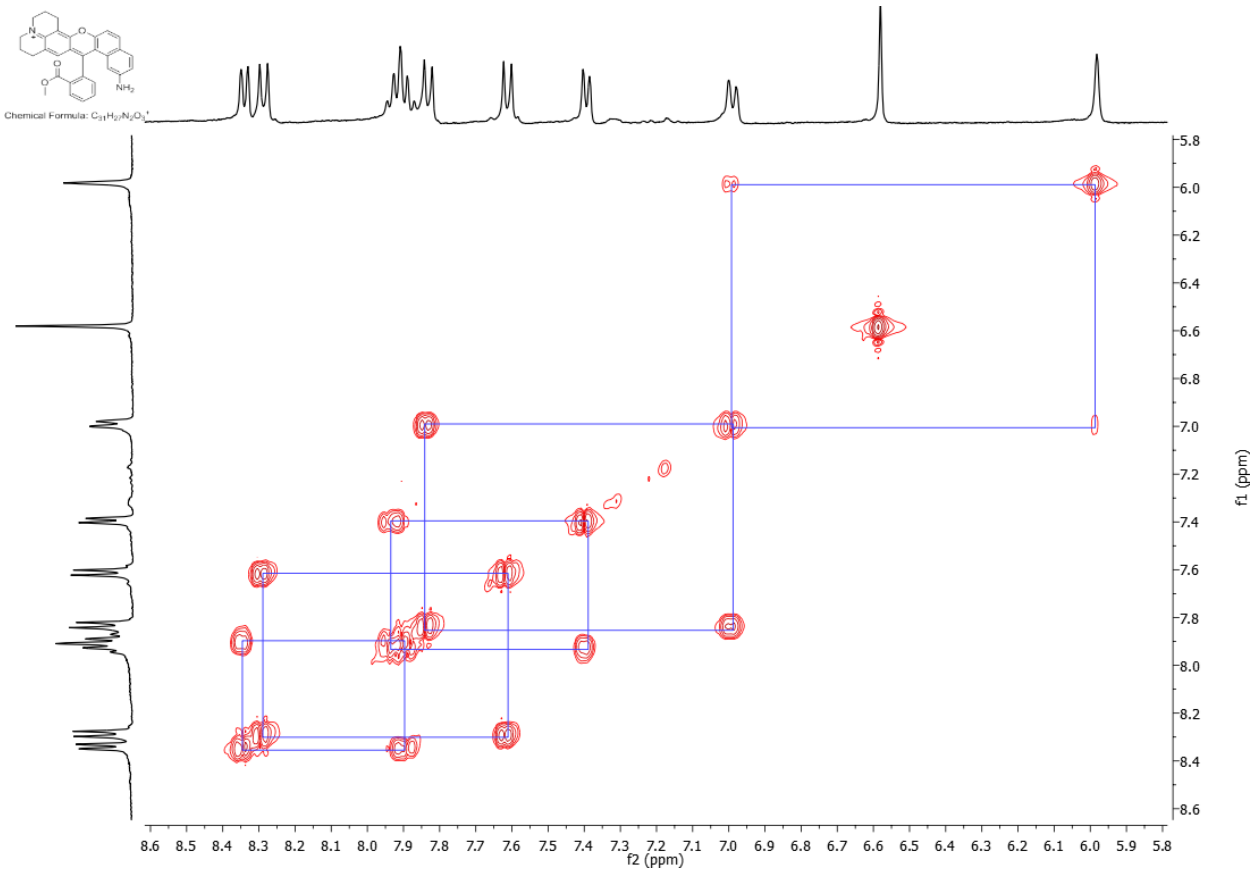

*Figure S29: ^{1}H 2D correlation (COSY) NMR spectra for Compound **3**.*

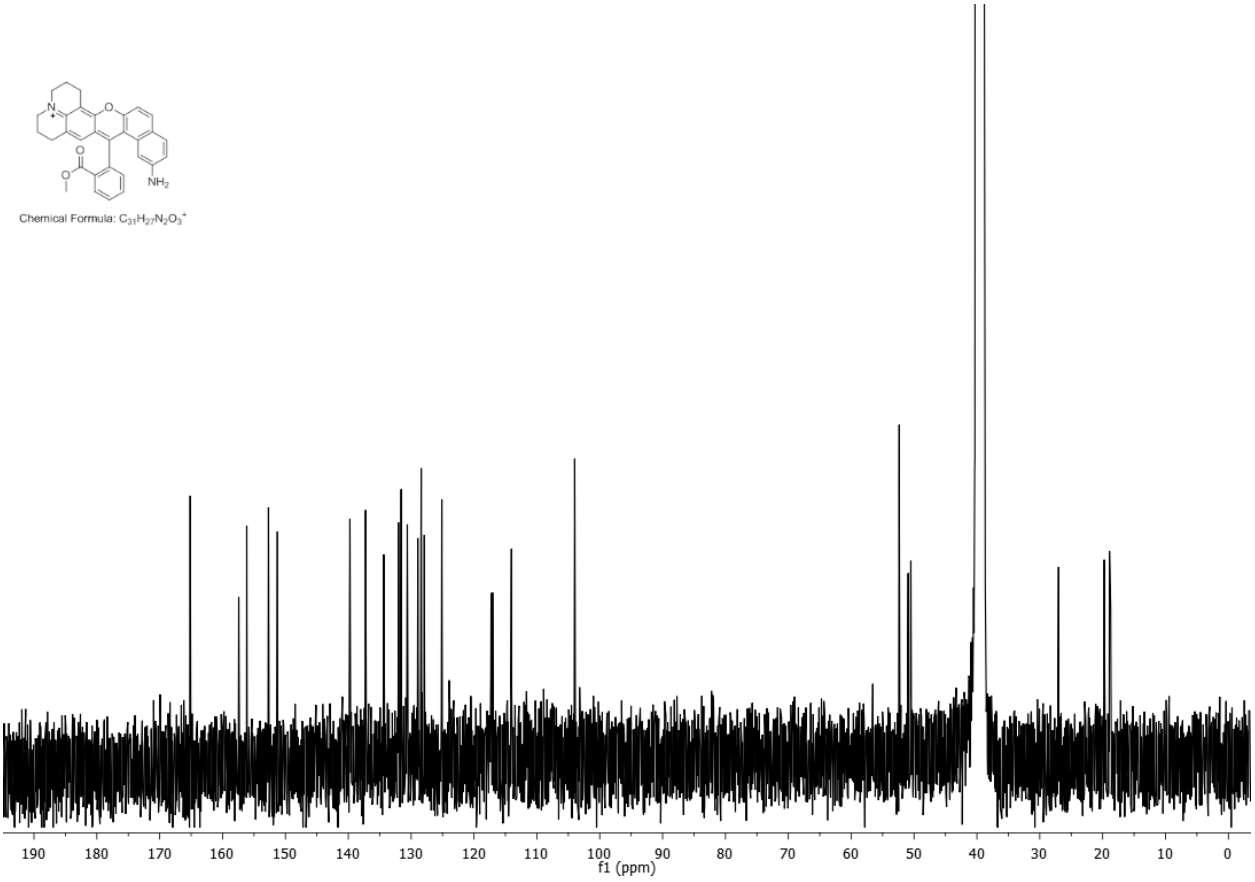

*Figure S30: ^{13}C NMR spectrum for Compound **3**.*

Mass Spectra

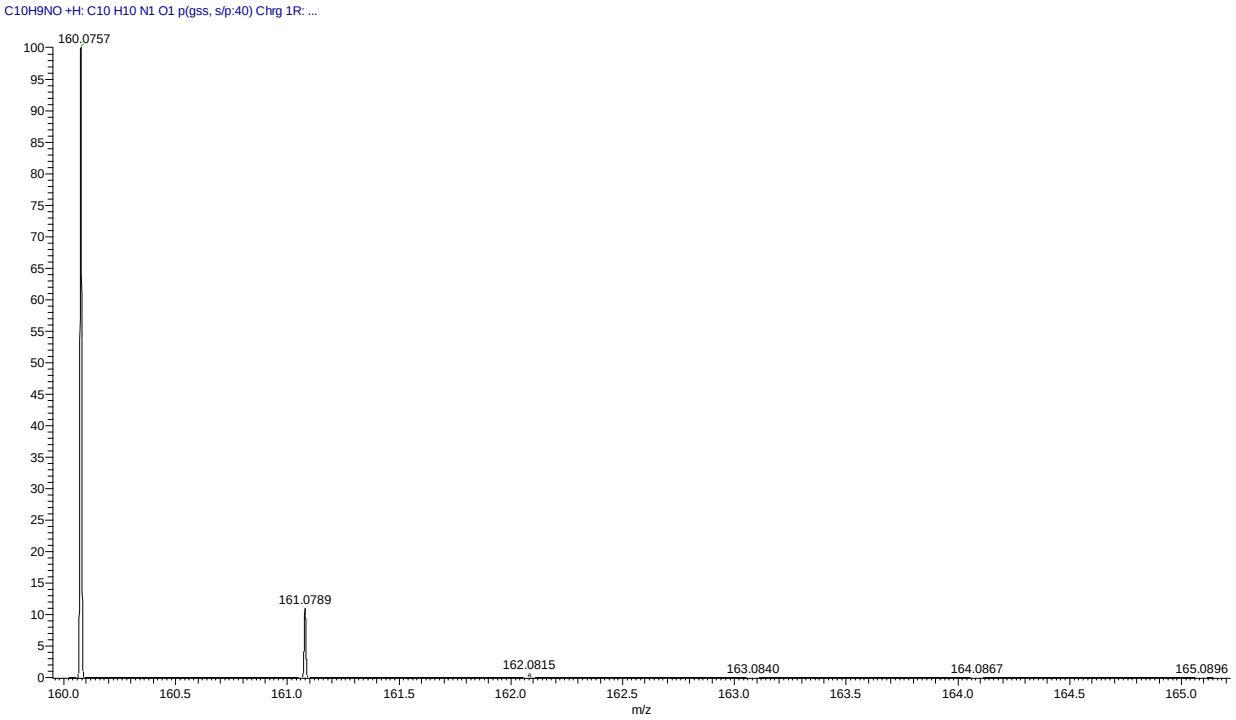

Figure S31: Calculated mass spectrum $(M+H)^+$ for 7-amino-2-naphthol.

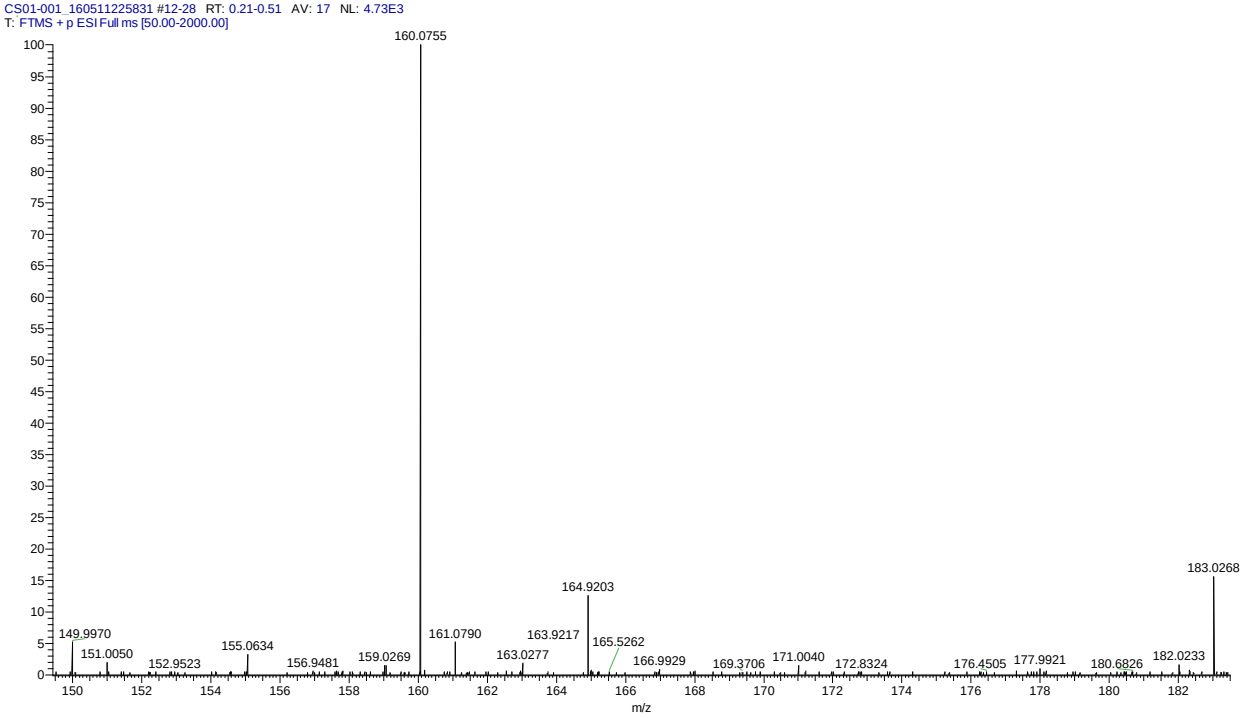

Figure S32: Measured mass spectrum $(M+H)^+$ for 7-amino-2-naphthol.

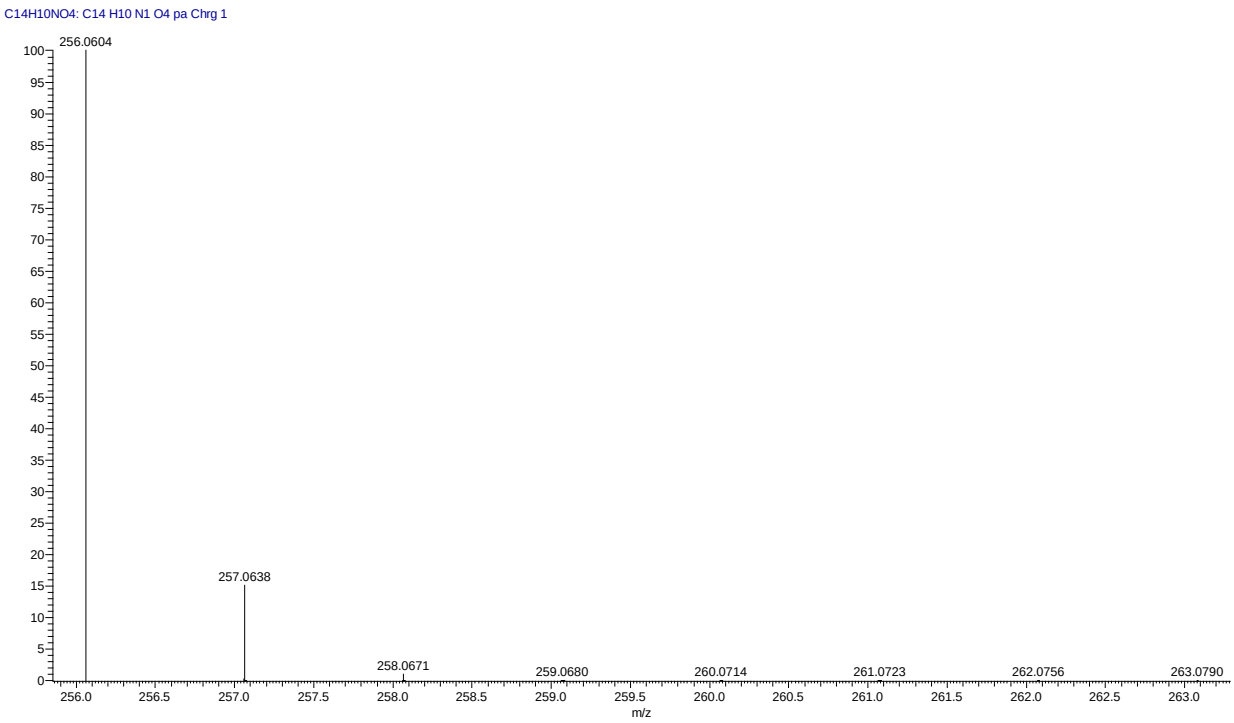

Figure S33: Calculated mass spectrum $(M+H)^+$ for 2-(4-amino-2-hydroxybenzoyl)benzoic acid.

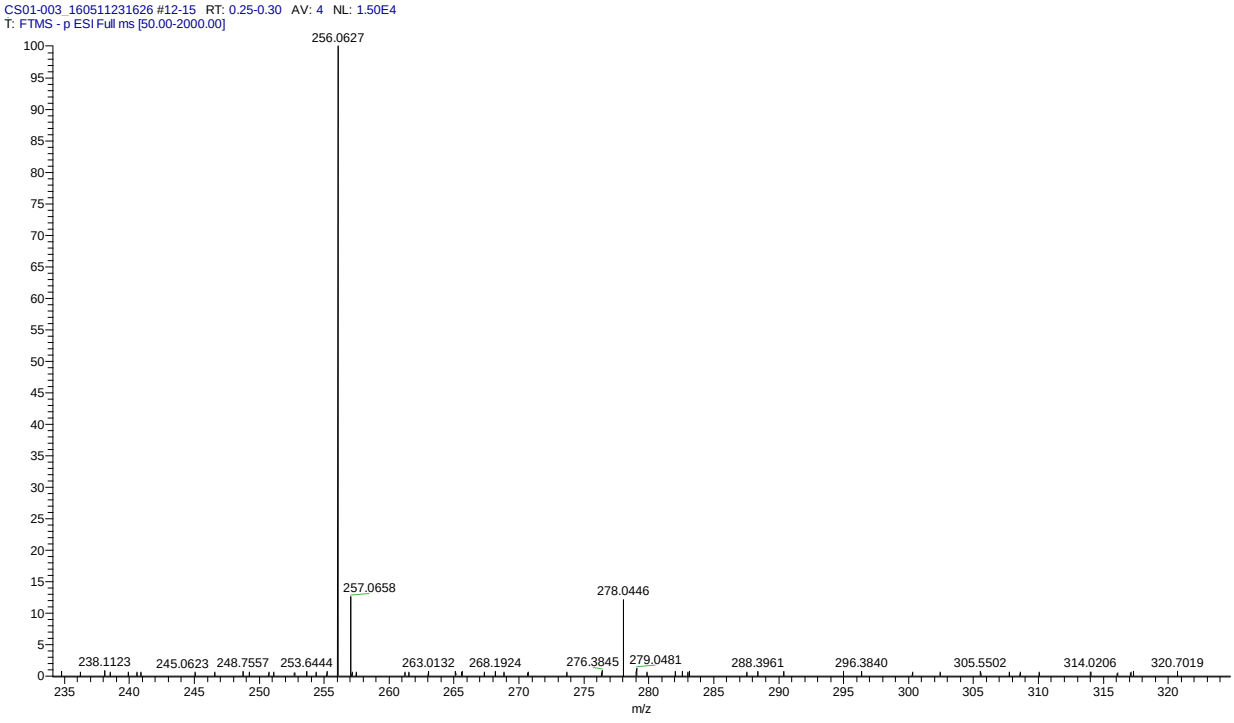

Figure S34: Measured mass spectrum $(M+H)^+$ for 2-(4-amino-2-hydroxybenzoyl)benzoic acid.

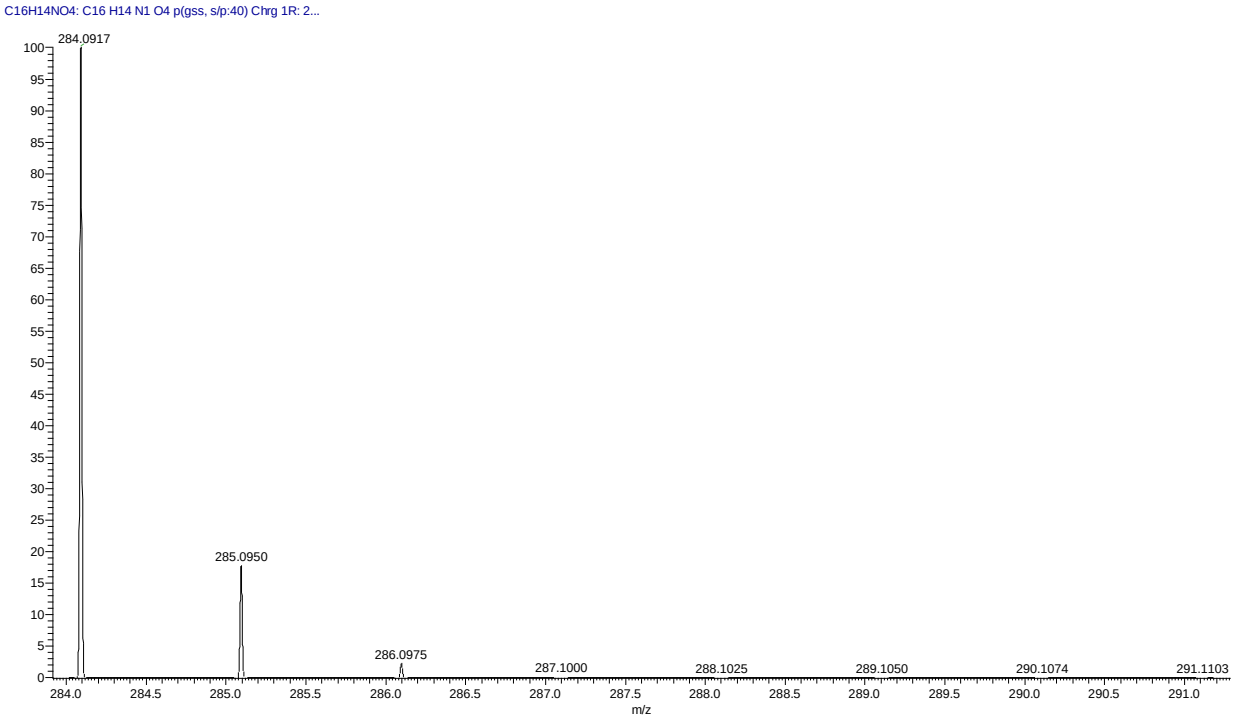

Figure S35: Calculated mass spectrum $(M+H)^-$ for 2-(4-(dimethylamino)-2-hydroxybenzoyl)benzoic acid.

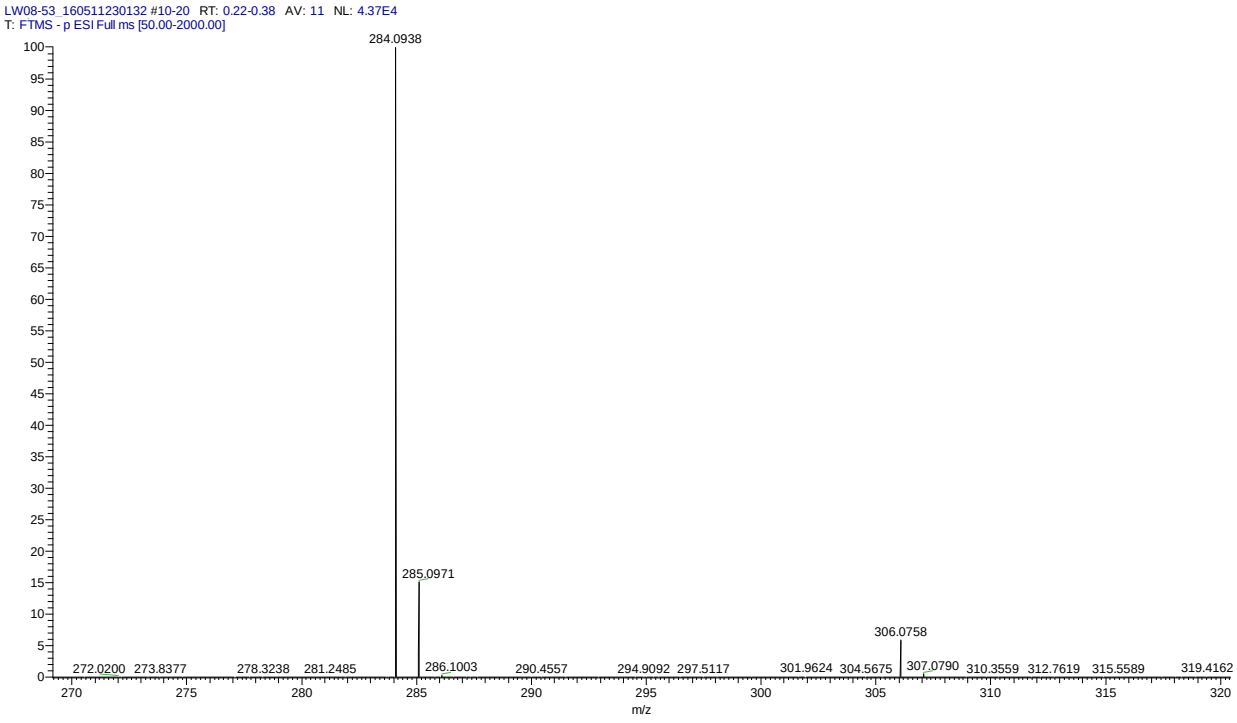

Figure S36: Measured mass spectrum $(M+H)^-$ for 2-(4-(dimethylamino)-2-hydroxybenzoyl)benzoic acid.

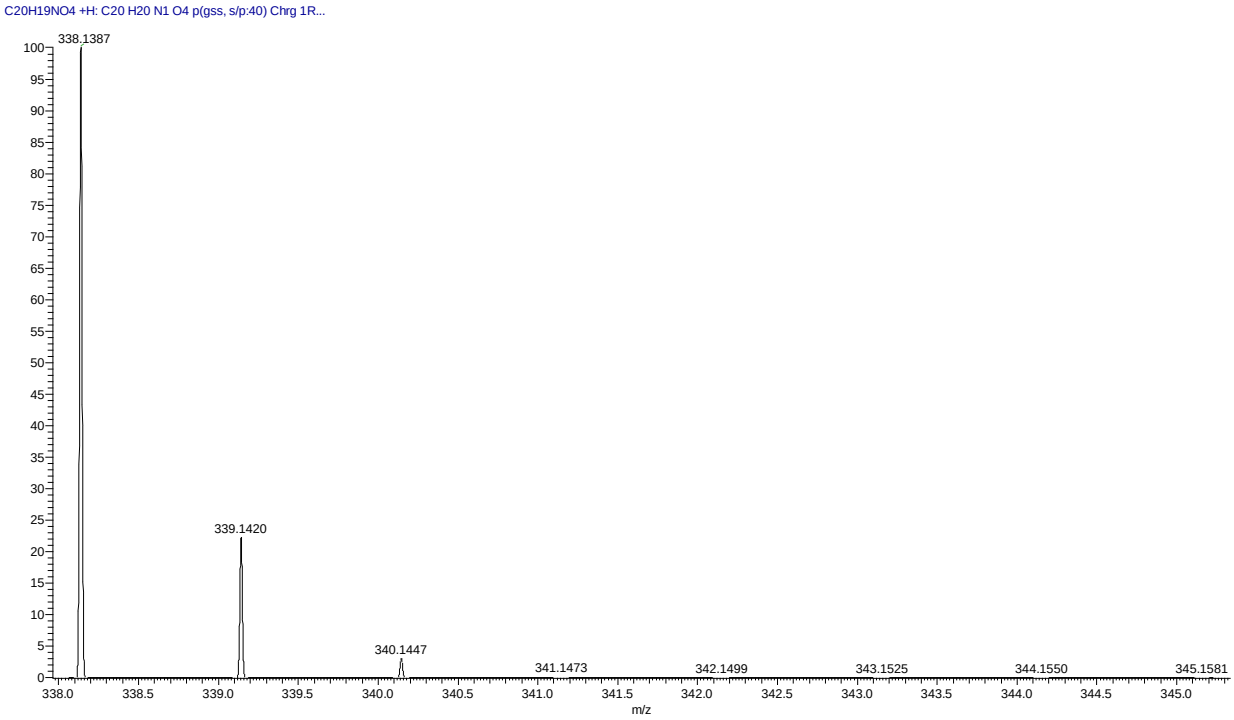

Figure S37: Calculated mass spectrum $(M+H)^+$ for 2-(8-hydroxy-1,2,3,5,6,7-hexahydropyrido[3,2,1-ij]quinoline-9-carbonyl)benzoic acid

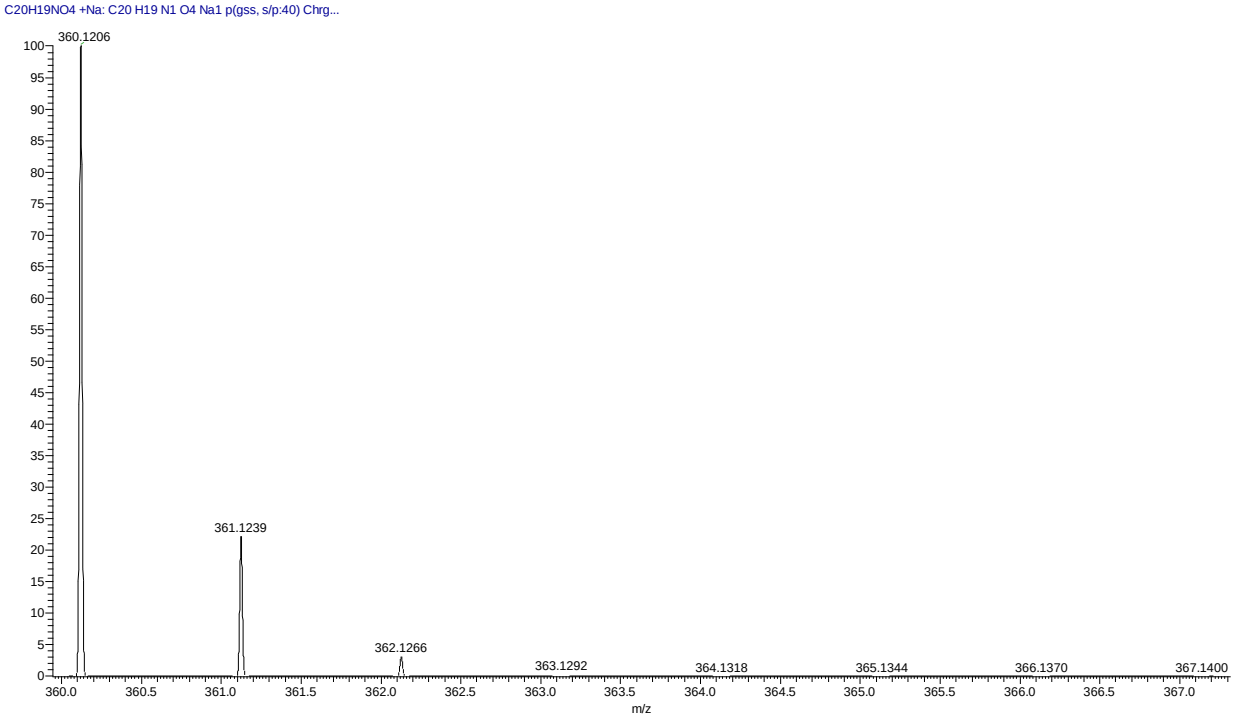

Figure S38: Calculated mass spectrum $(M+Na)^+$ for 2-(8-hydroxy-1,2,3,5,6,7-hexahydropyrido[3,2,1-ij]quinoline-9-carbonyl)benzoic acid

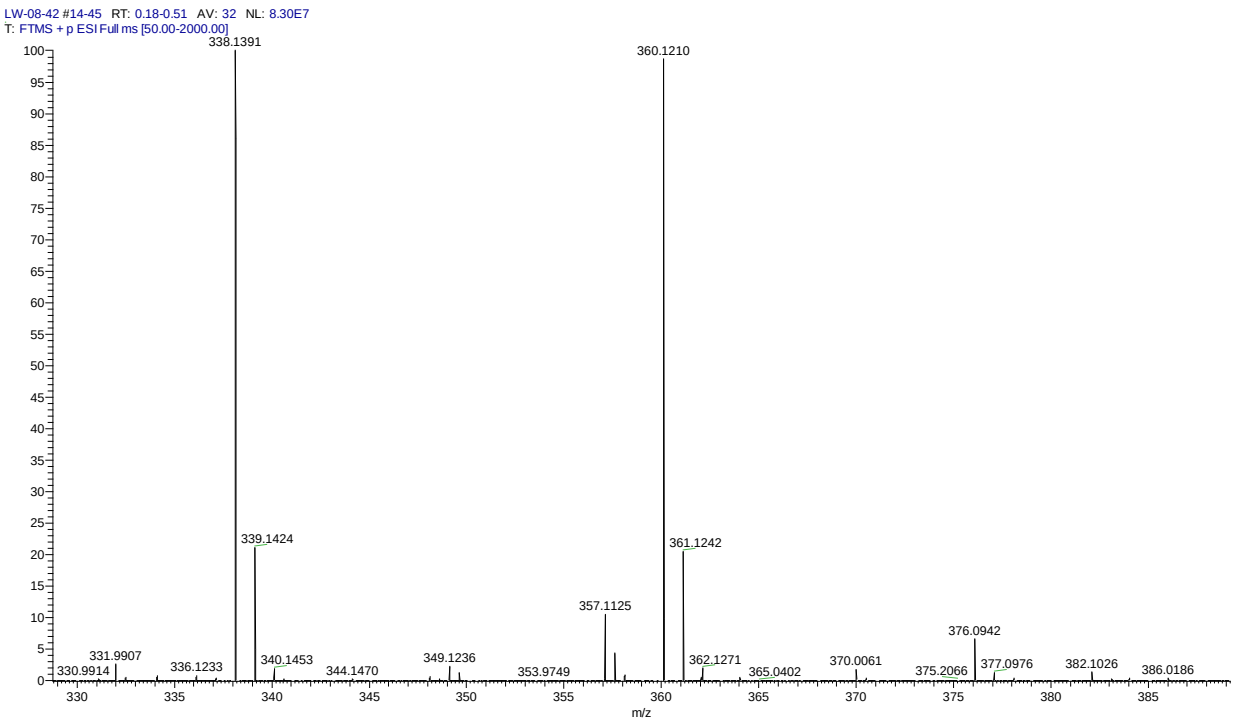

Figure S39: Measured mass spectrum $(M+H)^+$, $(M+Na)^+$ for 2-(8-hydroxy-1,2,3,5,6,7-hexahydropyrido[3,2,1-ij]quinoline-9-carbonyl)benzoic acid

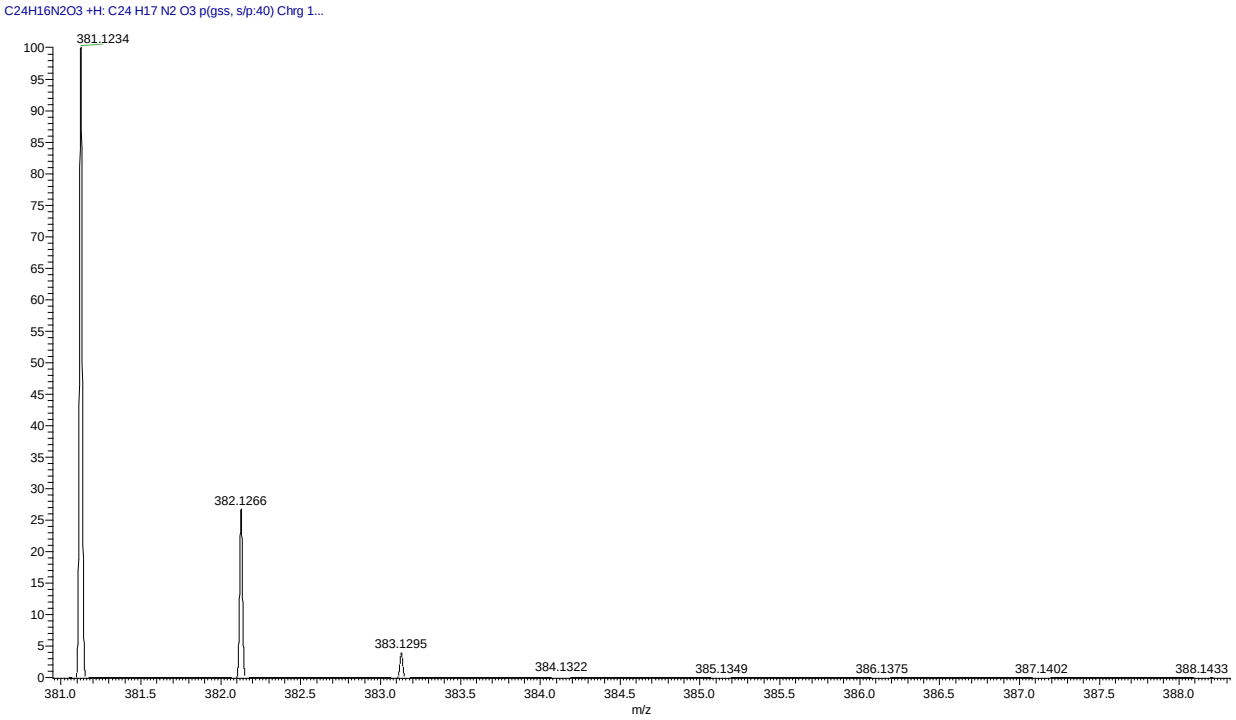

*Figure S40: Calculated mass spectrum $(M+H)^+$ for spiro **1***

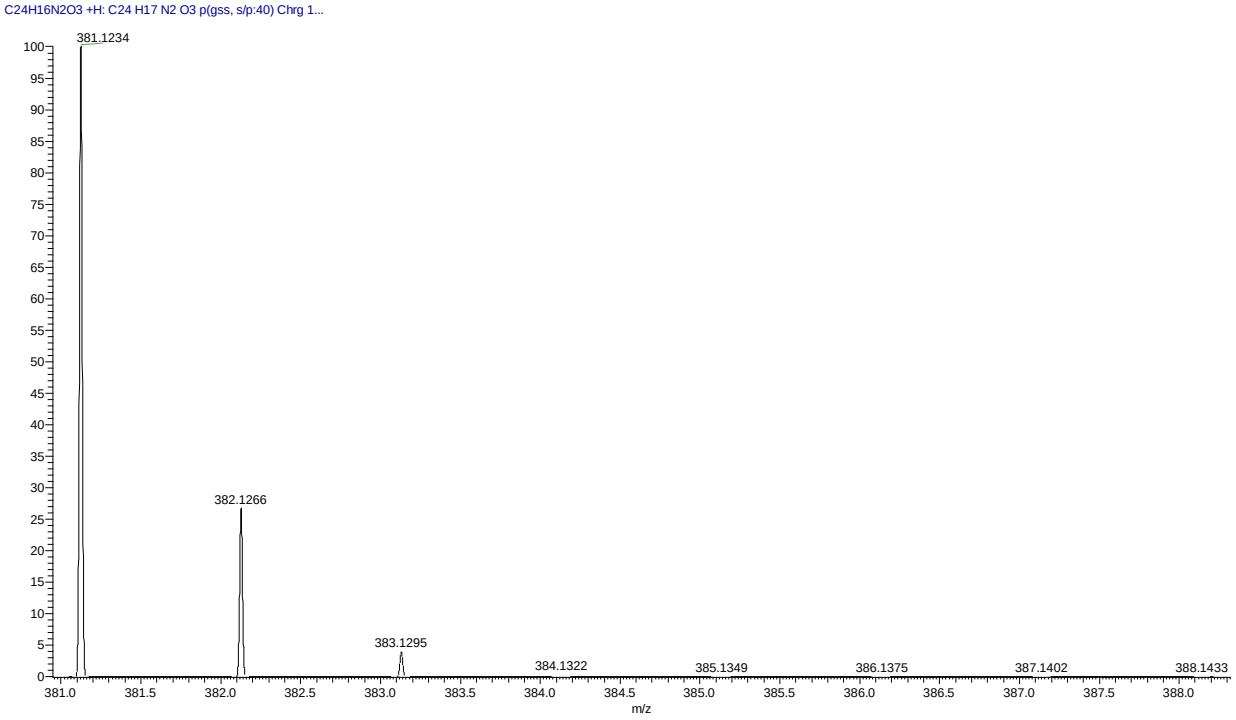

*Figure S41: Calculated mass spectrum $(M+Na)^+$ for spiro **1***

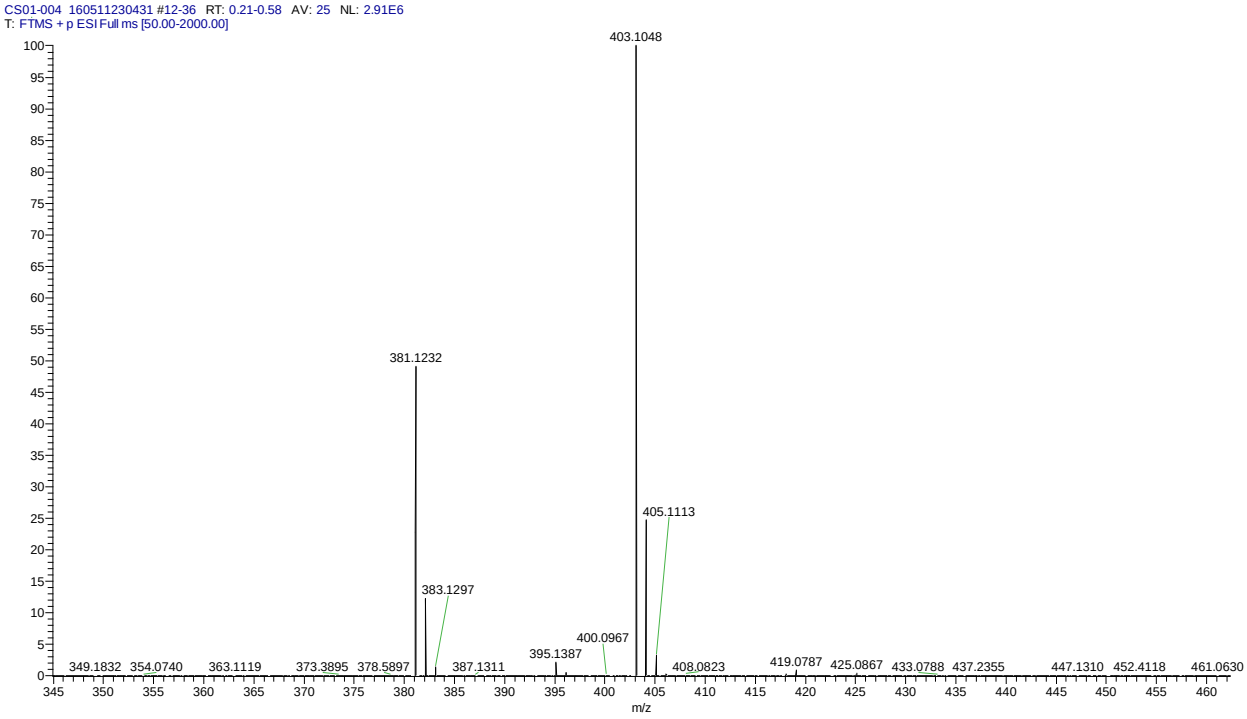

*Figure S42: Measured mass spectrum $(M+Na)^+$ for spiro **1***

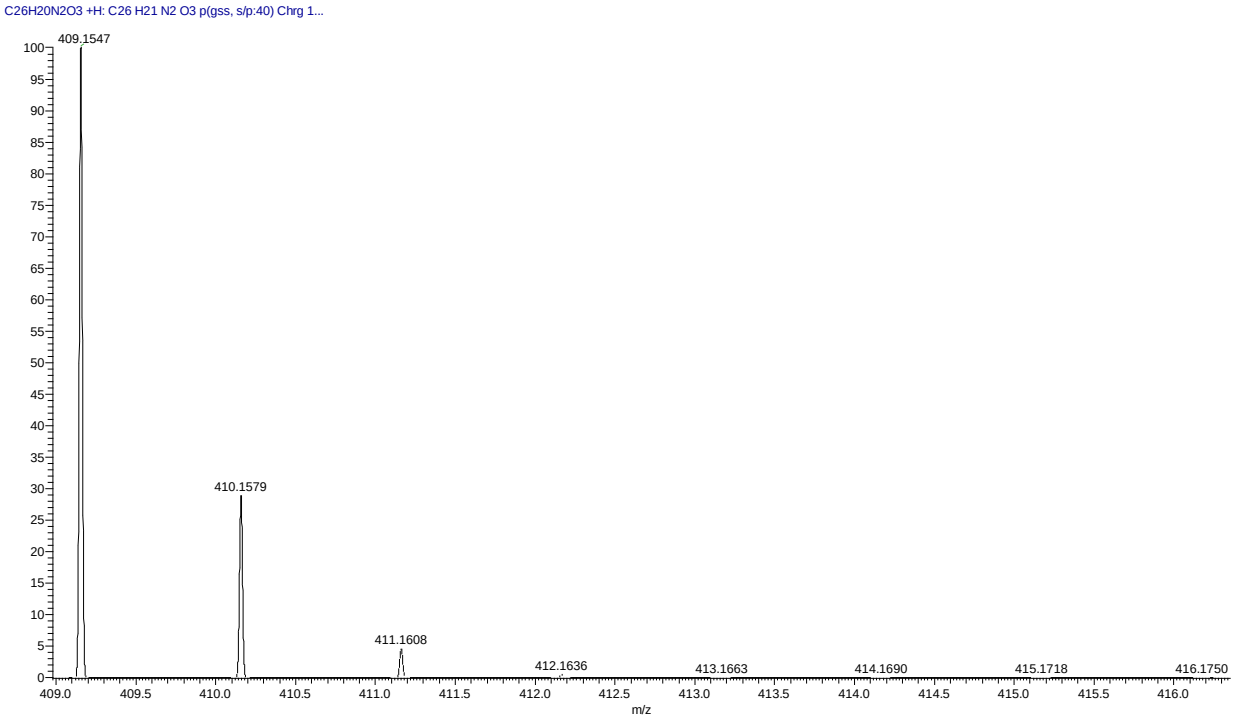

*Figure S43: Calculated mass spectrum $(M+H)^+$ for spiro **2***

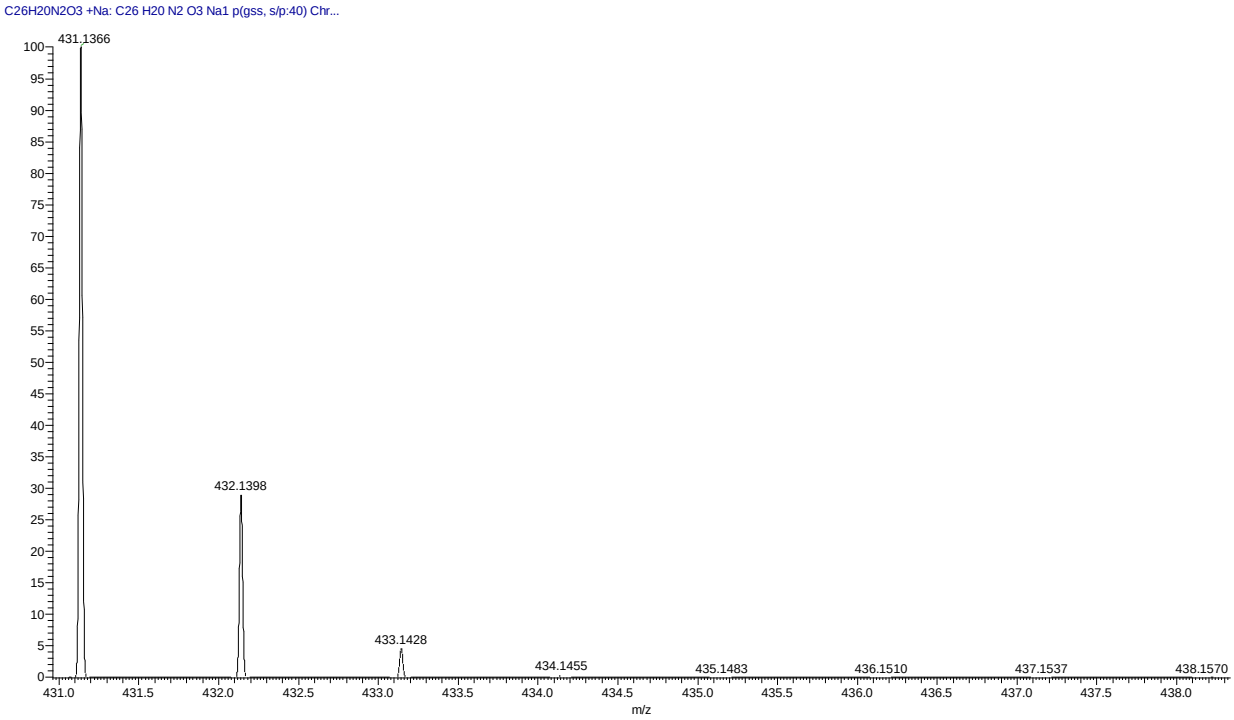

*Figure S44: Calculated mass spectrum $(M+Na)^+$ for spiro **2***

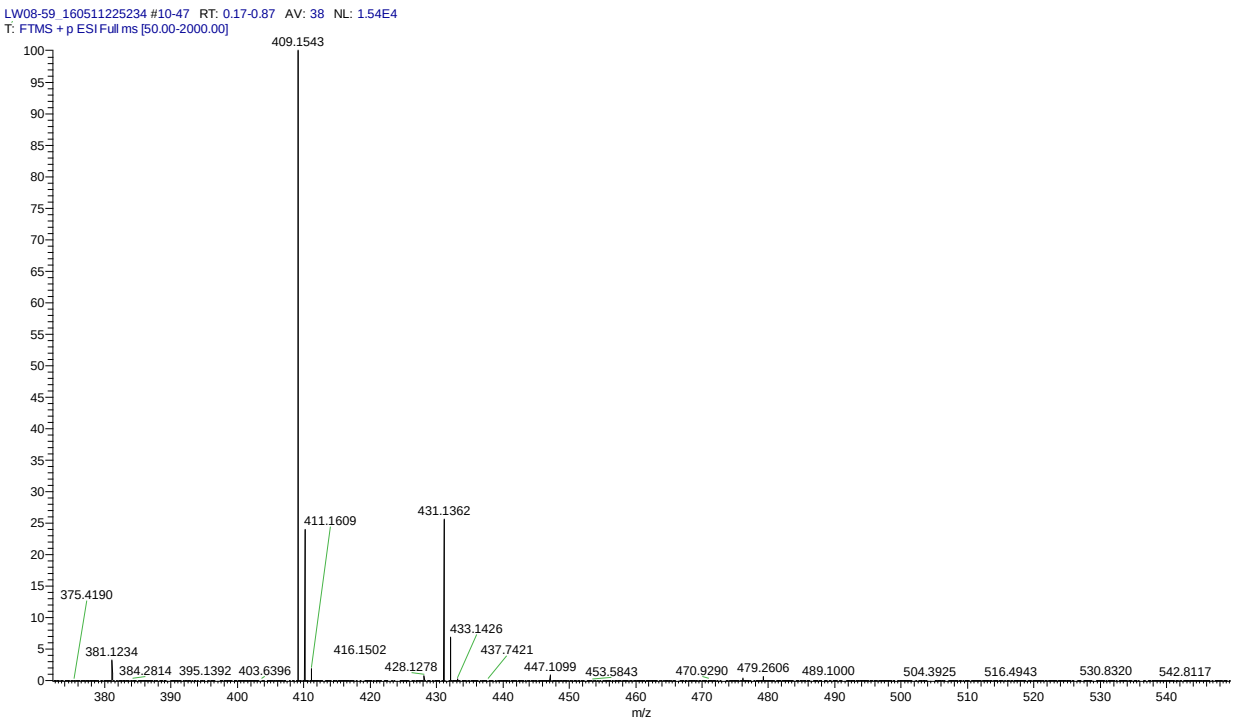

*Figure S45: Measured mass spectrum $(M+H)^+$ for spiro **2***

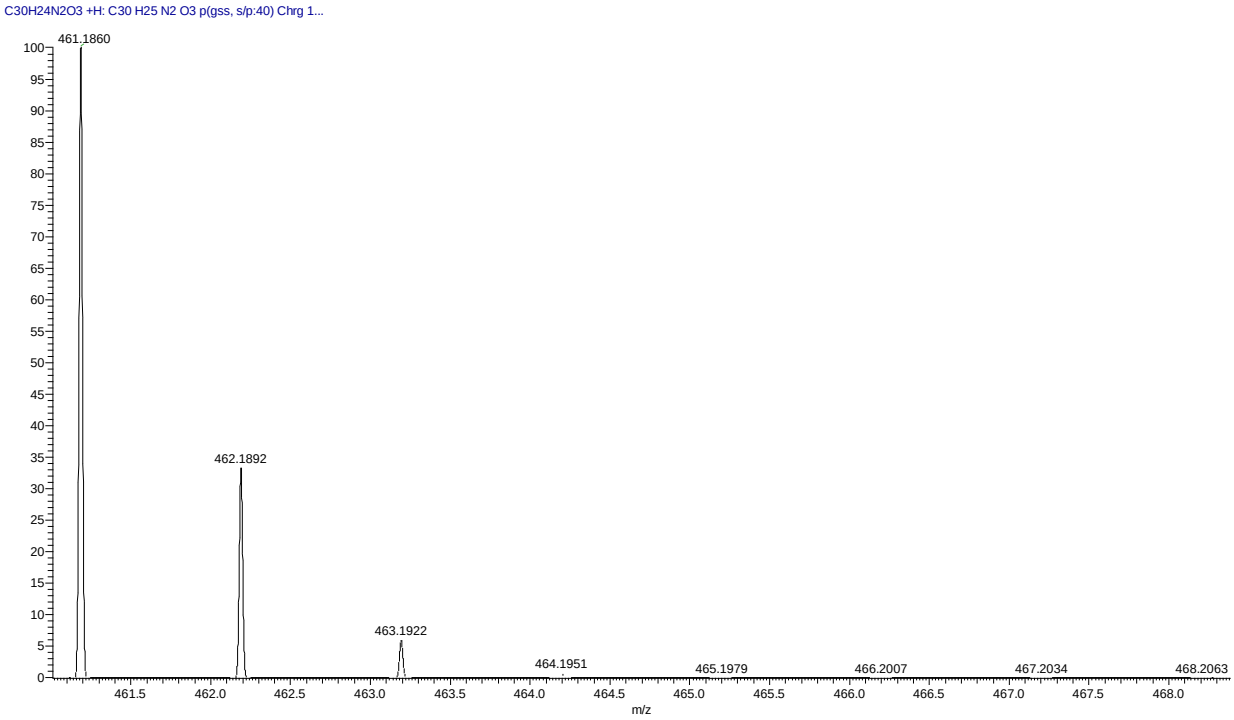

*Figure S46: Calculated mass spectrum $(M+H)^+$ for spiro **3***

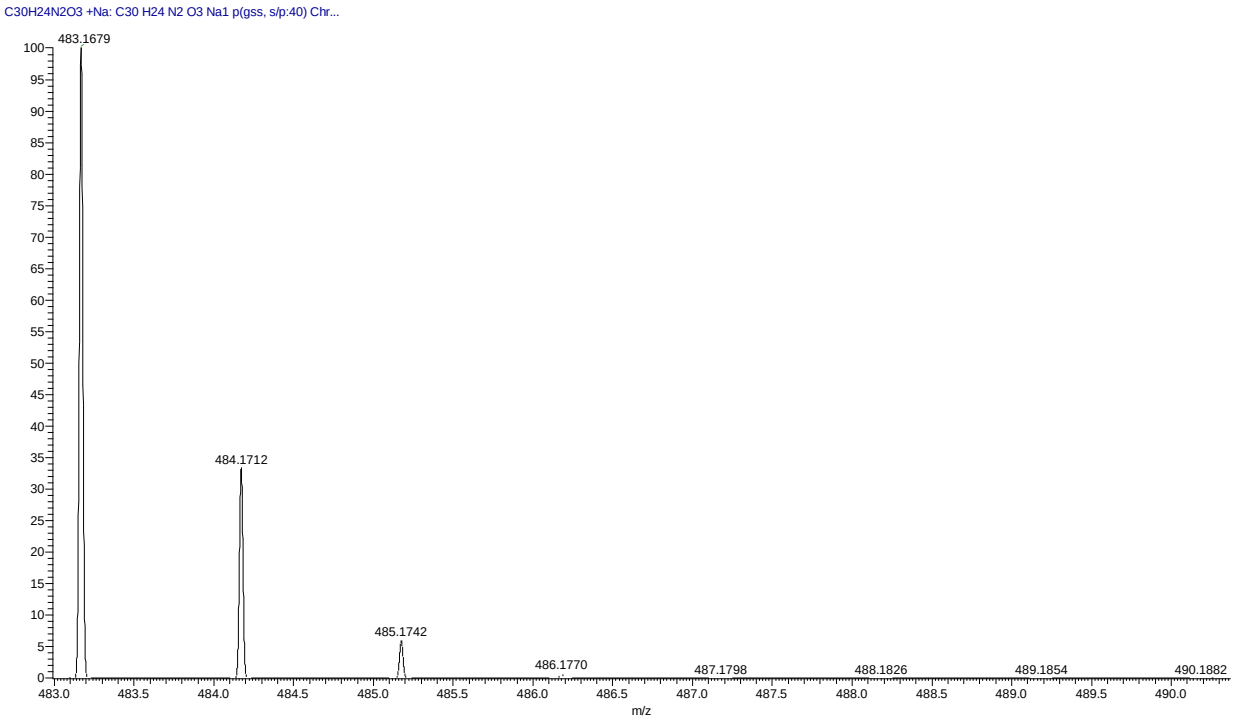

*Figure S47: Calculated mass spectrum $(M+Na)^+$ for spiro **3***

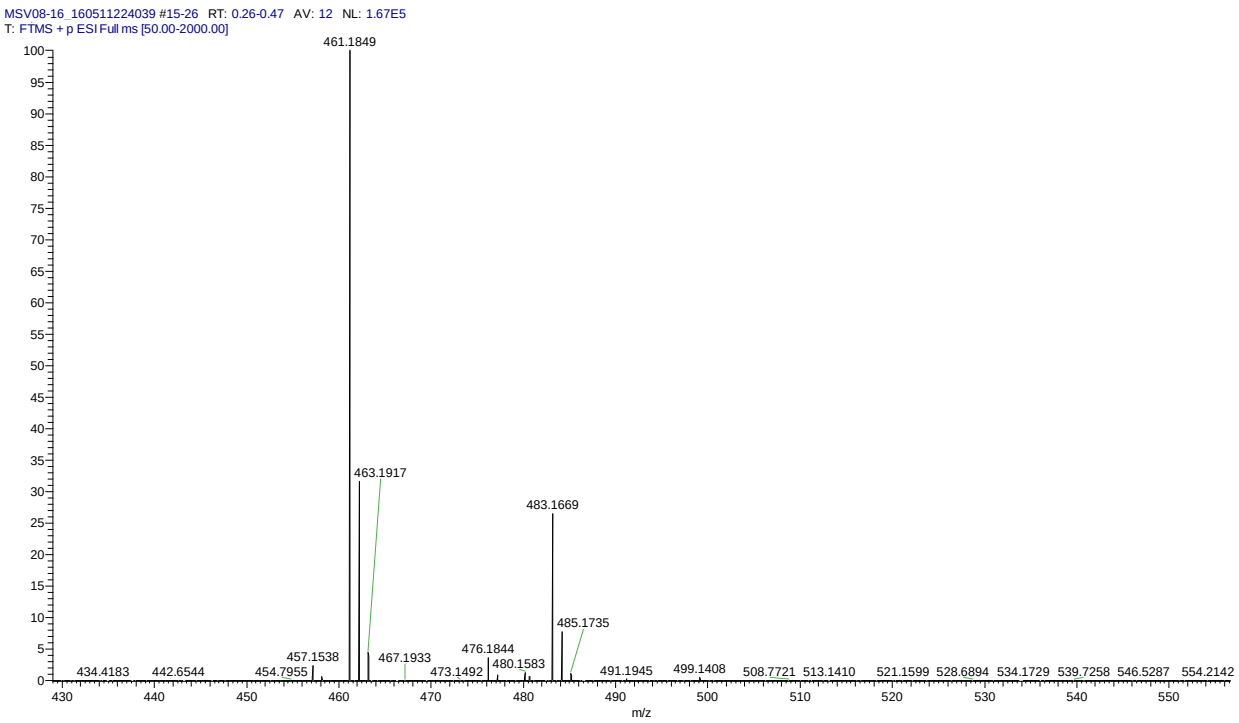

*Figure S48: Measured mass spectrum $(M+H)^+$ for spiro **3***

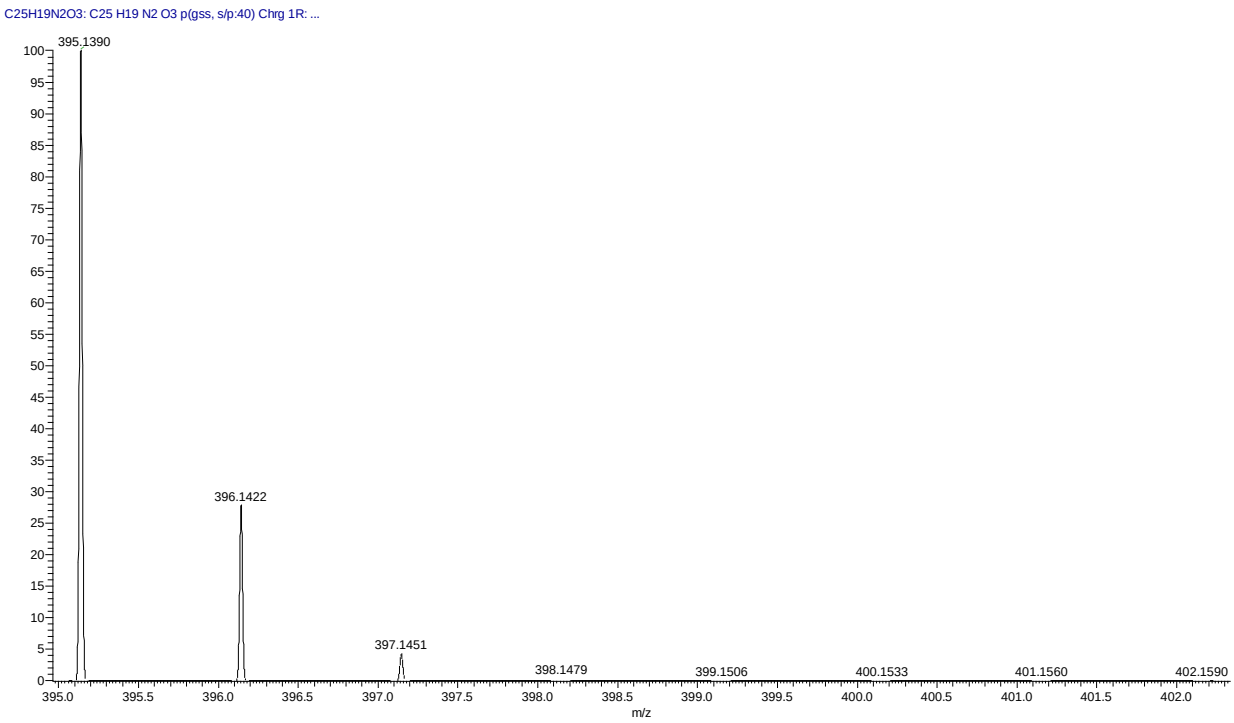

*Figure S49: Calculated mass spectrum (M peak) for Compound **1.***

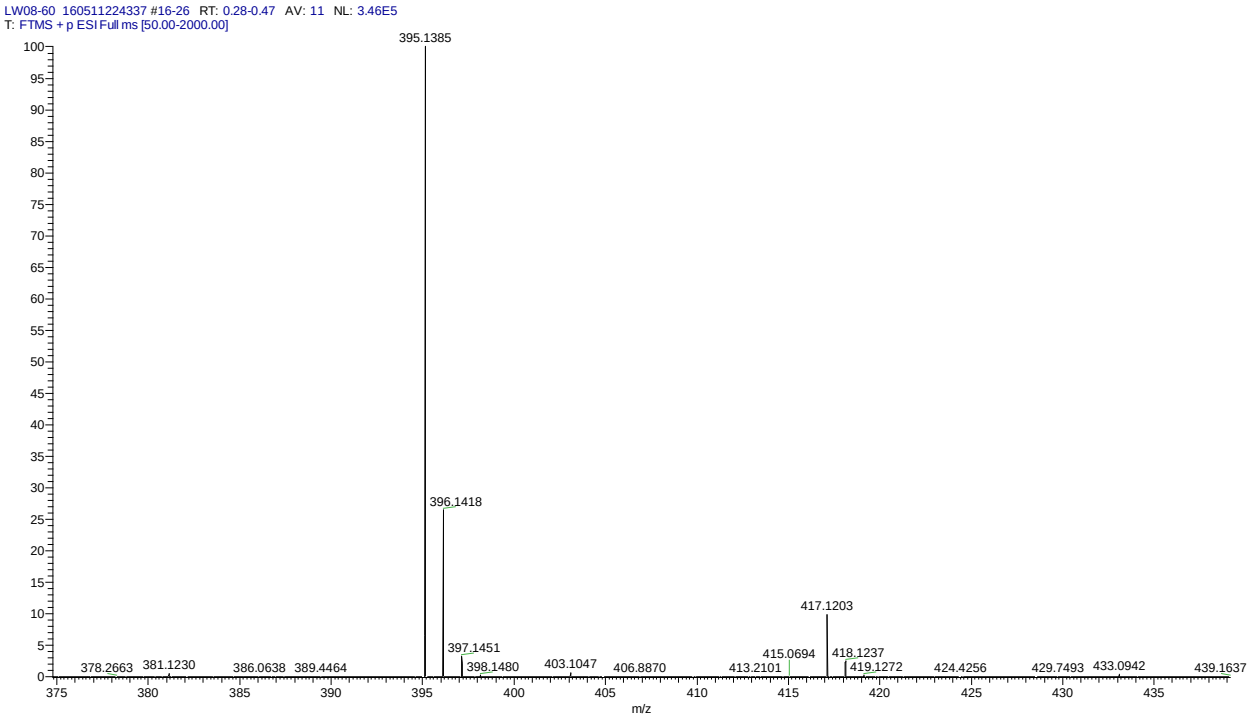

*Figure S50: Measured mass spectrum (M peak) for Compound **1.***

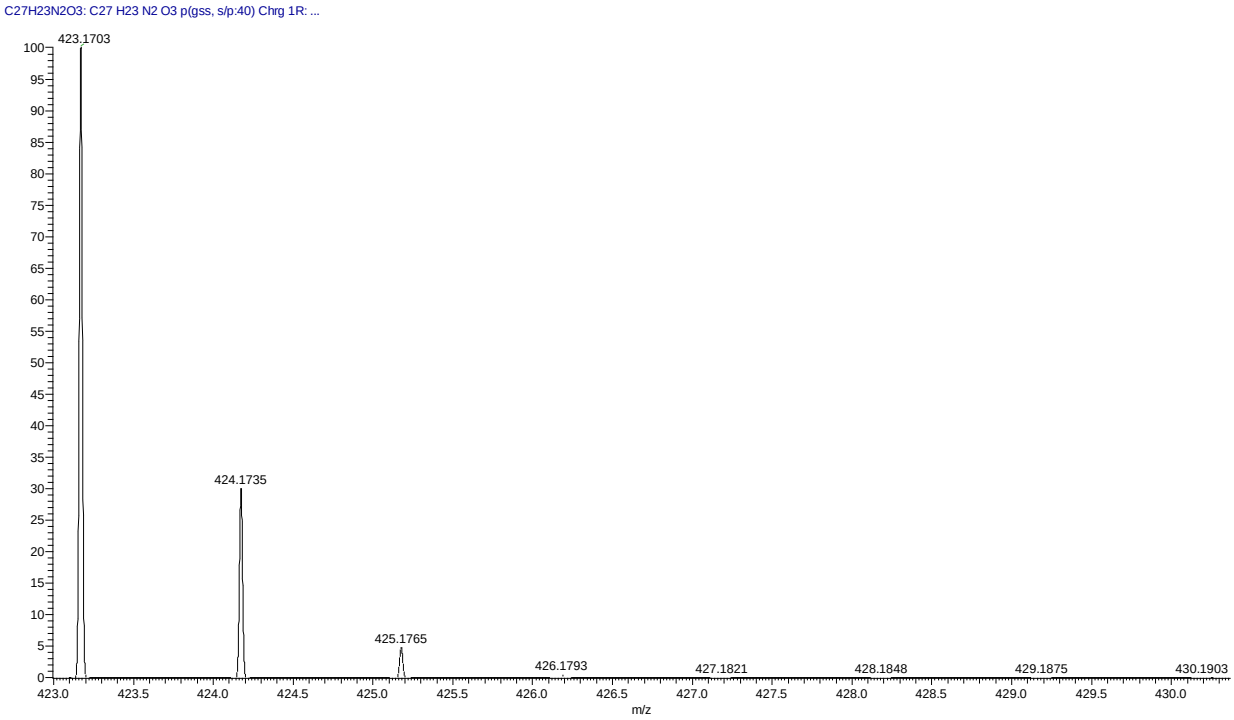

*Figure S51: Calculated mass spectrum (M peak) for Compound **2**.*

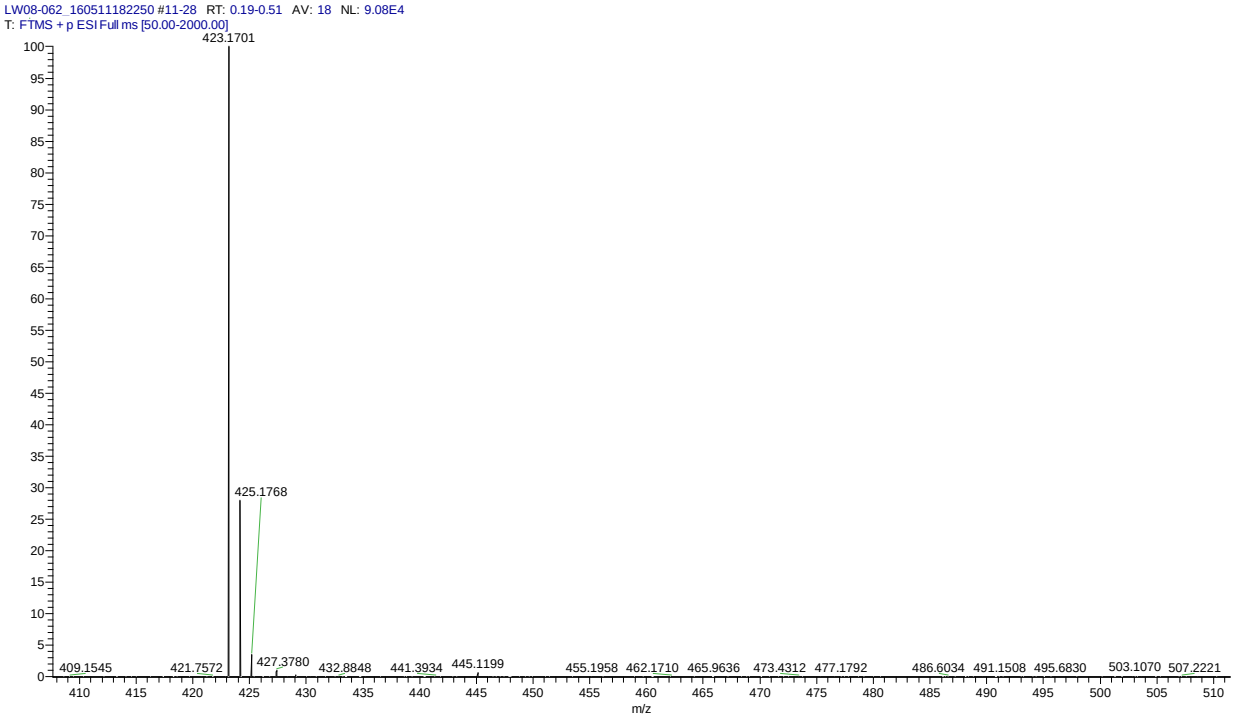

*Figure S52: Measured mass spectrum (M peak) for Compound **2**.*

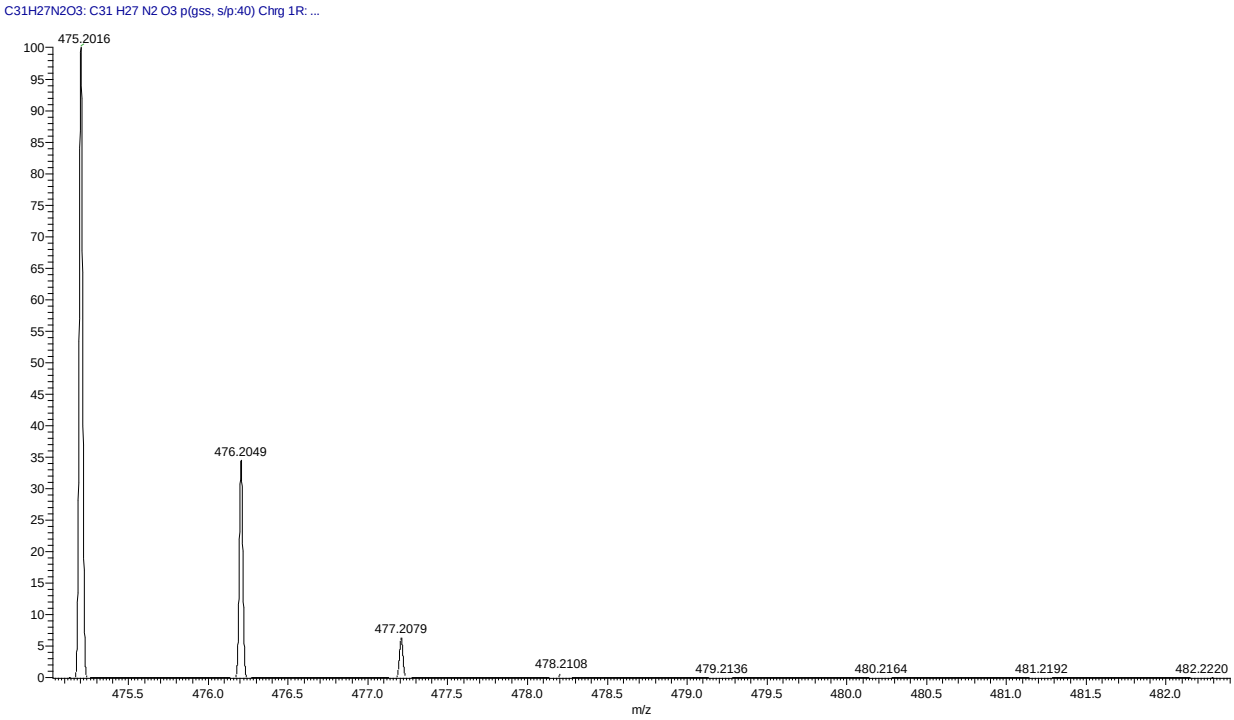

*Figure S53: Calculated mass spectrum (M peak) for Compound **3**.*

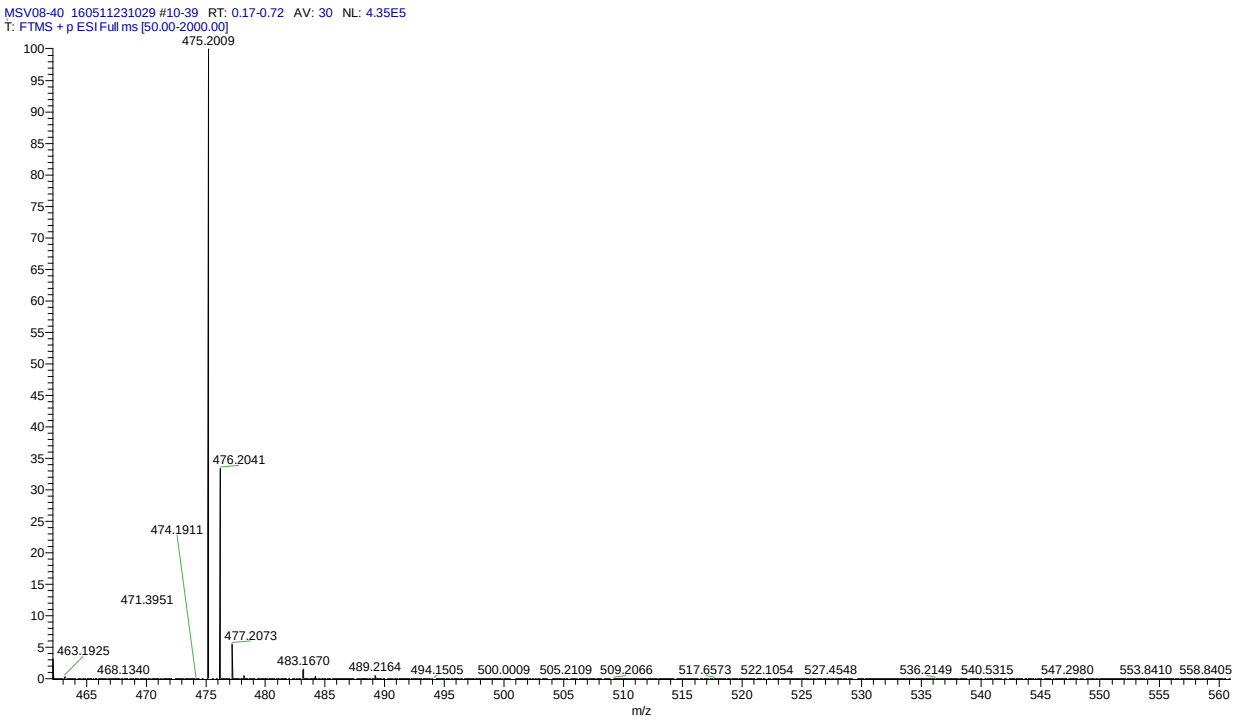

*Figure S54: Measured mass spectrum (M peak) for Compound **3**.*

Fluorescence EEM Contour Plots

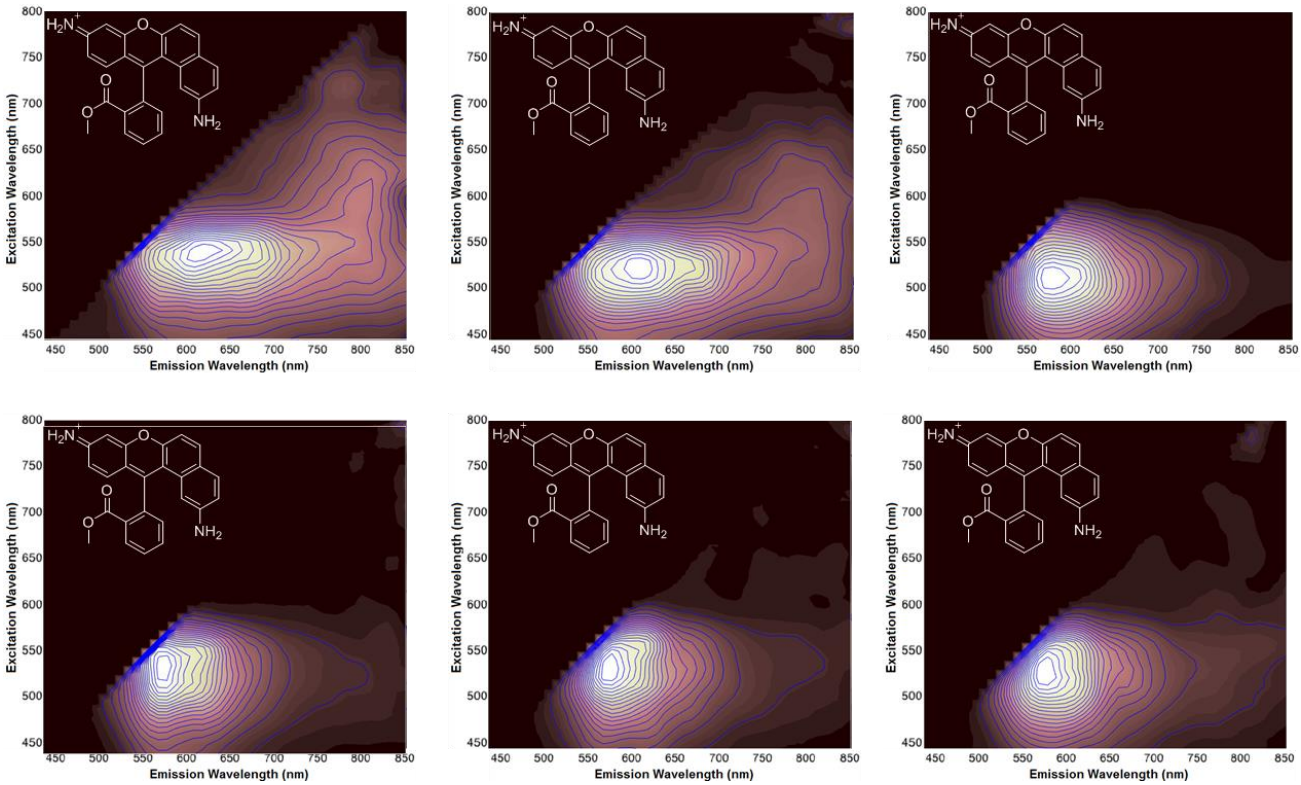

*Figure S55: EEM contour plots for compound **1** (15 μM)**.** The top row shows DMSO (left), MeOH (center, in 10% DMSO), and pH 1.9 (right) aqueous solution. The bottom row shows pH 6 (left), 7.4 (center), and 9 (right) phosphate buffer in 10% DMSO.*

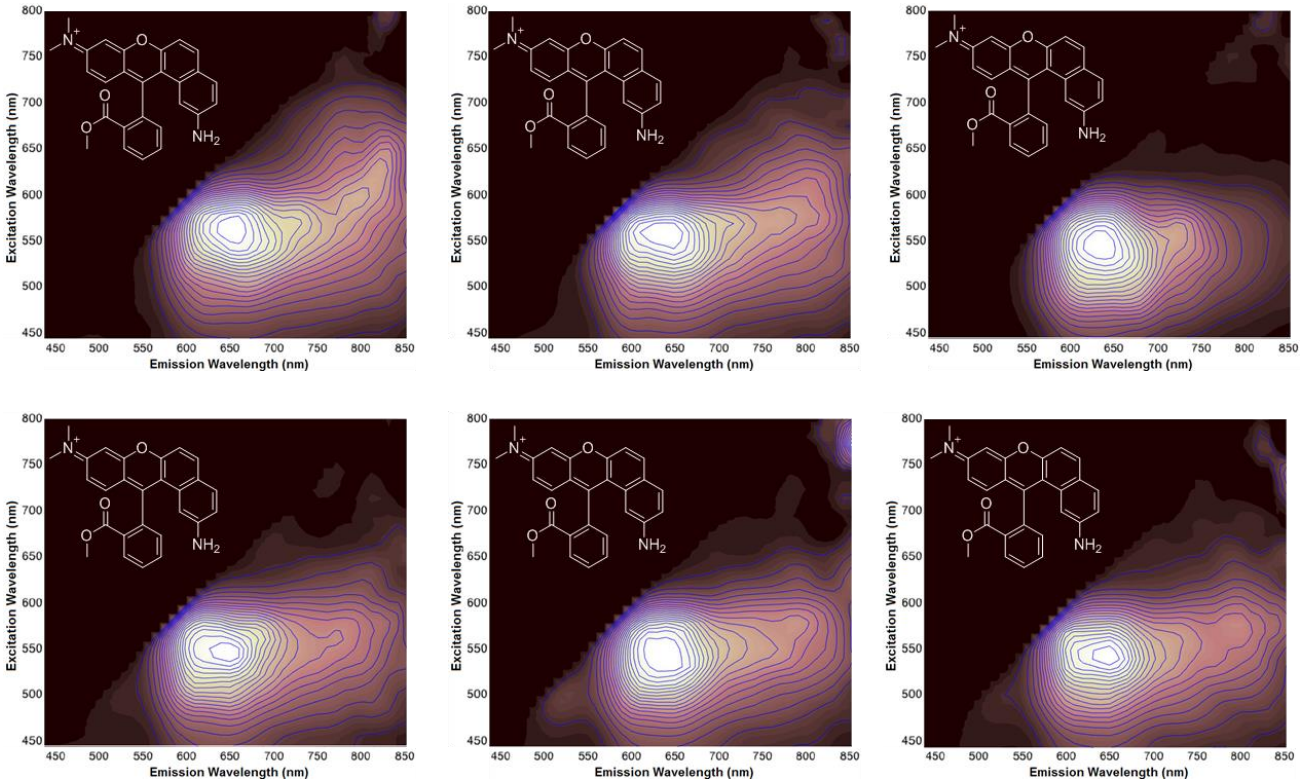

*Figure S56: EEM contour plots for compound **2** (15 μM)**.** The top row shows DMSO (left), MeOH (center, in 10% DMSO), and pH 1.9 (right) aqueous solution. The bottom row shows pH 6 (left), 7.4 (center), and 9 (right) phosphate buffer in 10% DMSO.*

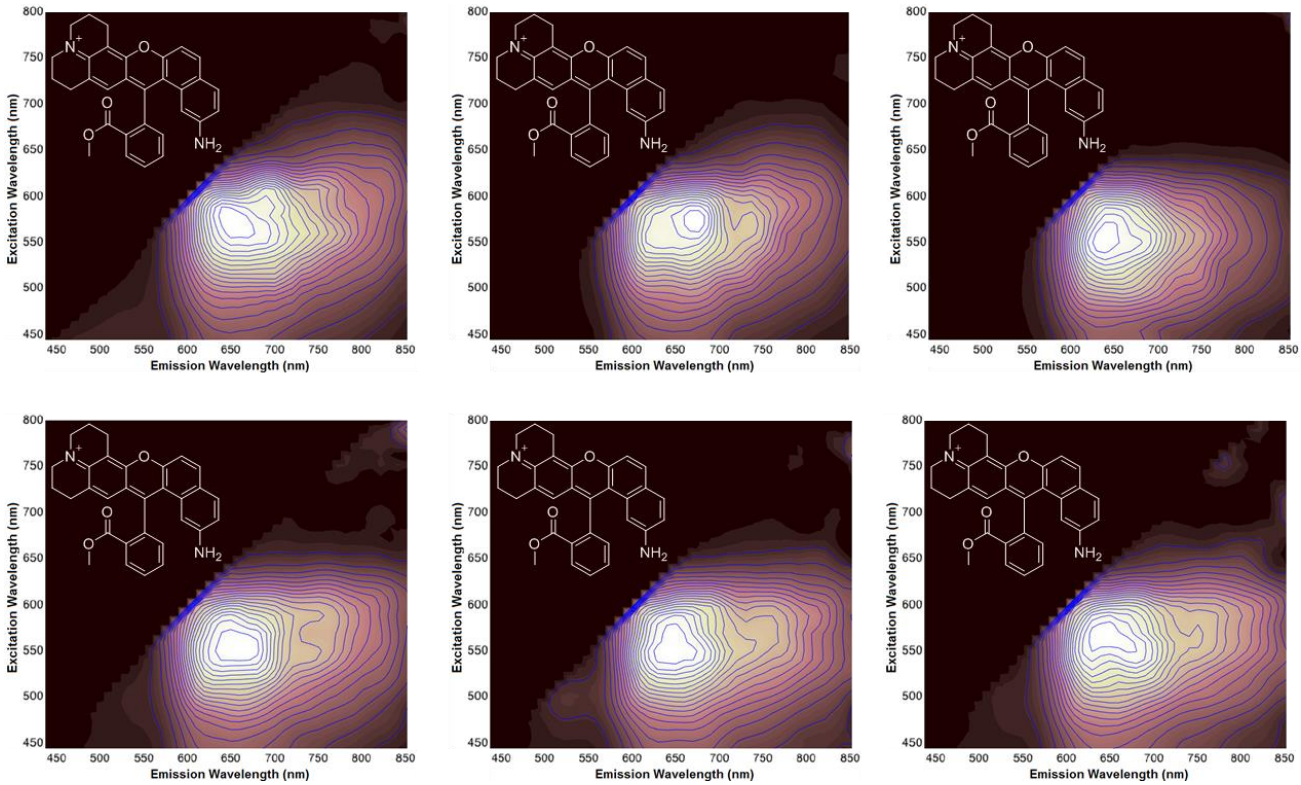

*Figure S57: EEM contour plots for compound **3** (15 μM)**.** The top row shows DMSO (left), MeOH (center, in 10% DMSO), and pH 1.9 (right) aqueous solution. The bottom row shows pH 6 (left), 7.4 (center), and 9 (right) phosphate buffer in 10% DMSO.*